

" AN INVESTIGATION INTO  
THE MECHANICAL PROPERTIES  
OF COMPOSITE MATERIALS  
REINFORCED WITH THE LOCALLY  
OBTAINED NATURAL FIBRES. "

THIS THESIS HAS BEEN ACCEPTED FOR  
THE DEGREE OF Msc. 1993  
AND A COPY MAY BE PLACED IN THE  
UNIVERSITY LIBRARY

BY: CYRUS CONCELLOR MUTHURI / KIRIMA.

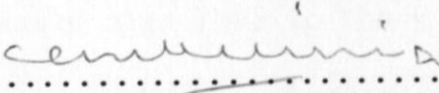
(Bsc. (Hons), Nairobi, 1987).

A thesis submitted in partial fulfilment for  
the award of a master of science degree of  
the University of Nairobi.

December, 1993

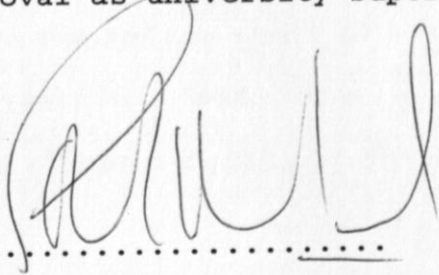
DECLARATION

I declare that "This thesis is my original work and has not been presented for a degree in any other university".

Signature:.......... Date:.....24/12/93.....  
(Cyrus Concellor Muthuri Kirima)

To my Parents, Mr. and Mrs. M'ikirima,  
for the noble cause and foresight in  
providing for this valuable education.

"This thesis has been submitted for examination with my approval as university supervisor"

Signature:.......... Date:.....35/12/93.....  
(Dr. Stephen M. Mutuli)

## ACKNOWLEDGEMENT

I am greatly indebted to my supervisor, Dr. Stephen Mutuli for his guidance, encouragement and help throughout the course of this study. I would also like to register my deep appreciation to the staff of The Housing Research and Development Unit, for their friendliness and willingness attitude in passing information to me during the preliminary survey of the literature. I would also like to thank Dr. Masu and Mr. Ouma, of the Mechanical Engineering Department for their useful

## DEDICATION

suggestions and encouragement when I faced difficulties in finishing this work, their contributions and sympathies could not have come To my Parents, Mr. and Mrs. M'Ikirima, thank the Technicians of for the noble cause and foresight in Engineering Department, in providing for this valuable education. their kind assistance during the fabrication of the cement mortar-fibre specimens.

Finally, I would like to express my sincere appreciation to Athi River Portland Cement Factory, for donating the cement used in this research work. Last but not least, my sincere gratitude go to the entire staff of the Mechanical Engineering Department, teaching and non - teaching, for their contributions, either directly or indirectly to the completion of this work.

## ACKNOWLEDGEMENT

I am greatly indebted to my supervisor, Dr. Stephen Mutuli for his guidance, encouragement and help throughout the course of this study. I would also like to register my deep appreciation to the staff of The Housing Research and Development Unit, for their friendliness and willingness attitude in passing information to me during the preliminary survey of the literature. I would also like to thank Dr. Masu and Mr. Ouma, of the Mechanical Engineering Department for their useful suggestions and encouragement when I faced difficulties in finishing this work, their contributions and sympathies could not have come at a better time. I wish also to thank the Technicians of the Concrete Laboratory, Civil Engineering Department, in particular messrs Maina and Musembi for their kind assistance during the fabrication of the cement mortar-fibre specimens.

Finally, I would like to express my sincere appreciation to Athi River Portland Cement Factory, for donating the cement used in this research work. Last but not least, my sincere gratitude go to the entire staff of the Mechanical Engineering Department, teaching and non - teaching, for their contributions, either directly or indirectly to the completion of this work.

3.1	Experimental devices.....	34
3.1.1	The vibration table.....	34
3.1.2	The cube moulding machine.....	34
3.1.3	The flexure test rig.....	35
3.1.4	The tensile test specimen grips .....	35

CONTENTS

	<u>TITLE</u>	<u>PAGE</u>
	ing machine.....	
3.2	Experimental procedure.....	40
3.2.1	DECLARATION.....	i
3.2.1.1	DEDICATION.....	ii
3.2.1.2	ACKNOWLEDGEMENT.....	iii
3.2.2	ABSTRACT.....	viii
3.2.2.1	ABBREVIATIONS.....	x
3.2.2.2	NOTATION.....	x
3.2.2.3	LIST OF FIGURES.....	xii
	LIST OF TABLES.....	xv
3.2.3	The matrix constituents.....	43
1	INTRODUCTION.....	1
2	REVIEW OF LITERATURE.....	6
2.1	Introduction.....	6
2.2	Progress in cement matrix and fibre reinforcement.....	45 7
2.3	The mechanical properties.....	21
2.4	Efficiency factors.....	29
2.4.1	Fibre orientation efficiency factor....	29
2.4.2	Fibre randomness efficiency factor....	31
2.4.3	Fibre length efficiency factor.....	32
3	EXPERIMENTAL DEVICES AND EXPERIMENTAL PROCEDURE.....	48 34
3.1	Experimental devices.....	34
3.1.1	The vibration table.....	34
3.1.2	The cube moulding machine.....	34
3.1.3	The flexure test rig.....	35
3.1.4	The tensile test specimen grips .....	35
3.3.2	Fibre composites.....	54

3.1.5	The Instron universal .....	54
3.1.5.1	testing machine.....	36
3.2	Experimental procedure.....	40
3.2.1	The experimental programme.....	40
3.2.1.1	Reinforcing fibres.....	40
3.2.1.2	Fibre composites.....	41
3.2.2	Sample preparation.....	42
3.2.2.1	coconut fibre for tensile test.....	42
3.2.2.2	Chopped fibres.....	42
3.2.2.3	Sisal fibre for parallel	62
3.2.2.3.1	reinforcement.....	43
3.2.3	The matrix constituents.....	43
3.2.4	Calculations.....	44
3.2.4.1	The flexure beams.....	44
3.2.4.2	Tensile specimens.....	45
3.2.4.3	Cube specimens.....	45
3.2.5	Specimen preparation.....	46
3.2.5.1	Fresh mortar.....	46
3.2.5.2	Un-reinforced flexure test beams.....	47
3.2.5.3	Chopped fibre reinforced	65
3.2.5.3.1	flexure test beams.....	48
3.2.5.4	Parallel aligned reinforced	68
3.2.5.4.1	flexure test beams.....	48
3.2.5.5	Tensile test specimens.....	49
3.2.5.6	Cube specimens.....	49
3.3	Mechanical testing.....	51
3.3.1	coconut fibre.....	51
3.3.1.1	Fibre tensile test.....	51
3.3.1.2	Fibre density.....	52
3.3.2	Fibre composites.....	54

3.3.2.1	Flexure test.....	54
3.3.2.2	Tensile test.....	55
3.3.2.3	Interfacial bond strength.....	57
3.3.2.4	Composite density and Void volume.....	58
4	EXPERIMENTAL RESULTS.....	60
4.1	coconut fibre.....	60
4.1.1	Density of coconut fibre.....	60
4.1.2	Fibre tensile strength.....	60
4.1.3	Fibre cross-sectional area.....	61
4.2	Cement mortar - fibre composites.....	62
4.2.1	Workability of cement mortar and cement mortar fibre components.....	62
4.2.2	Flexural properties of cement mortar-fibre composites.....	63
4.2.2.1	Chopped sisal fibre reinforced flexural beams.....	63
4.2.2.2	Parallel aligned sisal fibre reinforced flexural beams.....	64
4.2.2.3	Chopped coconut fibre reinforced flexural beams.....	65
4.2.3	Tensile properties of cement mortar-fibre composites.....	68
4.2.3.1	Chopped sisal fibre reinforced tensile specimens.....	68
4.2.3.2	Parallel aligned sisal fibre reinforced specimens.....	69
4.2.3.3	Chopped coconut fibre reinforced tensile specimens.....	72
4.2.3.4	Composite density and void volume.....	75

4.2.3.5	sisal fibre-cement mortar	
	interfacial bond strength.....	78
5	DISCUSSION.....	80
5.1	coconut fibre.....	80
5.1.1	Tensile strength.....	80
5.1.2	Fibre cross-sectional area.....	82
5.1.3	Fibre Modulus of Elasticity.....	83
5.1.4	Fibre density.....	85
5.2	Cement mortar-fibre composite.....	86
5.2.1	Flexural strength.....	86
5.2.2	Tensile strength and Modulus of Elasticity.....	94
5.2.3	Interfacial bond strength.....	97
5.2.4	Density and Porosity.....	99
6	CONCLUSIONS AND RECOMMENDATIONS FOR FURTHER WORK.....	103
6.1	Conclusions.....	103
6.2	Recommendations for further work.....	106
7	REFERENCES.....	109
8.1	APPENDIX 1: Data.....	120
8.2	APPENDIX 2:.....	146
	Theory for minimum crack spacing of long fibres with Frictional Bond....	147



## ABSTRACT

This abstract summarizes the results of a research work done by Cyrus Concellor Muthuri Kirima, for a master of science degree thesis entitled "AN INVESTIGATION INTO THE MECHANICAL PROPERTIES OF COMPOSITE MATERIALS REINFORCED WITH THE LOCALLY OBTAINED NATURAL FIBRES". A thesis submitted in partial fulfilment for the award of a master of science degree of the University of Nairobi, in December, 1993.

The physical and mechanical properties of coconut fibre were investigated. The results obtained for the physical properties were; cross-sectional area,  $8.0 \times 10^{-8} \text{ m}^2$ , and density,  $5.3 \times 10^{-8} \text{ kgm}^{-2}$ . The cross-sectional area of the fibre varied between individual fibres and along its length. The following mechanical properties were obtained; tensile strength  $159.30 \text{ MNm}^{-2}$ , Yield stress  $70.53 \text{ MNm}^{-2}$ , Modulus of Elasticity  $4.02 \text{ GNm}^{-2}$  and an elongation at failure of 24.20%.

Sisal fibre was used to reinforce the cement mortar matrix in two forms; parallel aligned and chopped randomly aligned. The coconut fibre reinforced the matrix only in chopped form, randomly distributed in the matrix. The resulting composite was tested in flexure, (4-point bending) and direct tension to establish the effect of fibre reinforcement on the physical and mechanical properties.

Fibre reinforcement improved some mechanical properties of the composite. A linear increase in flexural and tensile strength with fibre volume fraction was obtained for parallel aligned sisal fibres. The increase in strength attained maximum values of  $9.46 \text{ MNm}^{-2}$  for flexure at 7.5% fibre reinforcement volume fraction and  $3.98 \text{ MNm}^{-2}$  in tension at 7% fibre volume fraction. Chopped sisal and coconut fibres generally increased the flexural and tensile strengths of the composite, but the maximum values obtained were low compared to the parallel aligned sisal fibre reinforcement. The maximum flexural strength occurred at 6% fibre volume fraction of  $4.74 \text{ MNm}^{-2}$  for sisal fibre reinforced composite and  $4.24 \text{ MNm}^{-2}$  at 8% volume fraction for coconut fibre reinforcement respectively. The maximum tensile strength values obtained were  $2.94 \text{ MNm}^{-2}$  for sisal fibre reinforcement and  $2.09 \text{ MNm}^{-2}$  for coconut fibre reinforcement. These occurred at 7% and 6% fibre volume fraction for sisal and coconut respectively. On the other hand, fibre reinforcement resulted into a linear decrease in the composite Modulus of Elasticity. Based on the above, the results obtained were therefore valid for the range of study.

Fibre addition into the cement mortar matrix gave a decrease in the composite density, while the amount of voids present increased. The interfacial bond strength between sisal fibre and the cement mortar matrix decreased with increase in fibre volume fraction. The calculated value tends to a mean value above a fibre volume fraction of 4%.

## ABBREVIATIONS

Abbreviations where otherwise not identified, will stand for the following:

ASTM	American Society for Testing and Materials
BRE	Building Research Establishment
BS	British Standards
HRDU	Housing Research and Development Unit
fib.	Fibre
r.p.m	Revolutions per minute
SFS	Specific fibre surface
SSP	Specimen
v.f.	Volume fraction

## NOTATION

The following symbols should be identified as follows:

A	Cross-sectional area
B	Breadth (bend test)
b	Width of specimen
c	Length in bond measurement
D	Depth of beam (bend test)
d	Diameter of fibre
E	Modulus of Elasticity
$E_c$	Composite Modulus of Elasticity
$E_f$	Fibre Modulus of Elasticity
$E_m$	Matrix Modulus of Elasticity
e	Fibre elongation
F	Force in tension
G	Energy absorbed by the composite
g	Gramme
J	Variable in summation
K	Fibre misalignment factor
Kg	Kilogramme
L	Span length in flexure test
l	Length
$l_c$	Critical length
M	Number of intervals in summation
N	Number of fibres crossing unit area of composite
P	Load in bending
$p_f$	Perimeter of fibre
r	Fibre radius
$U_m$	Work done to deform a matrix
uts	Ultimate in tension
V	Volume
$V_c$	Volume of composite

List of Figures

Figure	Description of Figure	Page
$V_{cr}$	Critical volume	
$V_f$	Fibre volume fraction	
$V_m$	Matrix volume fraction	
$V_{min}$	Minimum volume	
$V_v$	Volume of voids in the composite	12
$W$	Mass	
$w_a$	Amount of water absorbed by composite	
$X$	Minimum interfacial crack spacing (Aveston et al's theory)	14
$X''$	Final crack spacing (Krenchel's theory)	
$\alpha$	Scaling factor = $E_m V_m / E_f V_f$	
$\epsilon$	Strain	15
$\epsilon_c$	Strain in composite	
$\epsilon_f$	Strain in fibre	
$\epsilon_{fa}$	Strain in the fibre at the matrix failure strain	16
$\epsilon_m$	Strain in matrix	
$\eta_0$	Efficiency factor for fibre orientation	
$\eta_l$	Efficiency factor for fibre length	
$\rho$	Density	
$\sigma$	Stress	16
$\sigma_c$	Stress in composite	
$\sigma_f$	Stress in fibre	
$\sigma_{fa}$	Fibre stress at matrix failure strain	17
$\sigma_m$	Stress in matrix	
$\sigma_{ma}$	Matrix stress at fibre failure strain	
$\sigma_{mu}$	Matrix cracking stress	
$\sigma_s$	Splitting tensile strength	21
$\tau$	Interfacial bond strength	
$\tau_s$	Shear stress	
$\theta$	Angle between fibre principal direction and load direction	24
2.9	Strengthening behaviour of a fibre reinforced composite	26
2.10	Influence on flexural behaviour of a fibre composite by the critical fibre volume	26
2.11	Stress distribution of a fibre in a matrix	29
2.12	Variation of composite tensile Modulus of Elasticity with angle between applied stress and principal fibre direction	30
3.1	The flexure test rig showing the test arrangement	38
3.2	Specimen grips used in direct tensile test	39
3.3	Arrangement for loading flexure test pieces in four point bending	55

## List of Figures

<u>Figure No.</u>	<u>Title of Figure</u>	<u>Page</u>
2.1	Splitting tension test arrangement for loading cementitious specimens.....	12
2.2	Different composite fractures depicting different interfacial bond strength.....	14
2.3	Measurement of interfacial bond strength by critical length method.....	15
2.4	Direct fibre pull-out method for measuring the fibre-matrix interfacial bond strength.....	16
2.5	The strand perimeter technique of measuring the fibre-matrix interfacial bond strength.....	16
2.6	Determination of the interfacial bond strength using the peak load/embedment depth curve method.....	17
2.7	Aligned fibre composite tested in uniaxial tension.....	21
2.8	Graphical representation of equation [2.8] and the position of the critical fibre volume.....	24
2.9:	Strengthening behaviour of a fibre reinforced composite.....	26
2.10	Influence on flexural behaviour of a fibre composite by the critical fibre volume.....	26
2.11	Stress distribution of a fibre in a matrix.....	29
2.12	Variation of composite tensile Modulus of Elasticity with angle between applied stress and principal fibre direction.....	30
3.1	The flexure test rig showing the test arrangement.....	38
3.2	Specimen grips used in direct tensile test..	39
3.3	Arrangement for loading flexure test pieces in four point bending.....	55

4.1	Flexural strength of chopped sisal fibre reinforced cement mortar.....	66
4.2	Flexure strength of parallel aligned sisal fibre reinforced cement mortar.....	67
4.3	Flexure strength of chopped coconut fibre reinforced cement mortar.....	67
4.4	Crack patterns of failed flexure beams.....	68
4.5	Tensile strength of chopped sisal fibre reinforced specimens tested in direct tension.....	71
4.6	Tensile strength of parallel aligned sisal fibre reinforced specimens tested in direct tension.....	71
4.7	Tensile strength of chopped coconut fibre reinforced specimens tested in direct tension.....	72
4.8	Modulus of Elasticity for chopped sisal fibre reinforced cement mortar.....	73
4.9	Modulus of Elasticity for parallel aligned sisal fibre reinforced cement mortar.....	74
4.10	Modulus of Elasticity for chopped coconut fibre reinforced cement mortar.....	74
4.11	Variation of composite density with fibre volume fraction for sisal fibre reinforced cement mortar.....	76
4.12	Variation of composite density with fibre fraction for coconut fibre reinforced cement mortar.....	77
4.13	Variation of void volume with fibre volume fraction for sisal fibre reinforced cement mortar.....	77
4.14	Variation of void volume with fibre volume fraction for coconut fibre reinforced cement mortar.....	78
4.15	The sisal fibre-cement mortar interfacial bond strength.....	79
5.1	Flexure strength of glass reinforced cement composites for different fibre lengths.....	91

5.2	Relationship between fibre volume fraction and density of glass reinforced cement composite for different fibre length.....	101
<i>Table No.</i>		
5.3	Graph of density versus percent fibre (by mass) of wood-pulp reinforced cement mortar.....	101
2.1:	for various fibre-cement combinations.....	20
5.4	Multiple cracking in flexure test (parallel aligned reinforcement).....	102
2.2:	orientation relative to the direction.....	31
5.5	Single crack failure in direct tension (chopped fibre reinforcement).....	102
3.1:	Results of tensile test on sisal fibre.....	40
5.6	Multiple cracking in direct tension test (parallel aligned reinforcement).....	102
3.2:		
5.1:	Cell size for some natural fibres.....	82
5.2:	Typical fibre properties.....	83
5.3:	Critical fibre volume fraction of some common fibres.....	88
A.1:	Density of coconut fibre.....	121
A.2:	Results of tensile test performed on coconut fibre.....	122
A.3:	Summary of results on tensile test for coconut fibre.....	126
A.4:	Flexure strength of chopped sisal reinforced cement beams.....	127
A.5:	Results of flexure strength of cement mortar beams reinforced by parallel aligned sisal fibre.....	130
A.6:	Results of flexure test of cement mortar beams reinforced with 20 mm long chopped coconut fibre.....	133
A.7:	Ultimate tensile strength of tensile specimens reinforced with 20 mm long chopped sisal fibre.....	135
A.8:	Ultimate tensile strength of specimens reinforced with parallel aligned sisal fibre.....	138
A.9:	Ultimate tensile strength of specimens reinforced by 20 mm long chopped coconut fibre.....	141
A.10	The sisal fibre-cement mortar interfacial bond strength measured by the method of Aveston et al [53].....	143

## List of Tables

<u>Table No.</u>	<u>Title of Table</u>	<u>Page:</u>
2.1:	Some values of measured bond strength for various fibre-cement combinations.....	20
2.2:	Efficiency factors $n_0$ for given fibre orientation relative to the direction of stress.....	31
3.1:	Results of tensile test on sisal fibre.....	40
3.2:	Some mechanical properties of sisal fibre...	41
5.1:	Cell size for some natural fibres.....	82
5.2:	Typical fibre properties.....	83
5.3:	Critical fibre volume fraction of some common fibres.....	88
A.1:	Density of coconut fibre.....	121
A.2:	Results of tensile test performed on coconut fibre.....	122
A.3:	Summary of results on tensile test for coconut fibre.....	126
A.4:	Flexure strength of chopped sisal reinforced cement beams.....	127
A.5:	Results of flexure strength of cement mortar beams reinforced by parallel aligned sisal fibre.....	130
A.6:	Results of flexure test of cement mortar beams reinforced with 20 mm long chopped coconut fibre.....	133
A.7:	Ultimate tensile strength of tensile specimens reinforced with 20 mm long chopped sisal fibre.....	135
A.8:	Ultimate tensile strength of specimens reinforced with parallel aligned sisal fibre.....	138
A.9:	Ultimate tensile strength of specimens reinforced by 20 mm long chopped coconut fibre.....	141
A.10	The sisal fibre-cement mortar interfacial bond strength measured by the method of Aveston et al [53].....	143



## 1 INTRODUCTION

Ever since mankind started to produce artefacts, the problem of getting the most suitable material had to be solved. In very early times this might have resulted in a search for the best stones for axes or the strongest wood for arches. Often it was a choice based on the mechanical properties necessary for the specific task. Originally, the search for better materials was a search among the existing materials. However, today, with the knowledge of the basic mechanism involved in strong materials, the construction of new materials called **composites** started. This resulted in the process of searching for a single material structure with all the desired properties for a particular (case of a) design, which was found not to be in existence [1]. Consequently, composite materials became a subject for research on a wide range of problems, whereby, two or more materials whose properties are quite different are combined in a definite manner, resulting into a single structure that exhibits superior properties to the individual materials [2].

The history of composite materials is not a new concept. Reinforced materials (composites), both natural and man-made have existed since time immemorial. In natural form, composite materials are found in ; Wood, which is a composite consisting of cellulose and lignin, Bone, which is a composite of protein collagen and mineral apatite etc. [3]. The traditional man-made composites functioned in ways that resemble the deliberate choices available in the modern technology.

These traditional methods involved small percentage additions of fibre with considerable effect in improving the strength and toughness of weak, brittle materials; for example, straw in clay, horse hair in plaster, paper pulp in plaster of paris and asbestos fibre in phosphate cement, to mention but just a few [4]. Scientific methods have also been applied in trying to come up with new composite materials. This has mainly been due to the difficulty of getting a single material with unique properties to respond to particular practical design applications. As a result of this, many new composite materials have come into existence, the majority of which are fibre reinforced. The bulk of these fibre reinforced materials are plastics reinforced with different types of fibres such as carbon, boron, glass and synthetic fibres such as polypropylene etc. [5-14].

These materials have achieved superior properties more effectively enhanced by the properties of the reinforcing fibres, and have found extensive applications in aviation and automobile industries, space exploration, and ventures into the deep waters of the oceans. Apart from plastics, other materials have also been reinforced with fibres to achieve similar results.

Cement base materials such as concrete and mortar have also been a subject of a long on-going research, where they have been reinforced with different types of fibres both natural and artificial. These fibres have included asbestos, glass,

metal, jute, sisal and banana fibres [15]. This effort has predominantly been due to the poor properties of these materials which are very weak in tension and fail in a brittle fashion. These effects have been overcome by the incorporation of fibres in these materials, giving them high strength, stiffness, toughness and durability. Broadly speaking, the fibrous additions stop or deflect the cracks that, by propagating through concentrations of mean stresses well below theoretical expectations, make the material brittle.

In developing countries, eg. Malawi, Swaziland, Thailand and Kenya [16], the research work on fibre reinforcement in cement base materials has been going on for a while now. The fibres used in this case are natural fibres such as sisal and jute, which are obtained in large quantities as they grow locally and are comparatively cheaper. In Kenya, a lot of research work has been going on in trying to use sisal fibre as a reinforcement in cement base materials. This interest has partly been sparked off by the need to come up with cheap building materials and also to find an alternative application for sisal fibre which is currently facing stiff competition in foreign markets. The competition was caused by the coming of synthetic fibres in the hard fibre industry which include fibres like nylon, polypropylene, polyester, and others [17].

Extensive research study on this has been undertaken by the Housing Research and Development Unit (HRDU) of the University of Nairobi in low cost housing scheme. The Unit produces

roofing tiles and sheets by reinforcing cement mortar with chopped and parallel aligned sisal fibre. These products have been applied in various pilot stations wide spread in the country and have caused an impact in cheap rural constructions. Despite the on-going research work, these materials are already being produced in the informal sector of Kenya, and are finding applications in small but increasing scale in the building industry.

In view of the extensive applications that these materials are finding in the building industry, more research work therefore needs to be done, if they have to gain more diverse acceptance as construction and building materials. This will also provide a source of reliable data for publication and design, before these products can be put into more extensive use. It is therefore as a result of this that the work presented in this thesis was proposed, to try and establish properly, through a systematic experimentation the strength characteristics of cement mortar-fibre composites.

In this thesis an attempt has been made to evaluate the possibility of using sisal and coconut as reinforcing fibres in a cement mortar matrix to achieve better mechanical and physical properties. To be able to effectively examine the properties of the resulting composite materials, initial work was done on coconut fibre to establish various strength and physical properties. The properties of sisal fibre used in this research were obtained from the work by the fore-runner

s study, Mutuli, S.M. [18], who used the same grade of fibre used in this work. Hence the research programme has three sections of study: First a study of the properties of coconut fibre, secondly the effect of random and el aligned reinforcement of cement mortar matrix by fibre, in both flexure and direct tension, and thirdly effect of random reinforcement of cement mortar matrix by t fibre in both flexure and direct tension. tremendous h since the introduction of the so called advanced sites in the early sixties [4]. This growth has largely the result of a desire to apply these high strength and modulus but light weight materials in air transportation ms. While the investigation and prediction of the elastic four of these materials are fairly well documented and stood, their inelastic behaviour has presented engineers some very challenging problems. For instance, prediction failure in some particular analysis has proved to be cularly difficult. Over the past years, technological ess has continued quietly and unspectacularly to improve physical properties of these composites and equally tant, also to improve the understanding of how they may ed to the greatest effect. There has been extensive rch into the behaviour of composite materials under stic environmental conditions (corrosive environments, tional stress and extreme conditions of loading), and the e of the complex stress fields that occur in such ials due to their configurations, loading conditions and nal physical structure [5].

## 2 REVIEW OF LITERATURE

### 2.1 Introduction

A composite material has been defined [1,2,3] as any material consisting of two or more distinct constituents (or phases) that are insoluble in one another and whose separate identity is preserved throughout the life and service of the material. efficiency factors [19].

The field of composite materials has experienced tremendous growth since the introduction of the so called advanced composites in the early sixties [4]. This growth has largely been the result of a desire to apply these high strength and high modulus but light weight materials in air transportation systems. While the investigation and prediction of the elastic behaviour of these materials are fairly well documented and understood, their inelastic behaviour has presented engineers with some very challenging problems. For instance, prediction of failure in some particular analysis has proved to be particularly difficult. Over the past years, technological progress has continued quietly and unspectacularly to improve the physical properties of these composites and equally important, also to improve the understanding of how they may be used to the greatest effect. There has been extensive research into the behaviour of composite materials under realistic environmental conditions (corrosive environments, vibrational stress and extreme conditions of loading), and the nature of the complex stress fields that occur in such materials due to their configurations, loading conditions and internal physical structure [5].

## 2.2 Progress in cement matrix and fibre reinforcement

In recent years considerable progress has been made in the undertaking of a brittle matrix reinforced by continuous fibres aligned in the direction of the applied load. The extension of this analysis to the case where fibres are discontinuous and non aligned led to the introduction of efficiency factors [19].

Details on metal fibre reinforcement in cement matrix already exist and can be found in literature. Other reinforcement with artificial fibres such as polypropylene, carbon and glass have been considered extensively [20]. Literature on natural fibres eg. asbestos, which formed the pioneering work on fibre cements, and the current pre-occupation on other fibres eg. sisal, jute and coir is also widely available [21].

The work of Biryukovich et al [22] in the USSR, made it evident that glass fibres in the  $\text{Na}_2\text{O-SiO}_2\text{-ZrO}_2$  systems resisted the alkaline nature of portland cement, and the resulting composite was suitable for building applications. Pilkington Brothers Limited, [23], developed another alkali resistant glass fibre generation for the same application. Other glass composition considered suitable for cement reinforcement have been published in the patent literature at the Building Research Establishment (BRE) [24].

The effect of fibre reinforcement on other physical properties

Fibres added to the brittle cement matrix function so as to inhibit crack propagation, increase both tensile strength and

fracture energy and provide a degree of ductility in the behaviour of the material. The mechanism of energy absorption in cement composites have been shown to take place via fibre pull out and multiple cracking. The fibre pull out mechanism has greatly been studied and was first demonstrated by Kelly [25], who introduced the concept of critical length, on which complete stress transfer is assumed to take place. There was a progressive diminution of the load, giving the structure of Oakley and Proctor [26], while investigating the nature of cement-fibre bond strength, and fibre pull-out load, have demonstrated that majority of the fibre strands break before pulling out. In such circumstances, frictional forces play a big role in maintaining a very high proportion of the strand fracture. Fibre pull-out has further been studied by Nair [27], whose findings consequently led to other effects related to fibre pull-out. Among these effects are the substantial increase in the work of fracture, and the observed phenomenon of multiple cracking leading to a marked degree of pseudo-ductility, and the increased capacity to energy absorption during failure. Further investigations on fibre pull-out in aligned discontinuous fibre cement composites have revealed that for a multiple cracked system, this takes place at a single crack when the crack spacing is small compared with the fibre length [28].

The effect of fibre reinforcement on other physical properties of cement composites has not gone un-noticed. Parameswaran and Rajagopalan [29] observed that the phenomenon of fibre



pull-out was common with chopped fibre reinforced cement beams tested in flexure. In this case they noticed that the beams failed by fibre pull-out mode, with a single crack traversing straight through, up to the neutral axis of the beam at the cracking load of the matrix. Similar results were obtained by Swift and Smith [30], who, in addition observed that as the fibres gradually pulled out of the matrix, there was a progressive diminution of the load, giving the structure of superior post-cracking ductility and energy absorption.

To fracture fibre interfaces, a lot of energy is absorbed by fibres. A number of different energy absorbing mechanisms with various corresponding formulations have been proposed [31]. These are matrix fracture, fibre fracture, bond failure and fibre pull-out accounting differently in different materials for the total fracture toughness of the composite. The energy absorbed as the matrix fractures however depends on the volume fraction of the material. Cooper and Kelly [24], and Dharan [33], have proposed equations to predict the energy to deform a unit volume of matrix to failure and that required to debond the fibres respectively. The relative magnitudes of energy absorbing mechanisms vary in different composites depending on the mode of fracture which they have shown also to depend on the interfacial bond properties.

The following energy absorbing mechanisms have been proposed:  
 (i) Energy absorbed by the composite during fracture [32].

$$G_m = \frac{V_m^2 \sigma_m r U_m}{2 V_f \tau_s} \dots [2.1]$$

where  $U_m$  is the work done to deform a unit volume of matrix to failure and  $\tau_s$  is the shear stress.

(ii) The energy absorbed due to debonding of the fibres [33].

$$G = \frac{\sigma_f^2 r}{2 V_f E_f \tau_s} \left[ \frac{\sigma_f}{V_f} - \frac{(4 \tau E_f)^{\frac{1}{2}}}{r} \right] \dots [2.2]$$

where  $\tau$  is the bond strength

(iii) The work done in fracturing the fibres [34].

$$G = \frac{V_f \sigma_f^2 l_c}{6 E_f} \dots [2.3]$$

(iv) The energy absorbed due to pull-out of the fibres [33]

$$G = \frac{l_c V_f \tau l_c^2}{24 l r} \dots [2.4(a)]$$

for  $l > l_c$ , and

$$G = \frac{V_f \tau l^2}{24 r} \dots [2.4(b)]$$

for  $l < l_c$

Laws [35], working on fibre cement composites has shown that due to the tendency of the fibres to pull-out of the matrix, the maximum stress that the composite can carry is unlikely to be reached because the average length of the slipping fibres embedded into the matrix progressively decreases as they pull out from the matrix.

The flexural strength of cement base composite materials are improved considerably by the addition of uniformly distributed and randomly oriented short fibres. The findings of Swift and Smith [36] in their preliminary evaluation of the behaviour of sisal-cement composite materials, using parallel aligned fibres show an improved flexure strength up to 7% by volume of fibres, above which the composite strength decreased. Suitable choice of fibre length, content and mix preparation gave remarkable improvements in flexure strength by a factor exceeding three [36]. Other values have been reported by Majumdar [37] and later backed by Hannant et al [38].

Multiple cracking phenomenon reported by Kelly and Zweben [39] allows for strength increase in hardened cement matrix if the fibre Poisson's ratio is not unfavourable for this effect. They argue that the negative effect is eliminated by presence of shrinkage stresses and fibre surface asperities.

Others [40,41,42] have reported mechanical properties of cement mortar reinforced with various natural fibres to

achieve improved strength attaining their maxima at a fibre volume fraction of 8%.

However, direct tension method is seldomly used due to the The undertaking to evaluate tensile strength of cementitious specimens has previously been computed from splitting tensile strength using the formula derived from the theory of elasticity [43]. The cylinder specimen is loaded as shown in Figure 2.1, and the tensile strength calculated from the formula below [44].

$$\sigma_s = \frac{2P}{\pi l d} \quad \dots[2.5]$$

where

$\sigma_s$  = splitting tensile strength

P = maximum applied load

l = length of cylinder specimen

d = diameter of cylinder

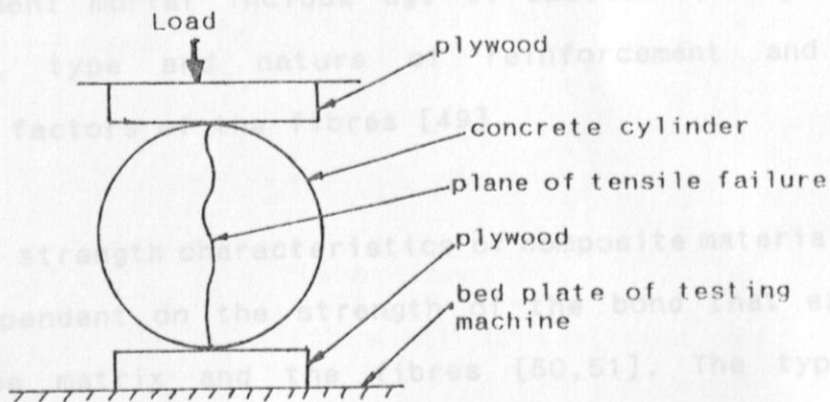


Figure 2.1: Splitting tension test arrangement for loading concrete specimens.

The tensile strength obtained using this method is usually 15% higher than that obtained through direct tensile loading. However, direct tension method is seldomly used due to the uncertainties of achieving uniform grip by the holding mechanism without introducing secondary stresses at the grip. It is also quite difficult to fabricate specimens to suit the testing arrangement for direct tension test.

Various researchers [45,46] have attempted to perform direct tensile test on cement and concrete specimens, although these have presented severe limitations due to the above factors and also the tendency to introduce different strain rates at different sections of the specimen. Allen [47], and Hannant et al [48] have reported encouraging increases in the first crack and ultimate tensile strength of the cement mortar composite resulting from additions of adequate volumes of fibre into the matrix. Other effects found to influence the tensile strength of the cement mortar include age of specimens, degree of compaction, type and nature of reinforcement and the efficiency factors of the fibres [49].

The general strength characteristics of composite materials is greatly dependent on the strength of the bond that exist between the matrix and the fibres [50,51]. The type of fracture surface is a good indicator of the type of bond at the interface, as the variation in the bond strength result in distinctively different fracture surfaces as shown in Figure 2.2 [52].

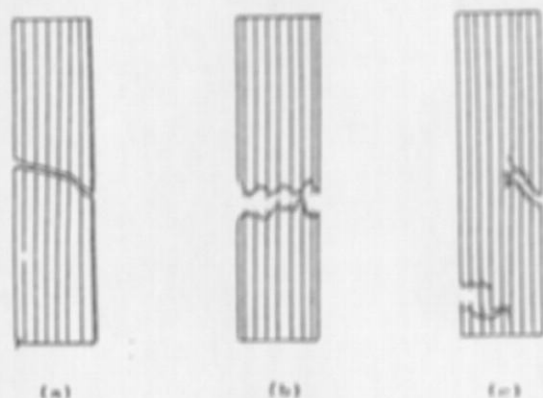


Figure 2.2: Different composite fractures depicting different interfacial bond strength  
 (a) specimen with strong bond.  
 (b) specimen with intermediate bond strength.  
 (c) specimen with poor bond strength.

Various techniques have been applied with a view to evaluating the strength of a fibre-matrix bond.

(a) The critical length ( $l_c$ ) method [50], Figure 2.2(a) is suitable for very thin, high bond strength composites. It yielded the average value of bond strength

$$\tau = \frac{d_f \sigma_{fu}}{4 l_c} \quad \dots[2.6]$$

where

$d_f$  = fibre diameter

$\sigma_{fu}$  = fibre ultimate strength

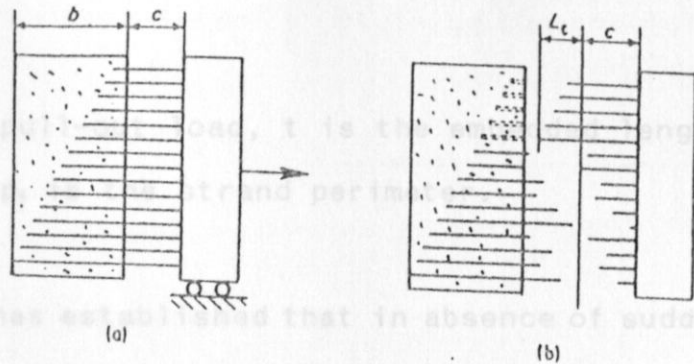


Figure 2.3: Critical length ( $l_c$ ) method for measuring interfacial bond strength.  
 (a) before pull-out.  
 (b) after pull-out.

(b) Direct pull-out method [50], Figure 2.4, is only used when the fibre critical length ( $l_c$ ) exceeds the thickness of the specimen ( $b$  in Figure 2.4). The average bond strength, determined from the pull-out load and the specimen geometry dimensions has yielded the following equation;

$$\tau = \frac{F}{\pi d_f b} \quad \dots[2.7]$$

Figure 2.4: Measurement of interfacial bond strength by direct pull-out method.

(c) The strand perimeter technique [26], Figure 2.5, is applied to determine the bond strength of fibres with high yield stress, such as steel and glass rods in single filament pull-out. If the bond between fibre and matrix is frictional in nature, the shear stress along the fibre in a pull-out test is constant, and equal to the bond strength. The bond strength is evaluated as;

$$\tau = \frac{F}{t p_f} \dots [2.8]$$

Where  $F$  is the pull-out load,  $t$  is the embedded length (disc thickness) and  $p_f$  is the strand perimeter.

This technique has established that in absence of sudden fibre fracture, the pull-out load increases linearly with the embedded length until the fibre failure stress is reached. At this stage, fibres then fracture before pull-out occurs and the failure load is constant.

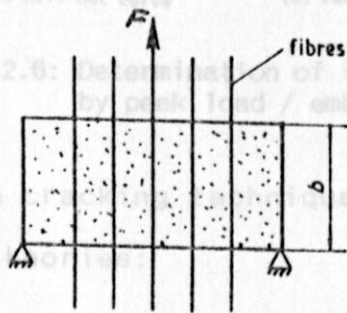


Figure 2.4: Measurement of interfacial bond strength by direct pull-out method.

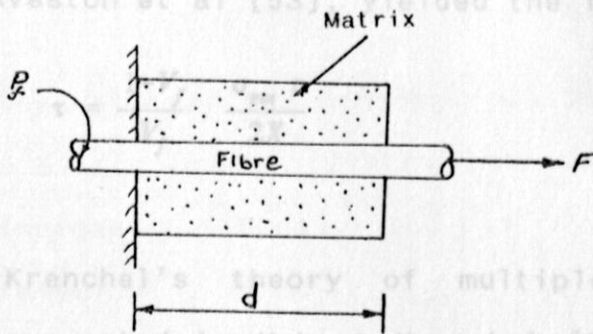
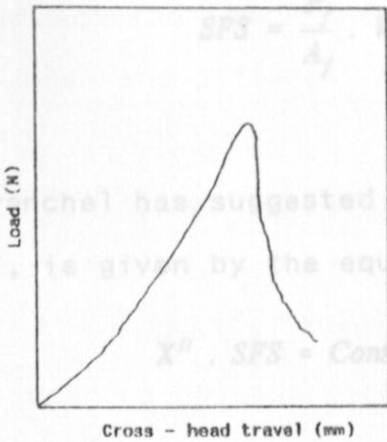


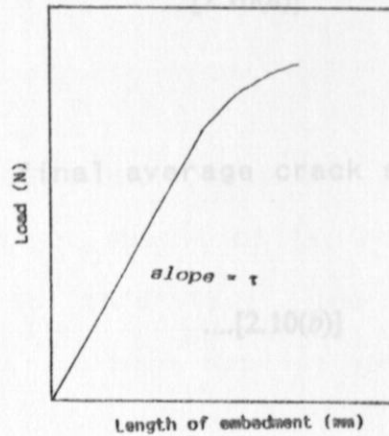
Figure 2.5: The strand perimeter technique of measuring interfacial bond strength.



(d) The peak load versus embedment depth plot curve method [26] depicted in Figure 2.6 has been used to measure the bond strength calculated by obtaining the initial slope of the curve.



(a) Multiple fibre - strand pull out curve



(b) Peak load versus length of embedment curve

Figure 2.6: Determination of interfacial bond strength by peak load / embedment depth curve method.

(e) The multiple cracking technique, has been split into two applicable theories:

(i) The interfacial crack spacing theory, introduced by Aveston et al [53], yielded the following equation;

$$\tau = \frac{1-V_f}{V_f} \cdot \frac{\sigma_{mu} r}{2X} \quad \dots[2.9]$$

(ii) Krenchel's theory of multiple cracking was suggested by Herbert Krenchel [54]. This approach uses the specific fibre surface, SFS, final crack

spacing and a constant in evaluating the bond strength.

In this theory, it has been shown that;

$$SFS = \frac{P_f}{A_f} \cdot V_f \quad \dots[2.10(a)]$$

Krenchel has suggested that the final average crack spacing,  $X''$ , is given by the equation;

$$X'' \cdot SFS = Constant \quad \dots[2.10(b)]$$

$$\tau = \frac{Constant}{\sigma_{ms} \cdot V_m} \quad \dots[2.10(c)]$$

In fact, the Krenchel's equation has been related to Aveston's equation as:

$$X'' \cdot \frac{V_f P_f}{A_f} = \frac{\sigma_{ms} V_m}{\tau} \quad \dots[2.10(d)]$$

The value of the constant has been reported to be 2.5 (for organic fibres) and close to unity (for inorganic fibres), and is evaluated from the relation:

$$\text{Constant} = X'' \cdot V_f P_f$$

....[2.10(e)]

It has been argued that the constant cannot be a universal one because the fibre - matrix bond strength varies for individual fibres and different matrices.

The Aveston et al's equation, takes account of fibre orientation, a factor which is not specifically included in the Krenchel's theory. Due to this fact, the equation therefore becomes more practical in most applications.

Most test reported on fibre cement bond strength have been conducted on steel and glass fibres because the conventional established methods [55] have been proved unsuitable for thin flexible synthetic and natural fibres. This is due to the difficulties in putting the fibres in the matrix in the prescribed manner. The interfacial bond strength in fibre cements has been found to be influenced by the curing conditions, and in most cases of fibre cements encountered the bond strength has been found to improve with age. Some values of fibre-matrix bond strength are given in Table 2.1. Low bond strength has been associated with large impact resistance of the composite, and poor tensile strength, (and for a good bond the converse applies). More practical results of bond strengths have been achieved by reinforcing cement based fibre composites with mixtures of fibres forming good and poor bond respectively [55].

### 2.3 The mechanical properties

The law of mixtures [10] has been applied accurately to predict the Modulus of Elasticity of a composite by considering a unit matrix reinforced with uniaxially aligned long fibres, Figure 2.1

Fibre	Matrix	Bond strength (N/mm <sup>2</sup> )	Age at testing (days)
Alkali resistant glass rod	Cement paste	5	3
'Cem - Fil' glass fibre	Cement paste	2 - 3	28
Steel fibre	Cement paste	6.8 - 8.3	14
Asbestos	Cement paste	0.88 - 3	-
Steel fibre	Cement mortar	5.4	28
polypropylene monofilament	Cement paste	0.7 - 1.2	180
Polycrystalline Alumina rod	Cement paste	11.7	20

Table 2.1: Some values of measured bond strength for various fibre-cement combinations [55].

### 2.3 The mechanical properties

The law of mixtures [10] has been applied accurately to predict the Modulus of Elasticity and tensile strength of a composite by considering a unit matrix reinforced with uniaxially aligned long fibres, Figure 2.7.

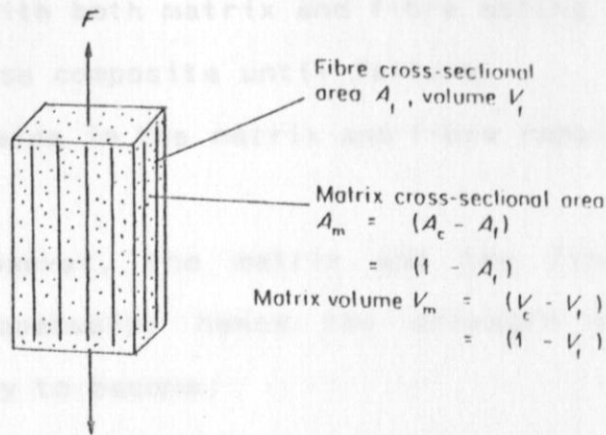


Figure 2.7: Aligned fibre composite tested in uniaxial tension.

This has resulted in the following equations for the composite Modulus of Elasticity and tensile strength:

$$E_c = E_f V_f + E_m (1 - V_f) \quad \dots [2.11(a)]$$

$$\sigma_c = \sigma_f V_f + \sigma_m (1 - V_f) \quad \dots [2.11(b)]$$

where the subscript c, f, and m represent composite, fibre and matrix respectively.

The two equations derived for tensile load depend only on the volume fraction of the constituents, and are subject to two major assumptions;

(a) the load carried by the composite is the sum of the loads carried individually by the matrix and the fibre with both matrix and fibre acting together as two phase composite until failure.

(b) the strains in the matrix and fibre remain the same.

In practice, however, the matrix and the fibres do not fracture simultaneously; hence the strength equation is modified slightly to become:

$$\sigma_c = \sigma_f V_f + \sigma_{ma} (1 - V_f) \quad \dots [2.12]$$

Where  $\sigma_{ma}$  represents the stress in the matrix at fracture strain of the fibres. This is a practical case where fibres fracture first as with the case of most thermoplastic materials.

In the case of brittle matrices (such as cementitious materials), the matrix fractures first at very low failure strains. Equation (2.11) for strength thus becomes [56];

$$\sigma_c = \sigma_{fa} V_f + \sigma_m (1 - V_f) \quad \dots [2.13]$$

Where  $\sigma_{fa}$  is the stress in the fibre at failure strain of the matrix.

The above equation is valid if the fibre volume fraction is greater than or equal to a minimum volume fraction [57]. i.e.

$$V_f \geq V_{min} \dots [2.14]$$

The minimum volume fraction is given by:

$$V_{min} = \frac{(\sigma_{mu} - \sigma_{ma})}{(\sigma_f + \sigma_{mu} - \sigma_{ma})} \dots [2.15]$$

Figure 2.8 Graphical representation of equation (2.11) and the position of the critical fibre volume.

Where  $\sigma_{mu}$  is the ultimate tensile strength of the matrix.

And for strengthening to take place, the fibre reinforcement volume fraction must be equal to or greater than the critical volume fraction [56]. i.e.

$$V_f \geq V_{cr} \dots [2.16]$$

Figure 2.8 gives a graphical representation of the position of  $V_{cr}$  in relation to equation 2.11 (b).

If the tensile strength of the matrix is less than that of the matrix, the critical volume fraction is evaluated from [56,58]

$$V_{cr} = \frac{(\sigma_{mu} - \sigma_{ma})}{(\sigma_f - \sigma_{ma})} \dots [2.17]$$

The critical fibre volume fraction is important in the strengthening of a composite as it allows a shift in its load-extension behaviour in Figure 2.9 from (a) to (b).

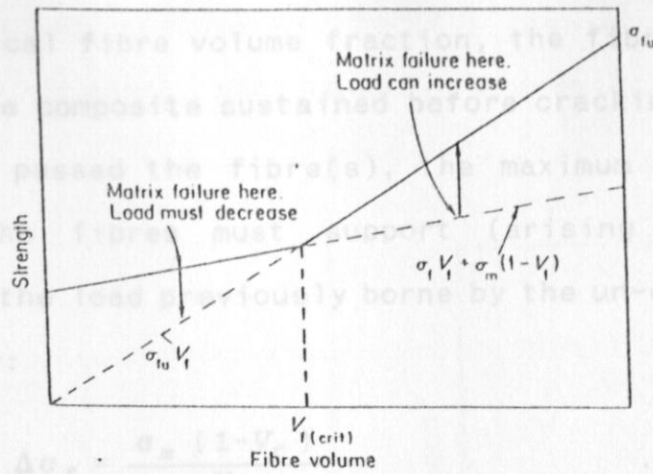


Figure 2.8: Graphical representation of equation [2.11] and the position of the critical fibre volume.

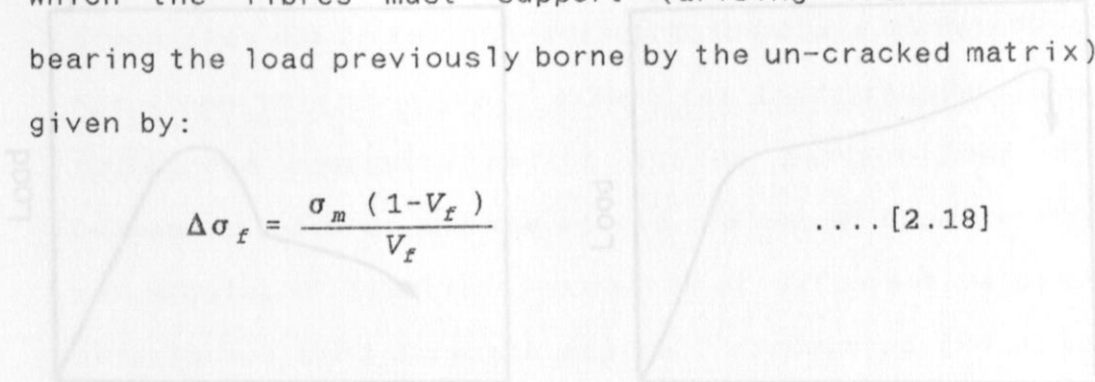
It can be seen in Figure 2.8 that the slope of the line  $\sigma_{fu}V_f$  greatly affect the intersection point at which the critical fibre volume for strengthening in direct tension occurs. Hence for the fibres which pull out at failure, the bond strength is the controlling influence on  $V_{cf}$ . It is also apparent from the Figure that the strength of the composite, where the critical volume fraction is exceeded is given by  $\sigma_{fu}V_f$  where  $\sigma_{fu}$  is the stress either at break or pull out of the fibres. At composite fracture when the fibre fracture strain is less than that of the matrix, the critical volume fraction is evaluated from [58,59]

$$V_{cr} = \frac{(\sigma_{mu} - \sigma_{ma})}{(\sigma_f - \sigma_{ma})} \dots [2.17]$$

The influence on the behaviour of a composite by the critical fibre volume fraction on flexural loaded beams has been studied extensively by [60]. The critical fibre volume fraction is important in the strengthening of a composite as it allows a shift in its load-extension behaviour in Figure 2.9 from (a) to (b).



At critical fibre volume fraction, the fibres carry the load which the composite sustained before cracking. When the crack tip has passed the fibre(s), the maximum additional stress which the fibres must support (arising from the fibres bearing the load previously borne by the un-cracked matrix) is given by:



$$\Delta\sigma_f = \frac{\sigma_m (1 - V_f)}{V_f}$$

.... [2.18]

At this stage, the fibres undergo an addition extension upon cracking of the matrix whose magnitude is given by:

$$\Delta e_f = e_{mu} \cdot \frac{(E_m V_m)}{(E_f V_f)} \quad \dots [2.19]$$

Figure 2.9: Stress-strain behaviour of a fibre reinforced composite.  
 (a) for  $V_f < V_{cr}$   
 (b) for  $V_f > V_{cr}$

Fibres may then pull out of the matrix if they are either;

- (i) Short ie.  $l_f < l_c$
- (ii)  $E_f V_f$  is much less than  $E_m V_m$  so that the resultant extension of fibres is so large that the frictional forces between the fibres and the matrix is reduced to a very small value [3].

The influence on the behaviour of a composite by the critical fibre volume fraction on flexural loaded beams has been studied extensively by Kelly [3]. Kelly relates the behaviour of flexure beams in two situations shown in Figure 2.10, to the critical fibre volume, where for  $V_f > V_{cr}$ , the tensile loaded side fails with multiple cracking if the reinforcement

is aligned and continuous. For the case when  $V_f < V_{cr}$  or the fibres are short and randomly arranged, the composite behaviour is similar to Figure 2.10 (b).

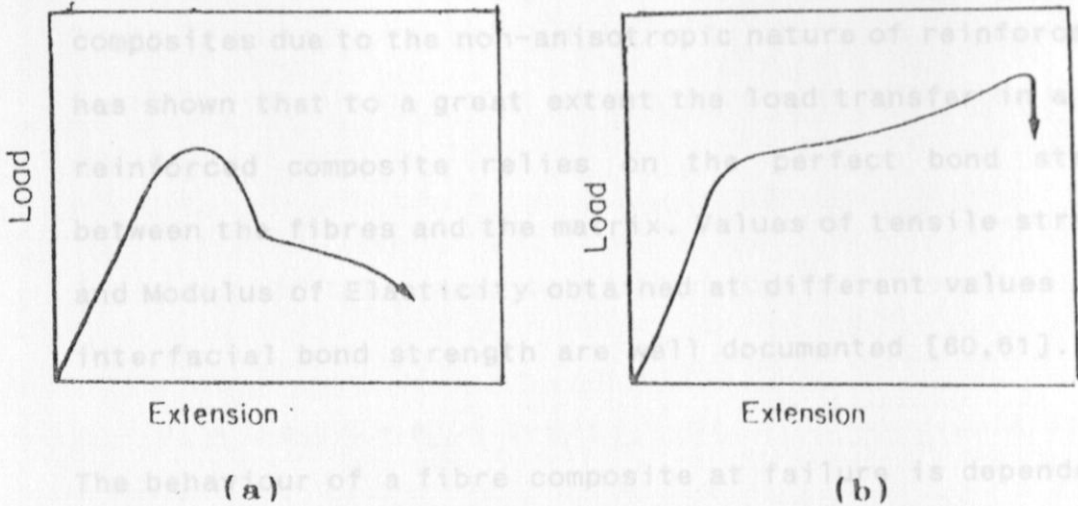


Figure 2.9: Strengthening behaviour of a fibre reinforced composite.

- (a) for  $V_f < V_{cr}$
- (b) for  $V_f > V_{cr}$ .

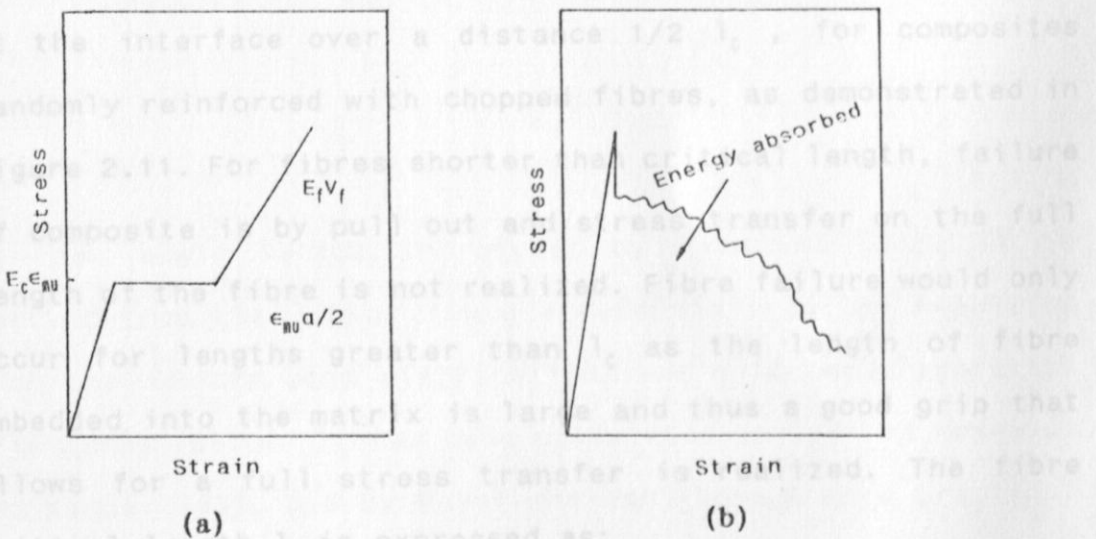


Figure 2.10: Influence on flexural behaviour of a fibre composite by the critical fibre volume.

- (a) continuous aligned fibres when  $V_f > V_{cr}$ .
- (b) short randomly aligned fibres when  $V_f < V_{cr}$ .

The extension of the law of mixtures to predict a composite strength and Modulus of Elasticity in the case of short fibres which find extensive application in fibre reinforced composites due to the non-anisotropic nature of reinforcement, has shown that to a great extent the load transfer in a fibre reinforced composite relies on the perfect bond strength between the fibres and the matrix. Values of tensile strengths and Modulus of Elasticity obtained at different values of the interfacial bond strength are well documented [60,61].

$$\sigma_c = C \sigma_f V_f + \sigma_m (1 - V_f) \quad \dots (2.21)$$

The behaviour of a fibre composite at failure is dependent on stress transfer between the matrix and the fibres. The complete stress transfer is only realized when the fibre length equals the critical fibre length [62]. In that state the load is transferred from the matrix to the fibre by shear at the interface over a distance  $1/2 l_c$ , for composites randomly reinforced with chopped fibres, as demonstrated in Figure 2.11. For fibres shorter than critical length, failure of composite is by pull out and stress transfer on the full length of the fibre is not realized. Fibre failure would only occur for lengths greater than  $l_c$  as the length of fibre embedded into the matrix is large and thus a good grip that allows for a full stress transfer is realized. The fibre critical length  $l_c$  is expressed as:

$$l_c = \frac{\sigma_f d}{2 \tau} \dots [2.20]$$

Where  $l_c$  is the critical length,  $d$  is the fibre diameter, and  $\tau$  is the interfacial bond strength between the fibre and the matrix.

The stress in the composite at fibre critical length is given by:

$$\sigma_c = C \sigma_f V_f + \sigma_{mi} (1 - V_f) \dots [2.21]$$

To deal with the more practical cases of discontinuous fibres randomly arranged in fibre cements and concretes, the concept of efficiency factors for orientation and length was introduced by Krenchel [55], to estimate how efficient discontinuous random fibres are as reinforcement in comparison with the case of continuous parallel aligned reinforcement.

$$C = \eta \left[ 1 - \frac{l_c}{2l} \right] \dots [2.22]$$

and

$$\left[ 1 - \frac{l_c}{2l} \right]$$

#### 2.4.1 Fibre orientation efficiency factor

$\eta$  is the length factor introduced by Krenchel [56]. It is derived from the linear fibre stress distribution resulting from the uniform bond distribution, and  $\eta$  is the orientation efficiency factor. It has been calculated as 0.41 by Romaul and Mandel [63], 0.5 by Parmi and Rao [64]. A more practical value of 0.637 has been given by the latter researchers.

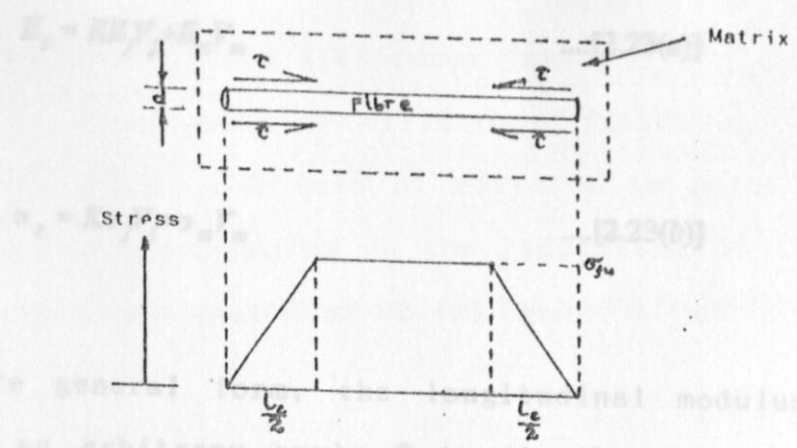


Figure 2.11: Stress distribution of a fibre in a matrix.

## 2.4 Efficiency factors

To deal with the more practical cases of discontinuous fibres randomly arranged in fibre cements and concretes, the concept of efficiency factors for orientation and length was introduced by Krenchel [55], to estimate how efficient discontinuous random fibres are as reinforcement in comparison with the case of continuous parallel aligned reinforcement.

### 2.4.1 Fibre orientation efficiency factor

For uni-directional composites, Tsai [65] uses a misalignment factor  $K$ , to correct for non-parallelism of fibres where  $K < 1$  such that the equation 2.11 derived from rule of mixtures is modified to:

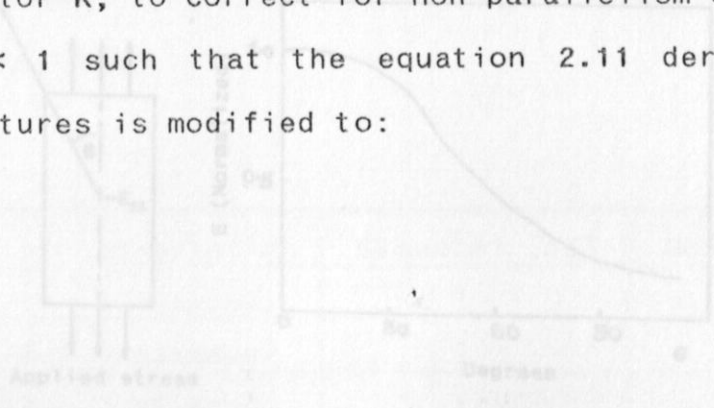


Figure 2.12: Variation of composite modulus with angle between applied stress and principal fibre direction.

$$E_c = KE_f V_f + E_m V_m \quad \dots[2.23(a)]$$

$$\sigma_c = K\sigma_f V_f + \sigma_m V_m \quad \dots[2.23(b)]$$

For a more general form, the longitudinal modulus and stress at an arbitrary angle  $\theta$  to the fibre direction, Nielson [66] has given the following equation:

$$\frac{1}{E_c} = \frac{\cos^4\theta}{E_{11}} + \frac{\sin^4\theta}{E_{22}} + \left[ \frac{1}{G_{12}} - \frac{2\nu_{12}}{E_{11}} \right] \cos^2\theta \sin^2\theta \quad \dots[2.24(a)]$$

$$\frac{1}{\sigma_c} = \frac{\cos^4\theta}{\sigma_{11}} + \frac{\sin^4\theta}{\sigma_{22}} + \left[ \frac{1}{\tau_{12}} - \frac{2\nu_{12}}{\sigma_{11}} \right] \cos^2\theta \sin^2\theta \quad \dots[2.24(b)]$$

Figure 2.12 shows the resulting variation of tensile Modulus of Elasticity with the angle between the applied stress and the principal fibre direction.

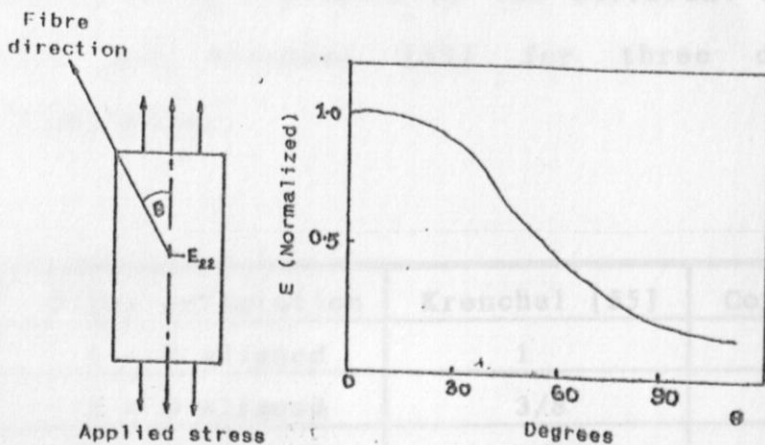


Figure 2.12: Variation of composite tensile Elasticity with angle between stress and principal fibre direction.

$$E_c = KE_f V_f + E_m V_m \quad \dots[2.23(a)]$$

$$\sigma_c = K\sigma_f V_f + \sigma_m V_m \quad \dots[2.23(b)]$$

For a more general form, the longitudinal modulus and stress at an arbitrary angle  $\theta$  to the fibre direction, Nielson [66] has given the following equation:

$$\frac{1}{E_c} = \frac{\cos^4\theta}{E_{11}} + \frac{\sin^4\theta}{E_{22}} + \left[ \frac{1}{G_{12}} - \frac{2\nu_{12}}{E_{11}} \right] \cos^2\theta \sin^2\theta \quad \dots[2.24(a)]$$

$$\frac{1}{\sigma_c} = \frac{\cos^4\theta}{\sigma_{11}} + \frac{\sin^4\theta}{\sigma_{22}} + \left[ \frac{1}{\tau_{12}} - \frac{2\nu_{12}}{\sigma_{11}} \right] \cos^2\theta \sin^2\theta \quad \dots[2.24(b)]$$

Figure 2.12 shows the resulting variation of tensile Modulus of Elasticity with the angle between the applied stress and the principal fibre direction.

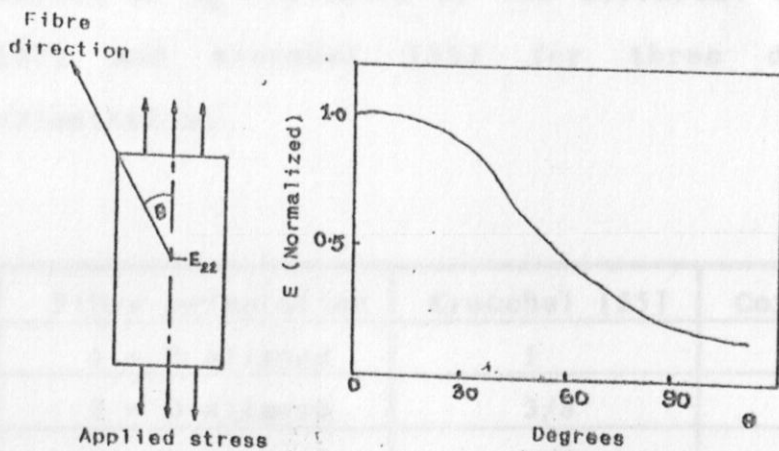


Figure 2.12: Variation of composite tensile Modulus of Elasticity with angle between applied stress and principal fibre direction.

### 2.4.2 Fibre randomness efficiency factor

COX [67], introduced an efficiency factor  $\eta_0$  into the equation derived from rule of mixtures to cater for the dependence of the modulus on the randomness of the fibre orientation, thus equations [2.11] become slightly modified to:

$$E_c = \eta_0 \eta_l E_f V_f + E_m [1 - V_f] \quad \dots[2.25(a)]$$

$$\sigma_c = \eta_0 \eta_l \sigma_f V_f + \sigma_m [1 - V_f] \quad \dots[2.25(b)]$$

He showed further that  $\eta_0$  took values of 1/3 and 1/6 for two and three dimensional fibre distributions respectively. However, it has been argued that the value of  $\eta_0$  for a given fibre orientation depends on the method of analysis used [66]. Table 2.13 gives a comparison of some typical values of  $\eta_0$  evaluated by two different researchers, Cox [67] and Krenchel [55] for three different fibre orientations.

Fibre orientation	Krenchel [55]	Cox [67]
1 - D Aligned	1	1
2 - D Aligned	3/8	1/3
3 - D Aligned	1/5	1/6

Table 2.2: Efficiency factors  $\eta_0$  for given fibre orientation relative to the direction of stress.



For a general case of planner fibre orientation, Krenchel [68] proposed that  $\eta_0$  be given the simple form;

$$\eta_0 = \frac{1}{2} \sum_{J=1}^M V_{fj} \cos^4 \theta_j \quad \dots [2.26]$$

where  $V_{fj}$  is the fibre volume fraction at an angle  $\theta$  to the principle axis, and M is the number of intervals in  $\theta$ .

#### 2.4.3 Fibre length efficiency factor

Allen [69] considered that for thin composites, apart from the efficiency factor  $\eta_0$  introduced by Cox, a second efficiency factor  $\eta_l$  was necessary where  $\eta_l$  depends on the fibre length. By incorporating this efficiency factor, the complete equation for the composite properties yields:

$$E_c = K\eta_0\eta_l E_f V_f + E_m [1 - V_f] \quad \dots [2.27(a)]$$

$$\sigma_c = K\eta_0\eta_l \sigma_f V_f + \sigma_m [1 - V_f] \quad \dots [2.27(b)]$$

The value of  $\eta_l$  is determined by the length of the fibre in relation to the critical length  $l_c$ .

The values of  $\eta_1$  given by Allen are;

3.1.1 The vibration table

$$\eta_1 = \frac{l}{2l_c} \dots [2.28(a)]$$

The vibration table consisted of a horizontal table, supported by for  $l_f < l_c$  springs, and mounted with an off-balance weight and The excitation motor was supplied from

$$\eta_1 = [1 - \frac{l}{2l_c}] \dots [2.28(b)]$$

When power is for  $l_f > l_c$  rotation of the motor excites the supporting springs, and owing to the presence of the out-of-

In the region before the matrix failure is reached, Laws [70] evaluated the value of  $\eta_1$  for aligned short fibre composite as 0.98 and proposed that it nearly approaches unity for most practical composites. The precise value of  $\eta_1$  is however not obtainable with accuracy because the critical fibre length is rarely known with any accuracy and will probably vary with age at test since the bond strength increases with age.

the cube mould, and a revolving shaft provided with an eccentricity. The set up of the machine is such that the revolving eccentric imparts an equal circular motion to all parts of the machine and mould, the motion being equivalent to equal vertical and horizontal simple harmonic vibration, 90° out of phase.

The drive is by means of an endless belt running on a crowned pulley on the motor, of synchronous type, and crowned pulley on the vibrator. The machine is equipped with mould clamp, hopper and mould supporting springs, and

### 3 EXPERIMENTAL DEVICES AND EXPERIMENTAL PROCEDURE

#### 3.1 experimental devices

##### 3.1.1 The vibration table

The vibration table consisted of a horizontal table, supported by compression springs, and mounted with an off-balance weight. The excitation motor was supplied from a 240 V mains supply.

When power is put on, the rotation of the motor excites the supporting springs, and owing to the presence of the out-of-balance weight, this combination causes vertical vibrations which are transmitted to the horizontal table via the supporting springs. The system was provided with a non-variable frequency amplitude control.

##### 3.1.2 The cube moulding machine

This consisted of a frame mounted on a coil spring to carry the cube mould, and a revolving shaft provided with an eccentricity. The set up of the machine is such that the revolving eccentric imparts an equal circular motion to all parts of the machine and mould, the motion being equivalent to equal vertical and horizontal simple harmonic vibration, 90° out of phase.

The drive is by means of an endless belt running on a crowned pulley on the motor, of synchronous type, and crowned pulley on the vibrator. The machine is equipped with mould clamp, hopper and mould supporting springs, and

had a normal running speed of eccentric shaft of 12000 r.p.m. The machine, in addition is provided with a timing mechanism that enables the selection of the duration of vibration. of the plates were roughed by spot welds.

### 3.1.3 The flexure test rig

The flexure test rig shown in Figure 3.1 was machined from a square cross-section bright mild steel piece to final dimensions of 115 mm width by 115 mm thickness and 520 mm length, according to BS 1881 part 118, 1983 [71]. The loading pins were turned on a lathe machine, and polished on a surface grinder to a final diameter of 20 mm.

The top plate measuring 20 mm thickness by 100 mm width and 200 mm length was machined out as shown in the same Figure, from bright mild steel piece. The slots on both the bottom rig and the top block were machined out on a horizontal milling machine. In order that point loading could be achieved on the top plate, a hemispherical slot for a 20 mm diameter steel ball was machined as shown on the top plate.

and changed. When in operation, the machine provides

### 3.1.4 The tensile test specimen grips

The difficulty in carrying out direct tensile testing is achieving a uniform stress distribution through out the test piece, without introducing stress concentration at the grips. To alleviate this problem, the gripping arrangement shown in Figure 3.2, suggested by Bessel and Mutuli [72] was fabricated.

The grips consisted of a square plate with four slots at 90° to each other. Through the slots, four vertical plates which form an open box section when in place were bolted. The inside of the plates were roughed by spot welds.

Before loading commences, the chart and crosshead speeds The instron machine pin was passed through the vertical pin of the grips at the top and bottom of the arrangement to secure it in the instron machine.

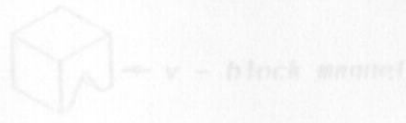
To calculate the strain in a test piece

### 3.1.5 The Instron universal testing machine

The 100 KN floor model available in the laboratory was used to test the specimens. This machine is made in such a way that several tests are possible under certain arrangements. These are; tensile, compression, flexure, and fatigue.

The machine incorporates a load cell designed to cover a specific test and range of loads. Load is applied by means of a moving crosshead which is operated by two vertical screws, powered by a main drive system. It is designed in such a way that a wide range of test speeds may be selected and changed. When in operation, the machine provides constant testing speeds through out the course of the test for all loads up to the capacity of the machine, while the rate of specimen extension remains constant through out the test. The strip chart , which is driven synchronously with respect to the crosshead records the extension of the test piece. Because of this synchronism, there is a correspondence between the individual motions of the chart

and crosshead, and the time axis of the chart becomes an accurate measure of the jaw positions and of the specimen extension.



Before loading commences, the chart and crosshead speeds are selected to give the desired magnification of the graph, and the machine calibrated by either dead weight for small load ranges or electronic calibration for high load ranges.

To calculate the strain in a test piece corresponding to a certain chart distance, the formula below is applied:

$$\text{Strain} = \frac{\text{Chart distance}}{\text{Magnification ratio} \times \text{gauge length}} \dots [3.1]$$

Where,

$$\text{Magnification ratio} = \frac{\text{Chart speed}}{\text{Loading speed}}$$

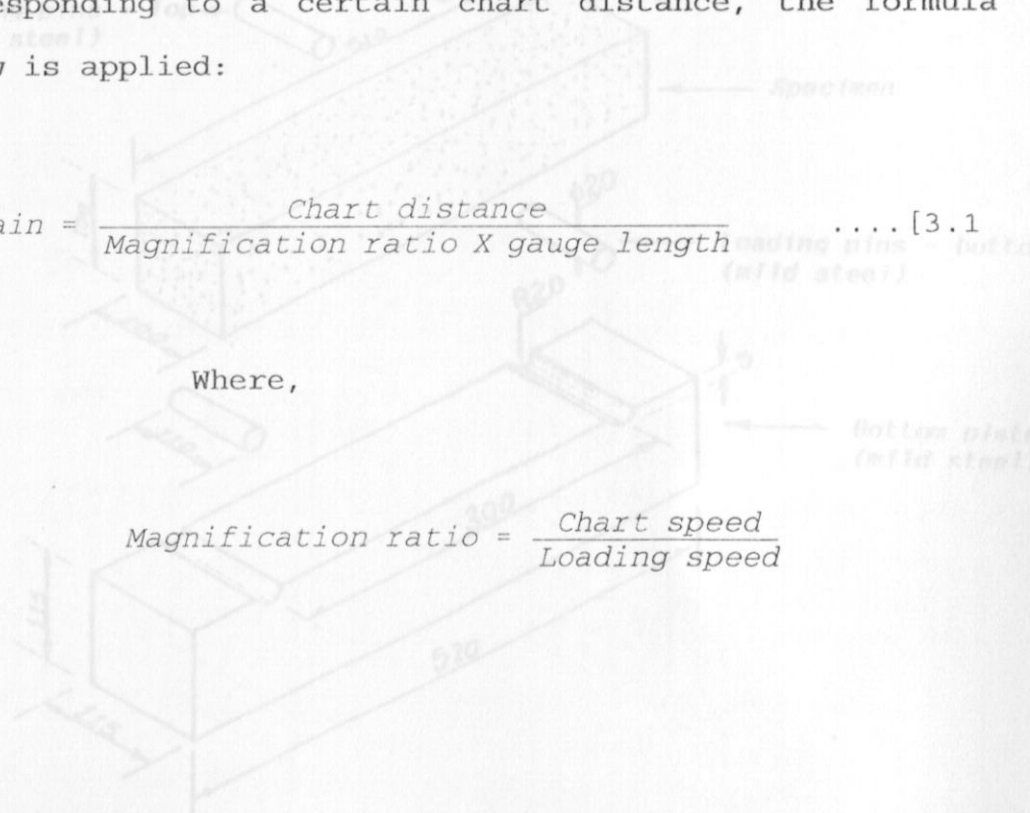


Figure 3.1: The flexure test rig showing the test arrangement (dimensions in mm).

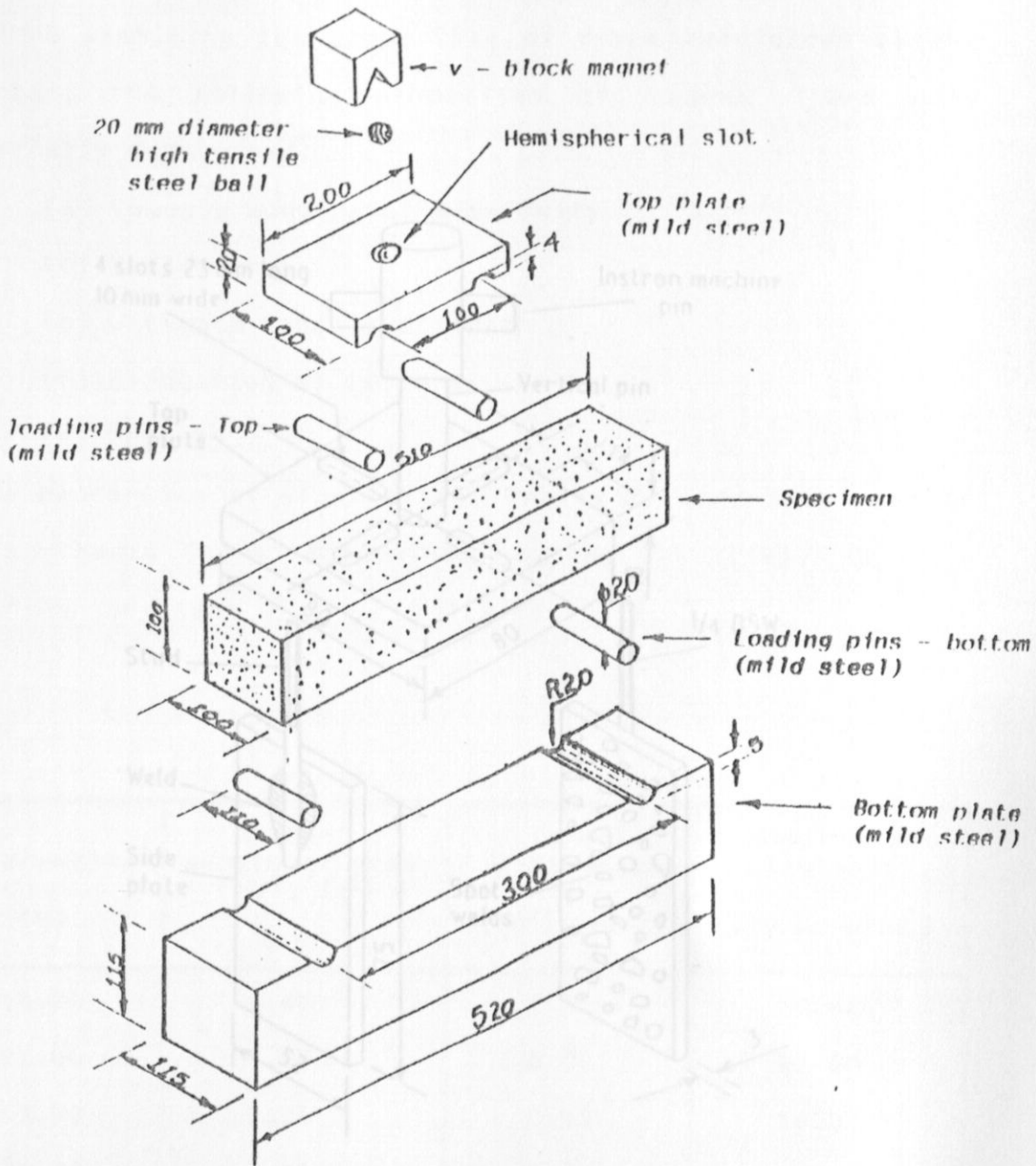


Figure 3.1: The flexure test rig showing the test arrangement (dimensions in mm).

### 3.2 Experimental procedure

#### 3.2.1 The experimental programme

##### 3.2.1.1 Reinforcing fibres

Before examining the properties of fibre reinforced cement mortar, the following properties of coconut fibre were initially determined.

##### (a) Young's Modulus of Elasticity

(b) 4 slots 23 mm long  
10 mm wide

(c) Ultimate tensile strength

(d) Elongation at failure

(e) Deformation

The properties of coconut fibre are given in Table 3.1 and 3.2, used in this thesis were obtained from [18]. Only a confirmatory test of

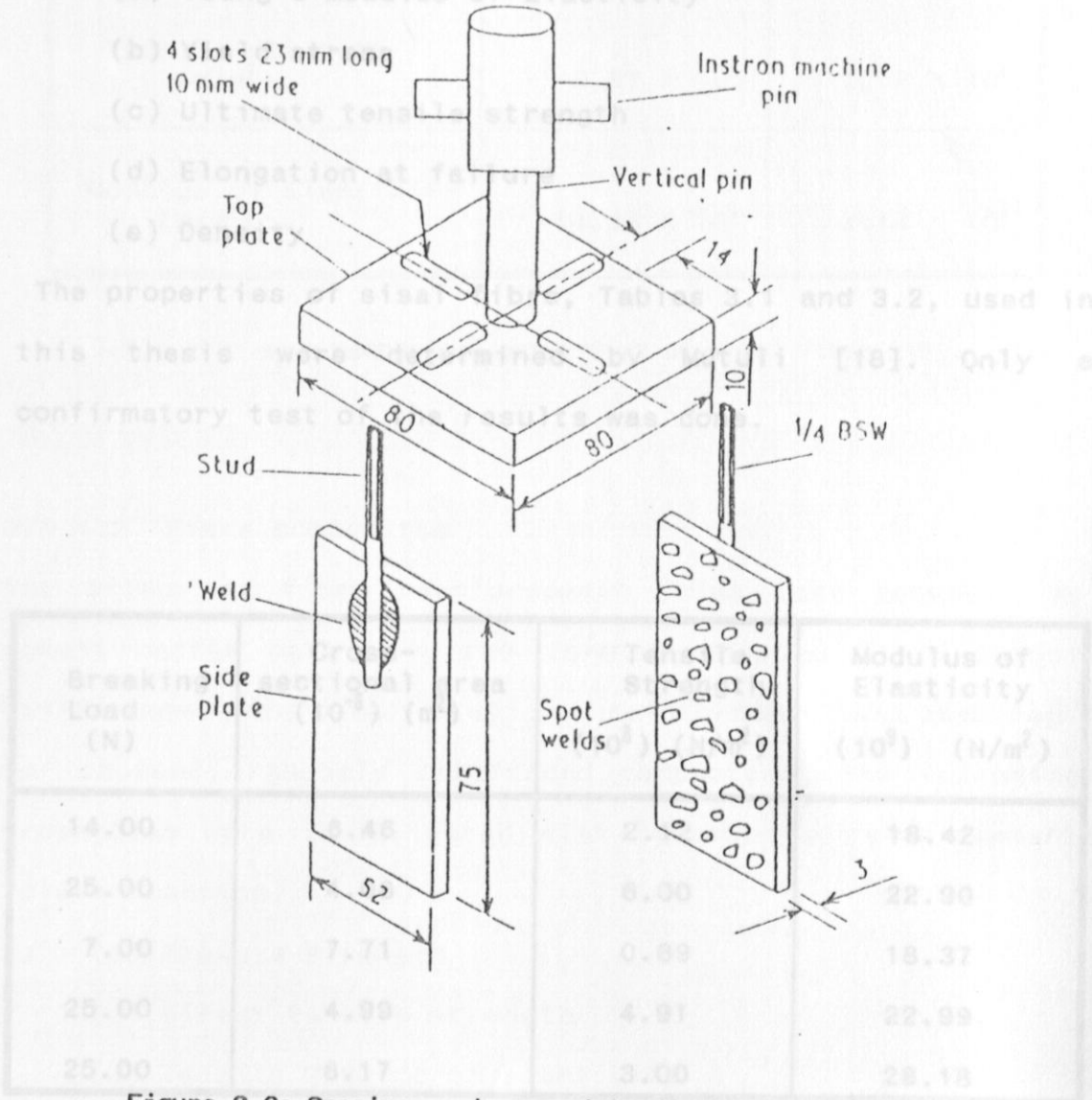


Figure 3.2: Specimen grips used in direct tensile test (dimensions in mm).

Table 3.1: Results of Tensile test on steel fibre [18].



## 3.2 Experimental procedure

### 3.2.1 The experimental programme

#### 3.2.1.1 Reinforcing fibres

Before examining the properties of fibre reinforced cement mortar, the following properties of coconut fibre were initially determined.

(a) Young's Modulus of Elasticity

(b) Yield stress

(c) Ultimate tensile strength

(d) Elongation at failure

(e) Density

The properties of sisal fibre, Tables 3.1 and 3.2, used in this thesis were determined by Mutuli [18]. Only a confirmatory test of the results was done.

#### 3.2.1.2 Fibre composites

The effect of fibre reinforcement (sisal and coconut) in

Breaking Load (N)	Cross-sectional area ( $10^{-8}$ ) ( $m^2$ )	Tensile Strength ( $10^8$ ) ( $N/m^2$ )	Modulus of Elasticity ( $10^9$ ) ( $N/m^2$ )
14.00	6.46	2.12	18.42
25.00	4.08	6.00	22.90
7.00	7.71	0.89	18.37
25.00	4.99	4.91	22.99
25.00	8.17	3.00	28.18

(d) Void volume variation

(e) Density

Table 3.1: Results of Tensile test on sisal fibre [18].

	Mean	Standard Deviation
Cross-sectional area (m <sup>2</sup> )	4.95 X 10 <sup>-8</sup>	1.38 X 10 <sup>8</sup>
Tensile strength (N/m <sup>2</sup> )	3.47 X 10 <sup>8</sup>	1.18 X 10 <sup>8</sup>
Modulus of Elasticity (N/m <sup>2</sup> )	14.28 X 10 <sup>9</sup>	3.14 X 10 <sup>9</sup>

Table 3.2: some mechanical properties of sisal fibre [18].

### 3.2.1.2 Fibre composites

The effect of fibre reinforcement (sisal and coconut) in cement mortar matrix in the form of chopped fibre random reinforcement and parallel aligned reinforcement was examined. For chopped, randomly reinforced composites, the following properties were investigated with respect to reinforcement volume fraction.

- (a) Flexure strength
- (b) Direct tensile strength
- (c) Tensile Modulus of Elasticity
- (d) Void volume variation
- (e) Density

In the case of parallel aligned reinforcement, the properties investigated were; overall lengths of 350 mm and 510 mm for (a) Flexure strength specimens respectively. They were then (b) Direct tensile strength of varying masses between 5 g (c) Modulus of Elasticity were found to have retained the bark (d) fibre - matrix interfacial bond strength up to their parallelism.

### 3.2.2 Sample preparation

#### 3.2.2.1 coconut fibre for tensile test

Pieces of coconut fibre, obtained from slumberland mattress factory, Nairobi, were selected carefully, avoiding the ones defective and the branched. Since the cross section of the fibres was found to vary greatly with length, an attempt was made to include only those with certain degree of uniformity. A gauge length of 100 mm was marked on each fibre using writing ink. In order to achieve a true representative of the properties of coconut fibre, a sample size of 120 was used. This was done in laboratory air at normal atmospheric conditions.

#### 3.2.2.2 Chopped fibres

Small bundles of both coconut and grade 'UG' sisal fibres obtained from Taita Estates, Nairobi were chopped on a hand shearing machine. They were then hand sorted to ensure that all unsuitable pieces (for example those that retained the bark) were eliminated from the sample. The fibres were chopped to a final length of 20 mm, in line with what is used at the HRDU.

### 3.2.2.3 sisal fibre for parallel reinforcement

These were cut in bundles at overall lengths of 350 mm and 510 mm for tensile and flexure specimens respectively. They were then grouped and stored in bundles of varying masses between 5 g and 520 g. The fibres that were found to have retained the bark were removed, taking care not to disrupt their parallelism.

(parallelism) were tested for every fibre volume fraction considered) was calculated as:

### 3.2.3 The matrix constituents

The specimen preparation was based on the mixture constituent ratio used in the HRDU, for making roofing sheets and tiles.

The mixture ratio by weight is as follows:

Constituent	weight (Kg)
cement	2 3.160
sand	5 2.640
*water	1 1.000

\* The amount of water used is one litre.

This has been taken as 1 Kg assuming a density that would be of 1000 Kg/m<sup>3</sup>.

In the work of HRDU, 150 g of grade "UG", 20 mm chopped sisal fibres are added, and compacted for about 2 minutes to make either a roofing sheet or tile. In the foregoing work, the same mixture ratio by weight was used.

For one cubic metre of the mixture;

$$\begin{aligned} C &= (2.64 + (2.5 \times 3.16) + (0.5 \times 3.16 \times 2.64)) \\ &= 2.64 \times 3.16 \times 1000 \\ &= 567.08 \end{aligned}$$

### 3.2.4 Calculations

#### 3.2.4.1 The flexure beams

The fixed ratio of cement : sand : water by weight described in section 3.2.3 was maintained ie. 2 : 5 : 1. The flexural moulds measured 100 mm X 100 mm X 510 mm internal dimensions. The total volume in cubic metres for five moulds (five specimens were tested for every fibre volume fraction considered) was calculated as:

$$\begin{aligned} \text{Cement} &= 5(100 \times 100 \times 510) \times 10^{-9} \text{ m}^3 \\ \text{Sand} &= 0.0255 \text{ m}^3 \\ \text{Water} &= 0.0051 \text{ m}^3 \end{aligned}$$

The following specific gravities of the constituents were used

#### 3.2.4 constituent specific gravity

constituent	specific gravity
cement	3.160
sand	2.640
water	1.000

The mixture ratio was expressed into volumes of cement, that would be adequate to form one cubic metre of the dry mixture, ie.

ie. constituent requirement (Kg)

cement	2.56
2 sand	6.40
or C water	1/2 C
or C	0.5 C

For one cubic metre of the mixture;

$$\begin{aligned} \text{Cube} &= \{2.64 + (2.5 \times 3.16) + (0.5 \times 3.16 \times 2.64)\} \\ \text{dimension} &= 2.64 \times 3.16 \times 1000 \\ \text{calculated} &= 567.08 \end{aligned}$$

And hence  $S = 2.5 C = 1417.70$  in section 3.2.4.1, from which the quantity  $W = 0.5 C = 283.54$  the cube specimens were calculated. The total required volume of cement mortar is  $0.0255 \text{ m}^3$ , the following were the requirements by weight:

constituent	requirement (Kg)
cement	14.46
sand	36.15
water	7.23

**3.2.4.2 Tensile specimens**  
The internal dimensions of the tensile moulds were 50.8 mm X 50.8 mm X 350 mm. The total volume of five moulds worked out to be  $4.516 \times 10^{-3} \text{ m}^3$ . The requirement in specific constituents worked out to make one cubic metre of mortar as in section 3.2.4.1 yielded:

constituent	requirement (Kg)
cement	2.56
sand	6.40
water	1.28

**3.2.4.3 Cube specimens**  
Cube specimens were casted in standard moulds whose internal dimensions were 70.7 mm X 70.7 mm X 70.7 mm. The total volume calculated for three moulds worked out to be  $1.06 \text{ m}^3$

The mixture required to make one cubic metre of the cement mortar was worked out as in section 3.2.4.1, from which the quantity required for the cube specimens were calculated. The following constituents were obtained:

constituent	requirement (Kg)
cement	0.60
sand	1.50
water	0.30

Clean, internally oiled steel moulds mentioned in section 3.2.4.1 were placed on a small table vibrator described in

### 3.2.5 Specimen preparation

#### 3.2.5.1 Fresh mortar

Enough mortar to fill each mould was Ordinary earthly sand was vibrated through a series of screens to yield sand with a maximum particle size of 2 mm. To ensure uniform and controlled moisture content, the sand was dried in a kiln for 12 hours at 100 °C. The hot sand was spread in a tray and left for further 12 hours to cool to room temperature and atmospheric humidity.

Fresh cement mortar was prepared by mixing cement, sand and

water in the ratio 2:5:1 by weight as described in section 3.2.3.

The raw specimens were covered with polythene papers to

The cement used was ordinary portland cement from Athi River Portland Cement Factory, Kenya. Initial preparation of this involved pre-mixing weighed quantities of cement and sand for about one minute in a horizontal rotating counter-flow electric mixture. The mixing was continued for a further one

minute while a weighed quantity of water was continuously and slowly added. When all the water had been added, the electric mixture was switched off. All the un-mixed dry material clogged between the blades or pan surfaces was mixed by hand. The resulting cement mortar, by feel of hand was considered ready for use.

#### 3.2.5.2 Un-reinforced flexure test specimens

Clean, internally oiled steel moulds mentioned in section 3.2.4.1 were placed on a small table vibrator described in section 3.1.1, provided with a non variable frequency amplitude control unit. Enough mortar to fill each mould was weighed on a beam balance, and spread carefully into the moulds, compacting slowly each time with the edge of a mason trowel.

The mortar rich moulds were then vibrated for about two minutes, adding a little mortar each time and checking critically for any overflow. When compaction was over, the top surface of each specimen was finished off smoothly by use of a smooth trowel to the level of the mould.

The raw specimens were covered with polythene papers to control the rate of dehydration and stored in a fog room at 90 % Relative Humidity until de-moulding 24 hours later. On de-moulding, the specimens were properly covered with wet gunny cloths and left to set in the fog room, until testing 28 days later.



### 3.2.5.3 Chopped fibre reinforced flexure test beams

Chopped fibres from section 3.2.2.2 were weighed (to control the fibre volume fraction) on an electronic digital balance to two decimals of accuracy. A quantity of mortar to fill the mould was weighed, allowing for the volume to be occupied by the fibres. The fibres and mortar were thoroughly mixed in a wetted bucket, to eliminate possibilities of the bucket extracting water from the wet mix. The raw composite mix was spread carefully in the steel moulds mentioned in section 3.2.4.1, compacting slowly with the edge of the trowel. They were then vibrated for about two minutes in the table vibrator described in section 3.1.1, adding some mix slowly and checking keenly for any imminent spillage.

When the mix was fully compacted, the specimens were stored to cure under conditions described in section 3.2.5.2.

### 3.2.5.4 Parallel aligned reinforced flexure test beams

A little mortar was spread in the steel moulds described in section 3.2.4.1, and slightly vibrated to ensure a level surface. sisal fibre bunches which had been prepared and stored as described in section 3.2.2.3 were sub-divided into four small and equal portions. Each portion was spread carefully on the cement mortar in the mould, and more mortar added, each time vibrating slightly to ensure that each layer of fibres added lay parallel to the previous one. The system of additions of mortar and fibres adapted in this section ensured that each specimen contained four layers of equally

spaced fibres, and five equal layers of mortar, also equally spaced. The individual layers of each constituent weighed exactly the same as the other respectively.

Finally, the moulds were vibrated by the machine in section 3.1.1 for a duration of two minutes to compact the specimens, and expel the entrapped air. The specimens were then stored to cure under the conditions in section 3.2.5.2

#### **3.2.5.5 Tensile test specimens**

These were prepared in a similar fashion as the flexure test specimens. The moulds used to cast the specimens were those mentioned in section 3.2.4.2 which were manufactured for the purpose.

For the case of parallel reinforced specimens, three layers of fibres, of equal weight, and equally distributed in a four layer cement mortar matrix prepared in a similar manner as in section 3.2.5.4 were used. The layers of cement mortar were formed from equally weighed portions of raw mixture. The specimen were then cured as in section 3.2.5.2.

#### **3.2.5.6 Cube specimens**

The cube specimens for density and void volume variation tests were casted in the moulds mentioned in section 3.2.4.3. The moulds were assembled for use by covering the contact at the bottom of the moulds, and the base plates, with a thin film of petroleum jelly to ensure no water escaped during vibration.

The joints between the halves of the moulds, were similarly smeared with petroleum jelly to ensure they were water tight during the vibration period. The interior faces of the assembly were treated with a thin coating of mould oil to avoid sticking of the composite upon setting. The mould assembly was placed on the table of the vibration machine described in section 3.1.2, and firmly held in position by means of a clamp. A hopper was securely attached on the top of the mould to facilitate filling, and maintained in position until the vibration period was over.

Chopped fibres prepared as in section 3.2.2.2 and cement mortar prepared as in section 3.2.4.3 were mixed thoroughly in a wetted bucket. The chopped fibre - cement mortar mixture for each specimen was weighed and placed in the hopper. The timer was adjusted for a duration of two minutes, and the mixture vibrated at 12,000 vibrations per minute. The specimens were then stored to cure as described in section 3.2.5.2.

### 3.3 Mechanical testing

#### 3.3.1 coconut fibre

##### 3.3.1.1 Fibre tensile test

Fibre specimens (one at a time) were mounted on the Instron special fibre grips, and by adjusting the movable cross-head of the Instron machine, the grips separation were set at the selected fibre gauge length of 100 mm. The fibres were loaded on the pre-calibrated Instron machine at a cross-head speed of 2 cm/min. and a corresponding chart speed of 2 cm/min. A plot of load versus deflection to fracture was recorded automatically via the servodrives mechanism of the Instron machine. It accurately to four decimal places using an electronic balance. The volume was determined by immersing it in water. To measure the fibre cross-sectional area, a microscope fitted with a calibrated square graticule at the eye piece was used. The fibres were cut just below the fractured end using a surgical knife, and then mounted vertically on a plasticine, stuck on the microscope slide. The cross-section was viewed and the slide adjusted accordingly until the observed area lay enclosed by complete and fractions of the square graticule. The cross-sectional area was determined by counting and summing up the full squares and fractions of squares covered by the seen cross-section. The yield stress, and ultimate tensile stress were obtained by dividing the fibre yield load, and the fibre ultimate load (obtained from the load-deflection curve recorded by the Instron machine), with the cross-sectional area. The strains in the fibres were determined from equation 3.1 in section 3.1.5. The Modulus of

Elasticity was calculated from a plot of stress versus strain, derived from the load-deflection curve plotted by the Instron machine.

### 3.3.1.2 Fibre density

Archimedes principle was applied in the determination of the density of coconut fibre. This was done in two parts: In the first part, the density of known mass of plasticine in laboratory air at normal atmospheric conditions of temperature and humidity (ie. 22 °C and 65 RH) was determined. To accomplish this, the mass of the plasticine was determined by weighing it accurately to four decimal places using an electronic balance. The volume was determined by immersing it in a calibrated measuring cylinder with tap water at normal atmospheric conditions mentioned above. The volume of the plasticine equal, to the volume of water displaced was read off from the marked graduations on the measuring cylinder. The density of water was assumed to be 1000 Kg/m<sup>3</sup>. In part two, a known mass of chopped coconut fibres were embedded in the plasticine of part one, taking care that none of the fibres protruded above the surface of the plasticine. The procedure was repeated several times each time varying the quantity of the embedded fibres. The fibre density was calculated as follows:

$$\begin{aligned} \text{Mass of plasticine in air} &= W && \dots [3.3] \\ \text{Volume of water displaced} &= V_1 \\ \text{Mass of water displaced} &= W_1 \end{aligned}$$

Therefore density of plasticine,  $\rho_m$  and  $m$  represent fibre and matrix respectively, (the fibre being coconut and the matrix being plasticine).

$$\rho_m = \frac{W}{V_1} \dots [3.1]$$

3.3.2 Mass of embedded fibres =  $W_f$

3.3.2 Mass of plasticine with embedded fibres =  $W_2$

Flexure Volume of water displaced =  $V_2$  3.2.5.2 to 3.2.5.4

Mass of water displaced =  $W_3$  according to the British

But mass of plasticine with embedded fibres equals mass of plasticine plus mass of embedded fibres, i.e. 3.1.5, was

used together with the workshop fabricated flexure rig described in section 3.1.5. The experimental set up was as

depicted in Figure 3.3. Load was transferred to the

And volume of plasticine with embedded fibres equals volume of plasticine plus volume of embedded fibres, i.e. diameter

steel ball, held in position by a V-block magnet.

$$V_2 = V_m + V_f$$

The span used in the flexure test was 300 mm, the Instron cross-head speed of 2 cm/min and a chart speed of 5 cm/min.

The results of the flexure test were recorded graphically

by the strip chart.  $\rho_f$  ultimate flexural strength was

$$V_2 = \frac{W_f}{\rho_f} + \frac{W}{\rho_m} \dots [3.2]$$

measured in four point loading as:

And by rearranging,  $P = \frac{PL}{BD^2} \dots [3.4]$

$$\rho_f = \frac{W_f \rho_m}{\rho_m V_2 - W} \dots [3.3]$$

Where  $P$  is the ultimate flexural load recorded during the test and corrected for load due to the top plate and loading pins,  $L$  is the specimen span,  $B$  is the specimen

breadth and  $D$  is the specimen depth.

Where  $\rho_f$  is the density and the subscripts  $f$  and  $m$  represent fibre and matrix respectively, [the fibre being coconut and the matrix being plasticine].

### 3.3.2 Fibre composites

#### 3.3.2.1 Flexure test

Flexure specimens prepared in sections 3.2.5.2 to 3.2.5.4 were tested in four point bending according to the British Standards, BS 1881 part 118, 1981, [73]. The Instron universal testing machine mentioned in section 3.1.5, was used together with the workshop fabricated flexure rig described in section 3.1.3. The experimental set up was as depicted in Figure 3.3. Load was transferred to the specimens via the two pins shown on the same Figure. A point load was applied to the top plate by a 20 mm diameter steel ball, held in position by a V-block magnet.

The test specimens prepared as described in section 3.2.5.5 were secured in the test arrangement described in 3.1.4. The span used in the flexure test was 300 mm, the Instron cross-head speed of 2 cm/min and a chart speed of 5 cm/min. The results of the flexure test were recorded graphically by the strip chart. The ultimate flexural strength was measured in four point loading as:

$$\sigma = \frac{PL}{BD^2} \quad \dots[3.4]$$

Where  $P$  is the ultimate flexural load recorded during the test and corrected for load due to the top plate and loading pins,  $L$  is the specimen span,  $B$  is the specimen breadth and  $D$  is the specimen depth.

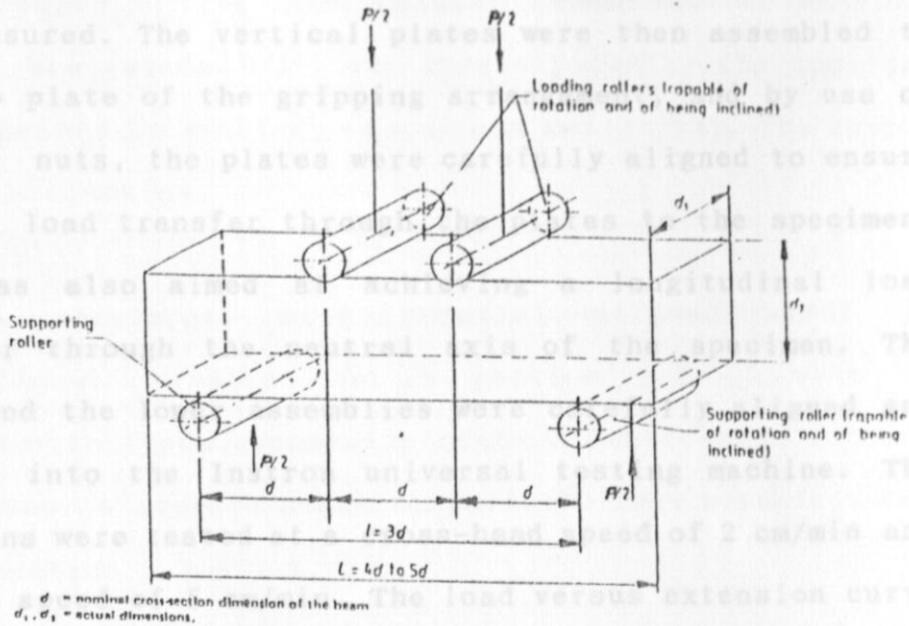


Figure 3.3 :Arrangement for loading flexure test pieces in four point bending [73].

### 3.3.2.2 Tensile test

The test specimens prepared as described in section 3.2.5.5 were secured in the test arrangement described in 3.1.4. First the faces to be gripped were serrated very lightly by use of a horizontal rotating fibre type stone cutter. "ISOPON" polyester paste, popularly known as car body filler, mixed with adequate hardener component to control its setting time was applied to the serrated surfaces of the specimens, and the glued faces were fastened to the four plates of the gripping arrangement. The plates were then held in place by small G-clamps, placed in a manner not to induce any stresses on the specimens owing to their gripping.



### 3.3.2.3 Interfacial bond strength

When the "Isopon" set, the gauge length of each specimen was measured. The vertical plates were then assembled to the top plate of the gripping arrangement, and by use of locking nuts, the plates were carefully aligned to ensure an even load transfer through the plates to the specimen.

This was also aimed at achieving a longitudinal load transfer through the neutral axis of the specimen. The upper and the lower assemblies were carefully aligned and mounted into the Instron universal testing machine. The specimens were tested at a cross-head speed of 2 cm/min and a chart speed of 5 cm/min. The load versus extension curve

was automatically recorded by the servodrive mechanism of the Instron machine. Five specimens for each fibre volume fraction chosen were tested. The ultimate tensile strength was determined from:

$$\sigma_{uts} = \frac{F}{A} \quad \dots[3.5]$$

Where  $F$  is the maximum load recorded by the Instron machine, and  $A$  is the initial cross-section area of the specimen.

The Young Modulus of Elasticity was computed by taking an incremental stress in the initial portion of the load-deflection curve, divided by the incremental strain. The incremental strain was calculated from equation 3.1 of section 3.1.5.

### 3.3.2.3 Interfacial bond strength & volume variation

The strength of the bond between cement mortar matrix and sisal fibre (grade "UG") was investigated by the application of the method by Aveston, Cooper and Kelly [53], the theory of multiple cracking. to remove the excess water. A digital

electronic balance was used to determine the mass of the Tensile specimens, with parallel aligned sisal fibre reinforcement prepared as in section 3.2.5.5 were first painted with three successive coats of white wash on all the four faces to improve crack visibility. They were then tested as in section 3.2.6.1.4. at fibre volume fractions. The average

amount of water absorbed at each fibre volume fraction was

At matrix failure, several cracks running perpendicular to the direction of load application appeared. The separation between individual cracks was measured in all the four faces to one place of decimal accuracy. The average crack separation in every face was calculated, and the averages of these were accordingly calculated. The interfacial bond strength,  $\tau$ , was calculated from equation 2.9 as:

Where  $w_p$  is the percentage water absorption value,  $w_d$  is the mass of saturated specimen and  $w_d$  is the mass of dry specimen

$$\tau = \frac{(1 - V_f) \cdot \sigma_{mm} \cdot r}{2 \cdot V_f \cdot X}$$

Where  $\tau$  is the interfacial bond strength in  $N/mm^2$ ,  $\sigma_{mm}$  is the ultimate tensile strength of the matrix,  $r = 0.126$  mm [18], is the average fibre radius and  $x$  is the average interfacial crack separation.

#### 3.3.2.4 Composite density and void volume variation

Oven dry specimens were immersed in a trough of clean tap water at ambient conditions for 24 hours. On removal from the trough, the saturated specimens were wiped slightly with a blotting paper to remove the excess water. A digital electronic balance was used to determine the mass of the saturated specimens. The saturated specimens were placed in an electric kiln and dried for 24 hours at 100 °C. They were then cooled for 12 hours at room temperature and humidity. The dry specimens were weighed again and the mass of each specimen determined for different fibre volume fractions. The average amount of water absorbed at each fibre volume fraction was calculated. The percentage water absorption value by weight was determined as follows:

$$w_a = \frac{[w_s - w_d]}{w_d} \cdot 100 \quad \dots[3.6]$$

Where  $w_a$  is the percentage water absorption value,  $w_s$  is the mass of saturated specimen and  $w_d$  is the mass of dry specimen.

The percentage void volume was determined according to ASTM C-220-75 [74], where the water absorption value was multiplied by the specimen density to yield the void volume value [42].

The results obtained for the density of coconut fibre tested in an indirect method as explained in section 3.2.6.1.2, are summarized in Table A1.1. A mean value of the fibre density of 0.53 g/cm<sup>3</sup> and a standard deviation of 0.02 g/cm<sup>3</sup> was obtained.

$$V_v \% = w_a \cdot \rho_c \quad \dots[3.7]$$

Where  $V_v$  is the void volume value and  $w_a$  and  $\rho_c$  are as determined above. The fibre density was seen to increase from 0.51 g/cm<sup>3</sup> to 0.56 g/cm<sup>3</sup> as the weight of fibre batches tested was decreased from 26.87 g to 14.40 g.

#### 4.1.2 Fibre tensile strength

The fibre tensile strength measured at atmospheric conditions in a laboratory air showed great variations as presented in Table A1.2. A mean value of the ultimate tensile strength of 159.30 N/mm<sup>2</sup> was obtained, as shown in Table A1.3, with the values varying greatly between individual fibres tested. The results indicate that the majority of the fibres tested had tensile strengths varying between 120 and 210 N/mm<sup>2</sup>. Few fibres gave fairly high tensile strengths with 322.45 N/mm<sup>2</sup> as the highest recorded value while others still gave low results - the lowest recorded value being 55.59 N/mm<sup>2</sup>.

The Modulus of Elasticity likewise showed quite a variation in the calculated results, see Table A1.2. These ranged from

## 4. EXPERIMENTAL RESULTS

### 4.1 coconut fibre

#### 4.1.1 Density of coconut fibre

The results obtained for the density of coconut fibre tested in an indirect method as explained in section 3.2.6.1.2. are summarized in Table A1.1. A mean value of the fibre density of  $0.53 \text{ g/cm}^3$  and a standard deviation of  $0.02 \text{ g/cm}^3$  was obtained. A substantial variation in the value of the density was seen between individual batches tested. The fibre density was seen to increase from  $0.51 \text{ g/cm}^3$  to  $0.56 \text{ g/cm}^3$  as the weight of fibre batches tested was decreased from 26.87 g to 14.40 g.

#### 4.1.2 Fibre tensile strength

The fibre tensile strength measured at atmospheric conditions in a laboratory air showed great variations as presented in Table A1.2. A mean value of the ultimate tensile strength of  $159.30 \text{ N/mm}^2$  was obtained, as shown in Table A1.3, with the values varying greatly between individual fibres tested. The results indicate that the majority of the fibres tested had tensile strengths varying between 120 and  $210 \text{ N/mm}^2$ . Few fibres gave fairly high tensile strengths with  $322.45 \text{ N/mm}^2$  as the highest recorded value while others still gave low results - the lowest recorded value being  $55.59 \text{ N/mm}^2$ .

The Modulus of Elasticity likewise showed quite a variation in the calculated results, see Table A1.2. These ranged from

1.21 GN/m<sup>2</sup> to 7.74 GN/m<sup>2</sup>. The results show that majority of fibres had the Modulus of Elasticity lying between 2.0 and 6.2 GN/m<sup>2</sup>. The mean value for the Modulus of Elasticity was calculated as 4.02 GN/m<sup>2</sup>.

A similar trend was noticed for the fibre yield stress and elongation at failure. A mean value of the fibre yield stress was calculated as 70.53 N/mm<sup>2</sup> while the percentage elongation at failure was calculated as 24.20 %.

#### 4.1.3 Fibre Cross-sectional area

The fibre cross-sectional area measured as in section 3.2.6.1.1 was found to be quite irregular. A great variation in the cross-sectional shapes was also noticed to the extent that it is not possible to generalize on the fibres cross-sectional shape.

The calculated areas were seen to vary tremendously between individual fibres tested. Values ranging from 0.03 mm<sup>2</sup> to 0.28 mm<sup>2</sup> were obtained. The mean value of the fibre cross-sectional area was calculated as 0.08 mm<sup>2</sup>.

Most fibres did not exhibit a clean fracture along the cross-section, but failed by severe splitting along the fibre length. Fibre splitting resulted in some audible sound from the failing sections of the fibre.

## 4.2 Cement mortar-fibre composites

### 4.2.1 Workability of cement mortar and cement mortar-fibre components

The workability of fresh cement mortar was found to be good as it was easily placed into the moulds for casting. The addition of fibres (sisal or coconut) into the mortar during the preparation of the respective composites greatly reduced the workability. As more and more of the fibres were added into the cement mortar, the workability was consequently reduced. The mixture became completely unworkable at some fibre volume fraction. Mixing became difficult as the fibre volume fraction was increased and it got fairly hard to achieve proper impregnation of the fibres with cement mortar.

Under the forementioned circumstances, bundling of the fibres took place with randomly distributed chopped fibres. In the case of sisal fibre, difficulty was experienced in the mixing operation at a fibre volume fraction of about 5-6%, while in the case of coconut fibre, this happened earlier at a fibre volume fraction of about 4%.

The tendency of the fibres to absorb water from the cement mortar during the mixing process and the inclusion of the fibres in the cement mortar as a foreign material may therefore be what contributed to the poor workability of the mixture.

## 4.2 Cement mortar-fibre composites

### 4.2.1 Workability of cement mortar and cement mortar-fibre components

The workability of fresh cement mortar was found to be good as it was easily placed into the moulds for casting. The addition of fibres (sisal or coconut) into the mortar during the preparation of the respective composites greatly reduced the workability. As more and more of the fibres were added into the cement mortar, the workability was consequently reduced. The mixture became completely unworkable at some fibre volume fraction. Mixing became difficult as the fibre volume fraction was increased and it got fairly hard to achieve proper impregnation of the fibres with cement mortar.

Under the forementioned circumstances, bundling of the fibres took place with randomly distributed chopped fibres. In the case of sisal fibre, difficulty was experienced in the mixing operation at a fibre volume fraction of about 5-6%, while in the case of coconut fibre, this happened earlier at a fibre volume fraction of about 4%.

The tendency of the fibres to absorb water from the cement mortar during the mixing process and the inclusion of the fibres in the cement mortar as a foreign material may therefore be what contributed to the poor workability of the mixture.



## 4.2.2 Flexural properties of cement mortar-fibre composites

### 4.2.2.1 Chopped sisal fibre reinforced flexural beams

Figure 4.1 gives the plot of flexural strength versus fibre reinforcement volume fraction for cement mortar beams reinforced with 20 mm chopped sisal fibre, tested after curing for 28 days. It is seen that the beams were seen to widen out gradually on the tensile side of the beams, with more fibres pulling out of the matrix.

It is observed that the mean flexural strength increased with increase in fibre reinforcement from a value of  $2.02 \text{ N/mm}^2$  for the unreinforced specimens to a maximum strength of about  $4.74 \text{ N/mm}^2$  at a fibre volume fraction of 6%. Above this value of reinforcement volume fraction, the flexural strength starts to fall gradually with further fibre additions. The strength increase decreases initially on introduction of fibres into the cement mortar, and starts to increase fairly rapidly from a fibre volume fraction of about 1.8%.

The rate of strength increase decreased with increase in fibre reinforcement and is seen to level up at a fibre volume fraction of 6%. A sharp decrease in the rate of strength increase is observed with further increase in fibre volume fraction. The results also show more scatter in the values obtained at fibre volume fractions greater than 5%. All the specimens tested were seen to fail with a single crack, illustrated in Figure 4.4, traversing through the neutral axis. As the crack opening became large, the bridging fibres

became visible, exhibiting a fibre pull out failure mode. The presence of fibres increased the area under the load-deflection curve which did not occur for the unreinforced specimens. This signifies fracture toughness and improved post cracking ductility. The crack in the case of fibre reinforced specimens was seen to widen out gradually on the tensile side of the beams, with more fibres pulling out of the matrix.

The flexural strength characteristics of chopped coconut fibre

#### 4.2.2.2 Parallel aligned sisal fibre reinforced flexural beams

obtained with reinforced specimens in section 4.2.2.1.

The results of parallel aligned sisal fibre reinforced flexural beams are plotted in Figure 4.2. The mean flexural strength was seen to increase steadily with fibre reinforcement, reaching a maximum value of  $9.46 \text{ N/mm}^2$  at a fibre volume fraction of 7.5%. The Figure indicates that the increase in flexural strength assumes a linear relationship up to a volume fraction of about 5%. At or about the maximum strength, the results are more uncertain as deviations and scatter become more apparent.

as poorer in the case of coconut fibre addition than the resulting mixture with same amount of

The flexural strength values for parallel aligned reinforced specimens were greater than the corresponding values obtained in the case of chopped fibre randomly reinforced specimens at the same value of fibre addition (volume fraction). It was noticed that unlike the case of chopped fibre reinforcement, the parallel aligned reinforced specimens did not exhibit an

initial drop in the flexural strength with introduction of the fibres into the cement mortar matrix, Figure 4.2. The specimens failed with multiple cracks initiated from the tensile side of the specimens, Figure 4.4, and load increase was seen to occur even with the presence of failure cracks.

#### 4.2.2.3 Chopped coconut fibre reinforced flexural beams

The flexural strength characteristics of chopped coconut fibre reinforced beams was seen to be similar to those obtained with chopped sisal fibre reinforced specimens in section 4.2.2.1. The strength increased with fibre addition, attaining a maximum value of  $4.24 \text{ N/mm}^2$  at a fibre volume fraction of 8%. The results indicate that at the same value of fibre reinforcement, lower values of flexural strength were obtained in the case of chopped coconut fibre reinforcement, for fibre reinforcements less than 7%. This behaviour could be linked to poor compaction due to poor workability of the cement mortar resulting from factors mentioned in section 4.2.1. The workability of cement mortar was poorer in the case of coconut fibre addition than the resulting mixture with same amount of sisal fibre inclusions.

The observed strength behaviour, Figure 4.3, was also identical to that obtained with chopped sisal fibre reinforcement. Other features such as failure by single crack, fibre pull out and post-cracking ductility were also dominant phenomenons. The

observed rate of crack opening was greater in the case of coconut fibre reinforced specimens as compared to that observed in the case of sisal fibre reinforced specimens. During the pulling out process of the coconut fibres, small particles were seen to de-bond from the parent mortar matrix progressively as the crack opening increased.

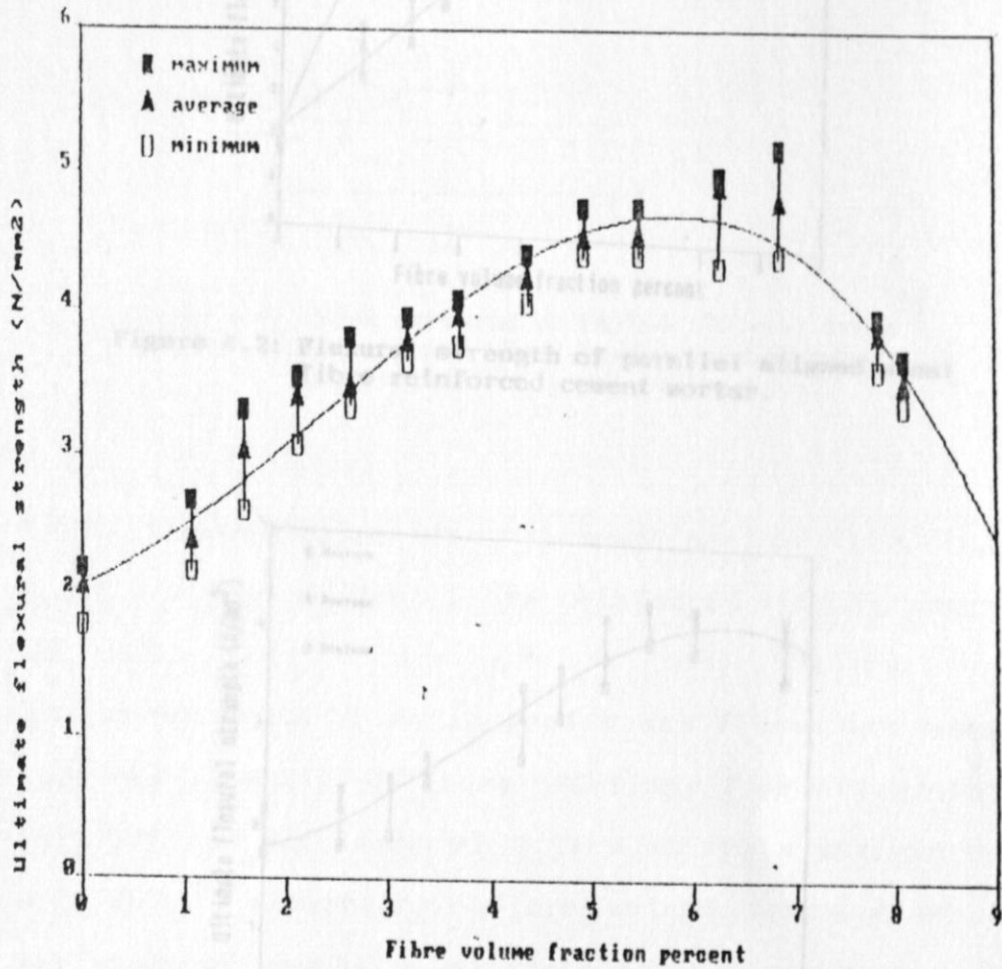


Figure 4.1: Flexural strength of chopped sisal fibre reinforced cement mortar.

Figure 4.3: Flexural strength of chopped coconut fibre reinforced cement mortar.

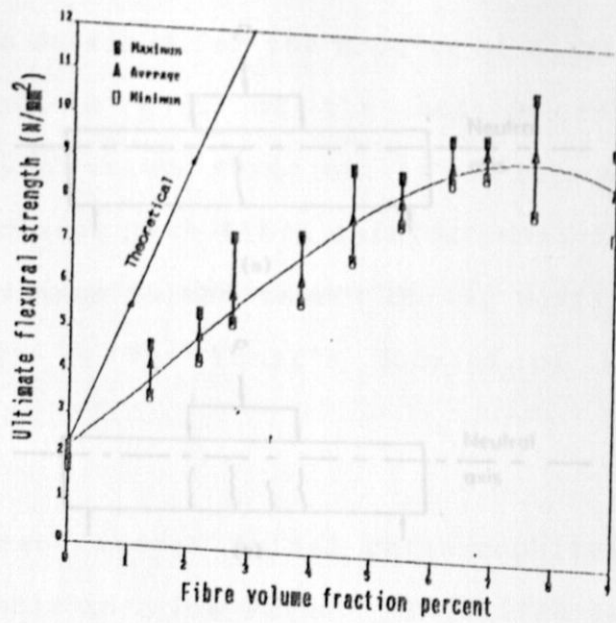


Figure 4.2: Flexural strength of parallel aligned sisal fibre reinforced cement mortar.

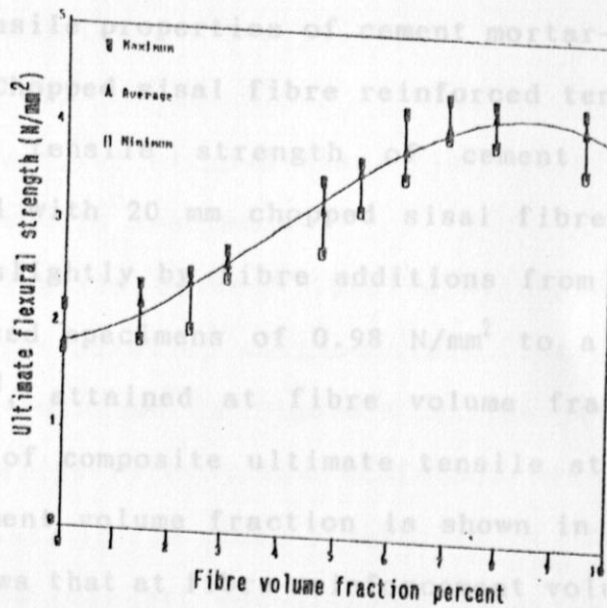


Figure 4.3: Flexural strength of chopped coconut fibre reinforced cement mortar.

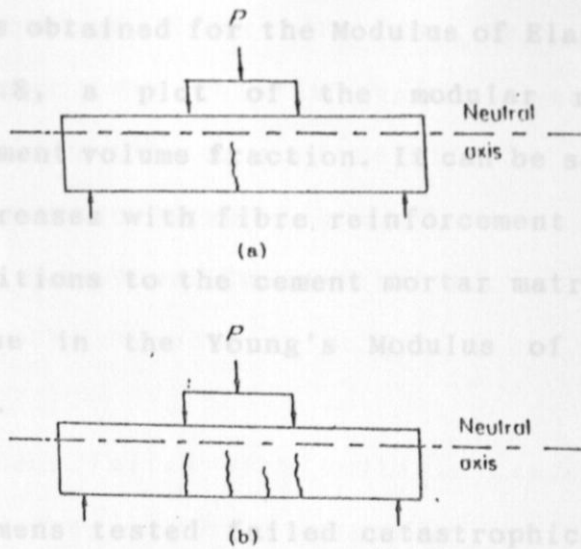


Figure 4.4: Crack patterns of failed flexural beams.

(a) chopped short random reinforcement.

(b) Parallel aligned reinforcement.

#### 4.2.3 Tensile properties of cement mortar-fibre composites

##### 4.2.3.1 Chopped sisal fibre reinforced tensile specimens

The mean tensile strength of cement mortar specimens reinforced with 20 mm chopped sisal fibres was seen to be improved slightly by fibre additions from the value of the unreinforced specimens of  $0.98 \text{ N/mm}^2$  to a maximum value of  $2.94 \text{ N/mm}^2$ , attained at fibre volume fraction of 7%. The variation of composite ultimate tensile strength with fibre reinforcement volume fraction is shown in Figure 4.5. The Figure shows that at fibre reinforcement volume fraction above 4%, the rate of strength improvement by fibre addition is reduced.

The values obtained for the Modulus of Elasticity are given in Figure 4.8, a plot of the modular ratio versus fibre reinforcement volume fraction. It can be seen that the modular ratio decreases with fibre reinforcement in a linear manner. Fibre additions to the cement mortar matrix therefore causes a decrease in the Young's Modulus of Elasticity of the composite.

The specimens failed with multiple cracks appearing on the The specimens tested failed catastrophically, and the load fell suddenly to a low value. The failed specimens showed no ability to sustain any load after the appearance of the failure crack. The specimens failed by an audible single crack traversing across the specimen cross-section, with the failure surface exhibiting fibre pull-out.aining even higher loads after the matrix fractured. The ability of the fractured

#### 4.2.3.2 Parallel aligned sisal fibre reinforced opening tensile specimens

The relationship between tensile strength and fibre volume fraction for parallel aligned sisal fibre reinforced tensile specimens is shown in Figure 4.6. The tensile strength was improved slightly by fibre addition, but increased steadily with increase in the added reinforcement. The maximum value of the tensile strength was attained at a fibre volume fraction of 6%, as can be seen from the Figure. Above 6% fibre reinforcement volume fraction, deviations in the results became evident, and cases of sudden fracturing of the matrix became apparent.

The values obtained for the Modulus of Elasticity are given in Figure 4.8, a plot of the modular ratio versus fibre reinforcement volume fraction. It can be seen that the modular ratio decreases with fibre reinforcement in a linear manner. Fibre additions to the cement mortar matrix therefore causes a decrease in the Young's Modulus of Elasticity of the composite.

The specimens failed with multiple cracks appearing on the The specimens tested failed catastrophically, and the load fell suddenly to a low value. The failed specimens showed no ability to sustain any load after the appearance of the failure crack. The specimens failed by an audible single crack traversing across the specimen cross-section, with the failure surface exhibiting fibre pull-out.aining even higher loads after the matrix fractured. The ability of the fractured

#### 4.2.3.2 Parallel aligned sisal fibre reinforced opening tensile specimens

The relationship between tensile strength and fibre volume fraction for parallel aligned sisal fibre reinforced tensile specimens is shown in Figure 4.6. The tensile strength was improved slightly by fibre addition, but increased steadily with increase in the added reinforcement. The maximum value of the tensile strength was attained at a fibre volume fraction of 6%, as can be seen from the Figure. Above 6% fibre reinforcement volume fraction, deviations in the results became evident, and cases of sudden fracturing of the matrix became apparent.



The Modulus of Elasticity too was affected by fibre reinforcement. The obtained values decreased linearly and gradually with additions of reinforcing fibres. The plot of the modular ratio versus fibre volume fraction, in Figure 4.9 shows this behaviour. The resulting graph showed less scatter in the results compared to chopped fibre reinforcement.

The specimens failed with multiple cracks appearing on the specimen gauge length on reaching the failure stress. The cracks were seen to be spaced at regular intervals and running almost parallel to one another along the specimen cross-section, and perpendicular to the loading direction. The stress/strain curves obtained exhibited a post-cracking ductility, with the specimens sustaining even higher loads after the matrix fractured. The ability of the fractured specimen to carry higher loads diminished after the crack opening became so large that the fibres could not carry the additional load. Fibre failure could be noticed as the load fluctuated at values above the first crack load. When a substantial amount of fibres had failed, the remaining fibres could no longer withstand high loads, the load then dropped gradually with load fluctuations being dominant.

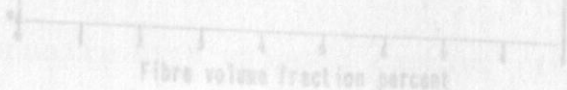


Figure 4.6: Tensile strength of parallel aligned sisal fibre reinforced specimens tested in direct tension.

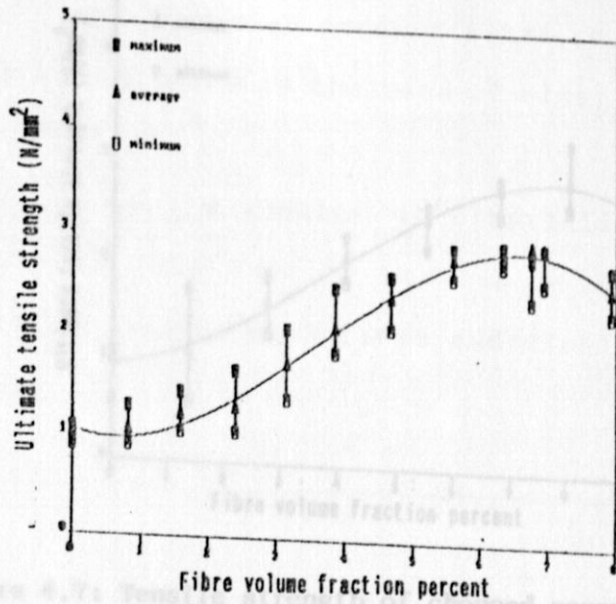


Figure 4.5: Tensile strength of chopped sisal fibre reinforced specimens tested in direct tension.

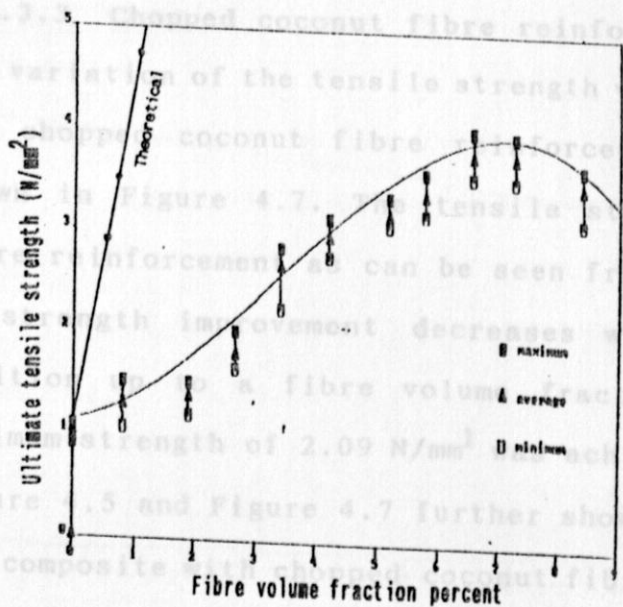


Figure 4.6: Tensile strength of parallel aligned sisal fibre reinforced specimens tested in direct tension.

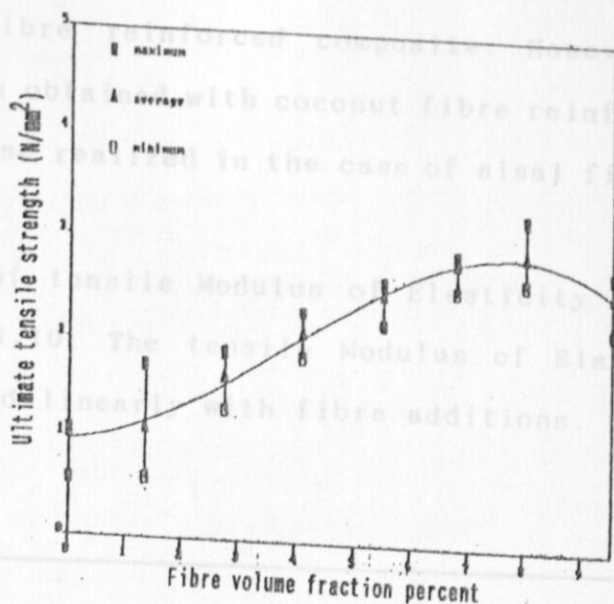


Figure 4.7: Tensile strength of chopped coconut fibre reinforced specimens tested in direct tension.

#### 4.2.3.3 Chopped coconut fibre reinforced tensile specimens.

The variation of the tensile strength with fibre reinforcement for chopped coconut fibre reinforced tensile specimens is shown in Figure 4.7. The tensile strength was improved by fibre reinforcement as can be seen from the Figure. The rate of strength improvement decreases with increase in fibre addition up to a fibre volume fraction of 6% at which a maximum strength of  $2.09 \text{ N/mm}^2$  was achieved. A comparison of Figure 4.5 and Figure 4.7 further show that the behaviour of the composite with chopped coconut fibre reinforcement is not different from that obtained with chopped sisal fibre reinforcement. The tensile strength in the case of coconut fibre reinforcement did not initially drop so much on

introduction of the fibres in the matrix as in the case of sisal fibre reinforced composite. However, the values of strength obtained with coconut fibre reinforcement were lower than those realized in the case of sisal fibre reinforcement.

Values of tensile Modulus of Elasticity are plotted in Figure 4.10. The tensile Modulus of Elasticity is seen to decreased linearly with fibre additions.

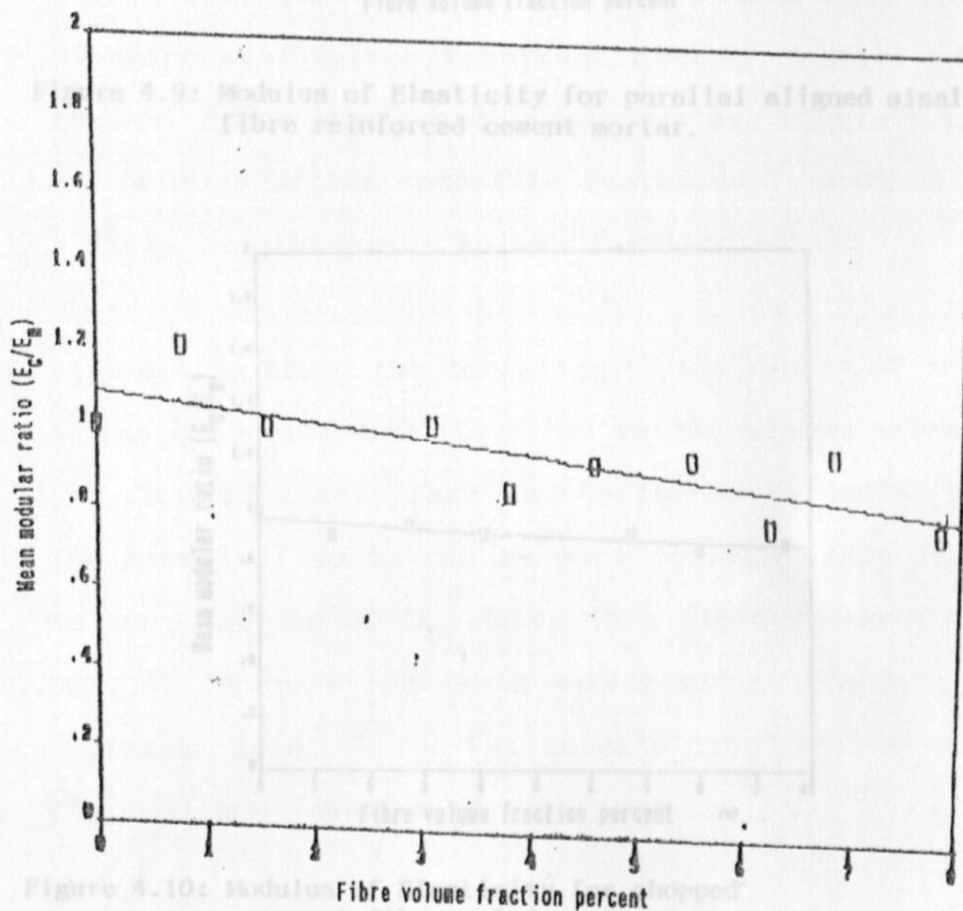


Figure 4.8: Modulus of Elasticity for chopped sisal fibre reinforced cement mortar.

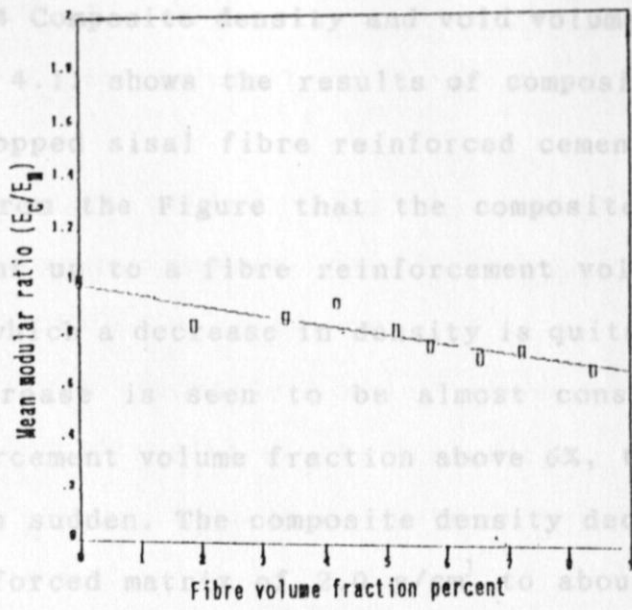


Figure 4.9: Modulus of Elasticity for parallel aligned sisal fibre reinforced cement mortar.

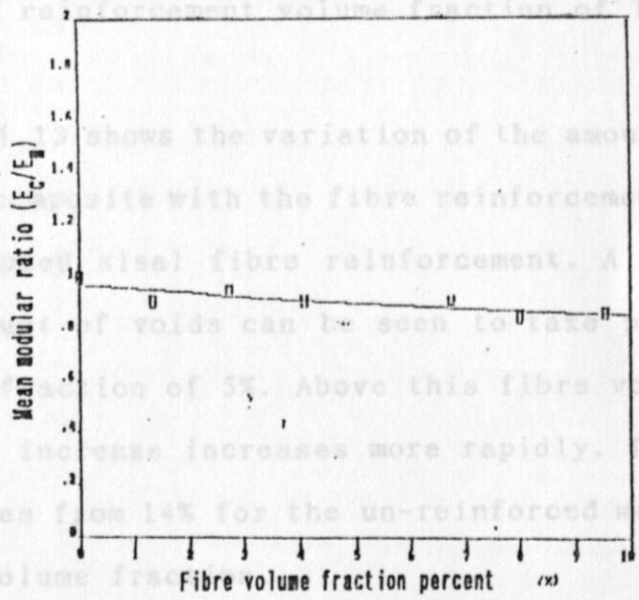


Figure 4.10: Modulus of Elasticity for chopped coconut fibre reinforced cement mortar.

#### 4.2.3.4 Composite density and void volume variation

Figure 4.11 shows the results of composite density obtained for chopped sisal fibre reinforced cement mortar. It can be seen from the Figure that the composite density is almost constant up to a fibre reinforcement volume fraction of 3%, above which a decrease in density is quite apparent. The rate of decrease is seen to be almost constant, but at fibre reinforcement volume fraction above 6%, the rate of decrease becomes sudden. The composite density decreases from that of unreinforced matrix of  $2.0 \text{ g/cm}^3$  to about  $1.57 \text{ g/cm}^3$  at 10% reinforcement volume fraction. Similar results are seen for coconut fibre reinforced cement mortar, Figure 4.12, in which the density of the composite decreases to about  $1.46 \text{ g/cm}^3$  at a fibre reinforcement volume fraction of 11%.

Figure 4.13 shows the variation of the amount of voids present in the composite with the fibre reinforcement volume fraction, for chopped sisal fibre reinforcement. A sudden increase in the amount of voids can be seen to take place up to a fibre volume fraction of 5%. Above this fibre volume fraction, the rate of increase increases more rapidly. The number of voids increases from 14% for the un-reinforced matrix to 26% at 10% fibre volume fraction.

Figure 4.14 shows that similar results were obtained for coconut fibre reinforced composites. The amount of voids present at fibre volume fraction above 11% seem to exceed more than double the number present in the un-reinforced matrix.

This shows that there is an increase of the number of voids from 14% for the unreinforced matrix to 30% at a fibre reinforcement volume fraction of 11.5%.

It is quite evident from the results that at any fibre reinforcement volume fraction, composites reinforced by coconut fibre have more number of voids than the corresponding sisal fibre composites, which consequently might affect the resulting strengths of the composites.

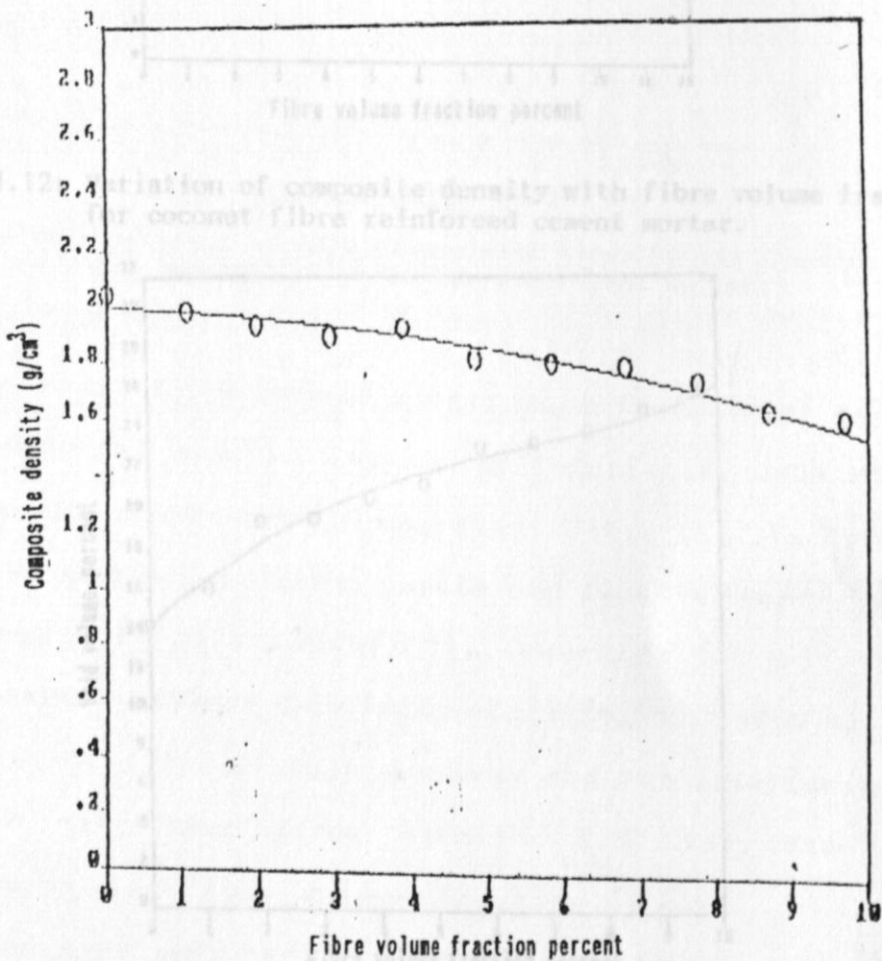


Figure 4.11: Variation of composite density with fibre volume fraction for sisal fibre reinforced cement mortar.

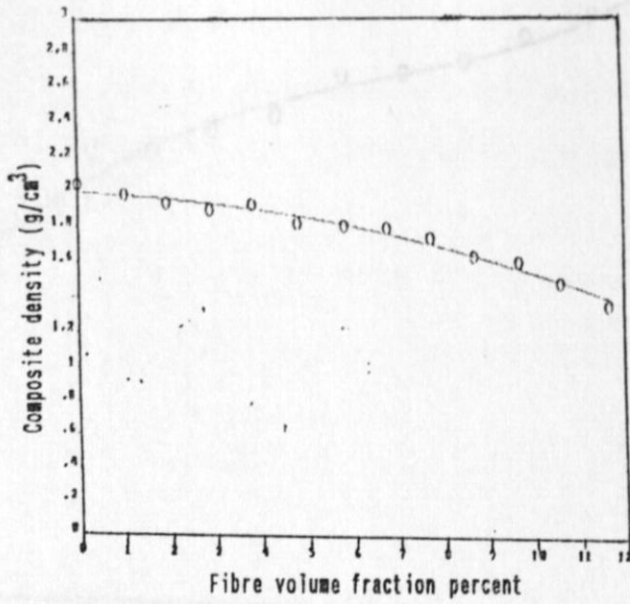


Figure 4.12: Variation of composite density with fibre volume fraction for coconut fibre reinforced cement mortar.

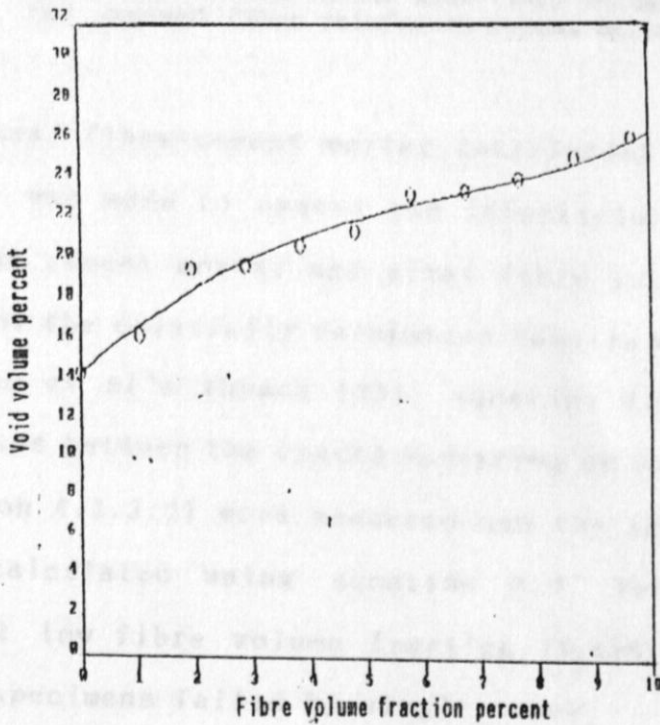


Figure 4.13: Variation of void volume with fibre volume fraction for sisal fibre reinforced cement mortar.



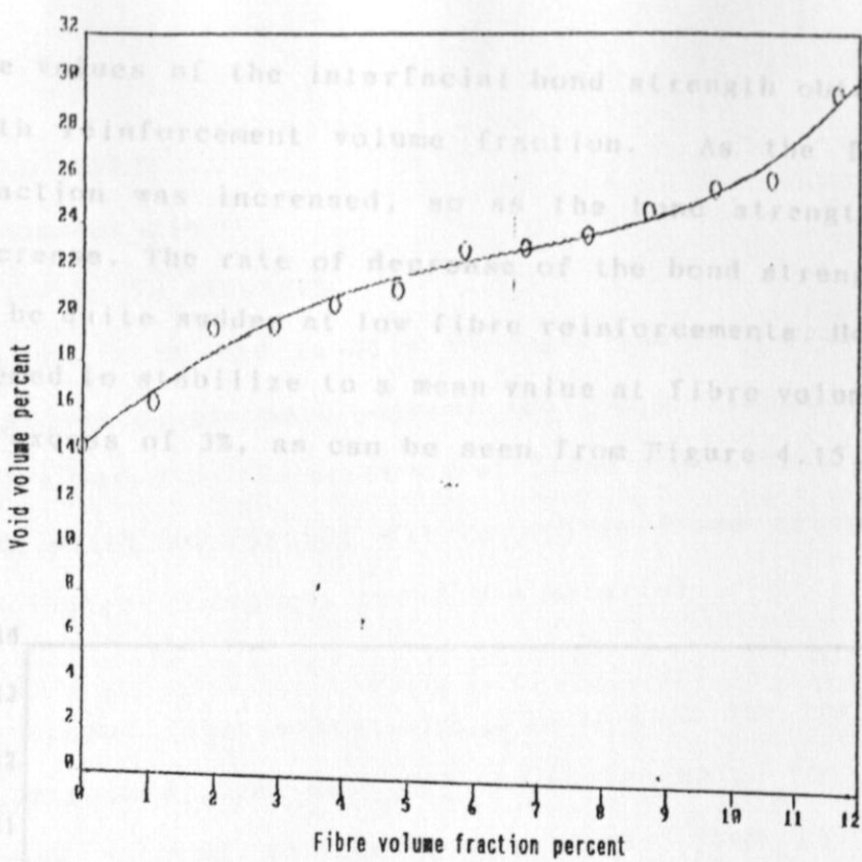


Figure 4.14: Variation of void volume with fibre volume fraction for coconut fibre reinforced cement mortar.

#### 4.2.3.5 Sisal fibre-cement mortar interfacial bond strength

An attempt was made to assess the interfacial bond strength between the cement mortar and sisal fibre interfaces. This was done for the uniaxially reinforced tensile specimens using the Aveston et al's theory [53], equation 2.8 section 2.2. The distances between the cracks appearing on loaded specimens (see section 4.2.3.2) were measured and the interfacial bond strength calculated using equation 2.9. Very few cracks occurred at low fibre volume fraction ( $V_f < 4\%$ ), and in some cases the specimens failed by single crack.

Figure 4.15: The sisal fibre-cement mortar interfacial bond strength.

The values of the interfacial bond strength obtained varied with reinforcement volume fraction. As the fibre volume fraction was increased, so as the bond strength tended to decrease. The rate of decrease of the bond strength was seen to be quite sudden at low fibre reinforcements. However, this seemed to stabilize to a mean value at fibre volume fractions in excess of 3%, as can be seen from Figure 4.15.

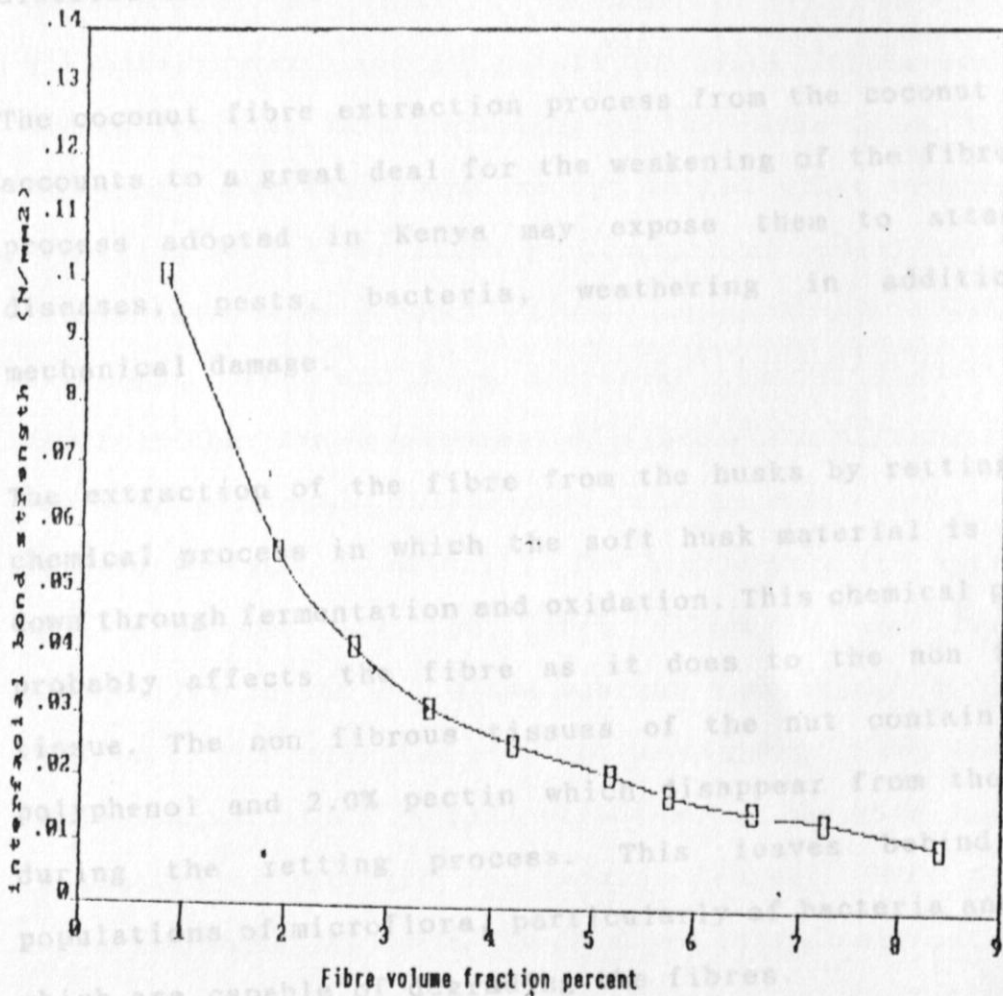


Figure 4.15: The sisal fibre-cement mortar interfacial bond strength.

## 5 DISCUSSION

### 5.1 coconut Fibre

#### 5.1.1 Tensile strength

The results on the tensile strength analysis showed great variations of strength between individual fibres. This could be attributed to the presence of flaws and natural variations which exist in natural fibres, these flaws being randomly distributed throughout the fibre material.

The coconut fibre extraction process from the coconut fruit accounts to a great deal for the weakening of the fibre. The process adopted in Kenya may expose them to attack by diseases, pests, bacteria, weathering in addition to mechanical damage.

The extraction of the fibre from the husks by retting is a chemical process in which the soft husk material is broken down through fermentation and oxidation. This chemical process probably affects the fibre as it does to the non fibrous tissue. The non fibrous tissues of the nut contain 7.3 % polyphenol and 2.0% pectin which disappear from the fibre during the retting process. This leaves behind heavy populations of microflora, particularly of bacteria and yeast which are capable of degrading the fibres.

The coconut fibre that was used in this investigation was obtained from Slumberland Mattress Factory, Nairobi, where the fibres are subjected to a mechanical fibre/coir dust

separation. It was established that, many fibres had been broken by machines, thus making the sample preparation a matter of chance.

Fibre	Length of cell (Micrometres)	Diameter of cell (Micrometres)
Ramie	150	40
Hemp	28	20
Flax	30	20

Apart from the variation of strength due to the presence of flaws in the fibre material, the growth and formation of the fibre also accounts for the varied results. During the fibre development, a number of discontinuities develop which ultimately would act as points of crack initiators. These discontinuities vary depending on the maturity of the nuts, and would also vary from one nut to the other, consequently resulting in the variation of strength of individual fibres. Commercial bulk coconut fibre consists of fibres from different nuts, and from different coconut plants. It is unlikely that the development of fibres from different plants would be identical, furthermore, the harvested nuts stand at different stages of maturity. The less mature the nut is, the less developed are the fibre ultimates and hence the variability in the cellulose content comprising the ultimate cell wall. The variation of fibre development along its length implies a variation in cell size ( which has been used as an indication of strength for natural fibres). This therefore explains the variation in the obtained tensile strength. Table 5.1 gives the cell size for some natural fibres [75]. It can be observed that coconut fibre has a low value of cell size as compared to other fibres. Hence the fibre probably would not fair very well if tested for strength as compared to the other fibres.

Fibre	Length of cell (Micrometres)	Diameter of cell (Micrometres)
Ranie	150	40
Hemp	28	20
Flax	20	25
Abaco	6	24
Aloe	2.5	24
Jute	1.9	17.5
Coir	0.9	20

Table 5.1: Cell size for some natural fibres [75].

### 5.1.2 Fibre cross-sectional area

The cross section of coconut fibre as seen through the microscope is irregular. This was seen to vary from fibre to fibre and also within individual fibres. The individual fibres were seen to lack uniformity along their lengths. This could be due to the factors highlighted in section 5.1.1, which affect the development of the fibre. The lack of uniform cross section of individual fibres would therefore imply that some sections of the fibre are more stressed than others when some load is applied longitudinally to the fibre. Consequently, the ultimate tensile strength of coconut fibre was lower than that of many artificial fibres such as nylon and polypropylene.

### 5.1.3 Fibre Modulus of Elasticity

The Modulus of Elasticity of coconut fibre was seen to be lower than that of the commercially applied non-metallic fibres used for matrix reinforcement. This is to be expected due to the high elongation recorded for coconut fibre. A comparison of coconut fibre and other high Modulus fibres is shown on Table 5.2. It is evident that coconut fibre has low tensile strength and Modulus of Elasticity, while the elongation at failure is much higher than that of the high Modulus fibres. Although these fibres, owing to their physical and mechanical properties, find extensive application in aerospace and deep water venture composites, coconut fibre too offer certain advantages. Due to its high percentage elongation at failure, it promises improvements in composite fracture toughness and impact strength, which would be important for the kind of reinforcement the fibre is likely to be used for.

Fibre	Density Kg/m <sup>3</sup> 10	Young's Modulus GN/m <sup>2</sup>	Tensile Strength MN/m <sup>2</sup>	Elongation at break %
Carbon	1.9	380	1,800	0.5
E - Glass	2.54	72	3,500	4.8
Kevlar 49	1.45	133	2,900	2.1
Stainless Steel	7.86	200	700	3.5
Nylon	1.14	< 4	750	13.5

Table 5.2: Typical fibre properties [21].

The post cracking ductility achieved on coconut fibre reinforced cement composites is highly attributed to the low modulus value of the fibre. Low modulus fibres have been shown to have large values of Poisson's ratio, this combined with their low moduli means that when stretched along their axis, they would contract laterally more than the other fibres. This leads to a high lateral tensile stress at the fibre - matrix interface, in the case when the fibre is used for reinforcing a matrix, and hence is likely to cause short aligned fibres to debond or pull out of the matrix gradually, thus prolonging the phenomenon of post cracking ductility. Although post cracking ductility would be important for fibre cement composites, such as coconut fibre reinforced cement mortar, the load carried by the composite after first crack is quite low thus rendering this phenomenon un-important in most practical applications of the composite. The possibility of using this fibre to reinforce a brittle matrix is limited. In addition, the modulus of the fibre being much less than that of the matrix, combined with the low volume fraction that can be added to achieve good interfacial bonding, means that the modulus of the resulting composite would not be greatly different from that of the matrix. This therefore puts coconut fibre at a disadvantage over high modulus fibres as a reinforcing fibre.

errors were minimized.

#### 5.1.4 Fibre density Fibre Composites

The density of coconut fibre is difficult to assess due to the fibre characteristics of absorbing most liquids brought into contact with it. On the other hand, if mercury is used, it tends to get squashed, thus reducing the effective fibre surface area. The indirect method used for determining the density gave little variations between individual batches taken. The fibre condition at the time that the test is carried out would cause variations in the obtained results. The moisture content of the fibres is affected by the atmospheric humidity, and since this keeps on varying, the calculated value of density would vary if the test is done under different atmospheric conditions. The batches selected in this case were sampled and tested at the same condition of temperature and humidity, which explains the consistency in the obtained results. The method adopted for measuring the density of the coconut fibre is indirect due to failure of the normal conventional methods. However, the method may have caused errors by the formation of void in the form of air pockets in the plasticine matrix.

By avoiding direct measurements of volume of coconut fibre, and applying the accurate weight measurements (and hence densities) of other constituents used in this method, the errors were minimized.

and coconut fibres being cellulose vegetable fibres have in them air pockets among their cells. The presence of these air pockets causes the fibres to have a high absorptivity for



## 5.2 Cement Mortar-fibre Composites

### 5.2.1 Flexural Strength

The results of flexure test on cement mortar-sisal fibre (both randomly and parallel aligned) and cement mortar-coconut fibre composites indicated an increase in the flexural strength with fibre additions, as seen in Figures 4.1, 4.2 and 4.3. This is in order as predicted from the rule of mixtures, see section 2.0. The rule of mixtures predicts a linear increase in the flexural strength with parallel aligned reinforcement giving a higher strength than chopped fibres randomly aligned reinforced specimens. This is due to the fibre length and fibre orientation efficiency factors, as described in section 2.4. This is shown in Figures 4.1 and 4.3, which give the variation of flexural strength with fibre reinforcement volume fraction obtained for chopped randomly oriented, sisal and coconut fibre reinforced cement mortar composites respectively. It is evident from these results that when a little quantity of short fibre is introduced into the cement matrix, the flexural strength is seen to decrease slightly before a significant increase in strength is noticed. The reason for this drop in strength can be explained by considering the effect of these fibres to the cement mortar matrix. First, the sisal and coconut fibres being cellulose vegetable fibres have in them air pockets among their cells. The presence of these air pockets causes the fibres to have a high absorptivity for the load is

water in the matrix. The introduction of a little quantity of the fibre in the matrix as a foreign material therefore breaks the homogeneity of the parent material through the formation of voids in the composite, thus weakening the material and hence lowering the strength. It has also been shown that in fibre reinforcement, strengthening of the matrix occurs if the fibre volume fraction is greater than the critical fibre volume fraction [56], equation 2.16. Table 5.3 gives some values of critical fibre volume fraction of some common fibres used to reinforce cement base matrices. The Table shows that the fibre critical volume is quite low, ranging between 0.1% and 1%. The results of flexural strength obtained for chopped fibre reinforcement show that steady strength increase takes place at a fibre volume fraction greater than one percent. Although it is difficult to determine the fibre critical volume fraction in the case investigated, the observed strength behaviour indicates that the fibre critical volume could probably be of the same magnitude as the values shown in the Table, thus resulting in strength drop in the range shown.

In the case of parallel aligned fibre reinforcement, no initial drop in flexural strength was noticed. This is because with little fibre additions, proper bonding is achieved, making the composite behaviour similar to that predicted by the rule of mixtures, where the load is

presumably shared between the fibres and the matrix. In this particular case, the fibres carry extra load, while the length efficiency and orientation factors greatly contribute to this behaviour.

Fibre	Critical $V_f$ %	Fibre	Critical $V_f$ %
Glass	0.2 - 0.1	Steel	0.5 - 0.2
Graphite	0.3 - 0.2	Polypropylene	1.0
Chrysotile Asbestos	-	Polycrystalline Alumina	0.8
sisal	0.6	Kevlar 49	0.2

Table 5.3: Critical fibre volume fraction of some common fibres [37].

Fibre additions into the cement mortar matrix improves the flexural strength of the composite. However this tends to reduce the workability of the mix, with more reduction in the case of chopped fibres. In this case, balling of the mix was evidenced at a fibre volume fraction of about 4%. When sisal fibres were carefully placed and aligned in the cement matrix (in parallel aligned reinforcement) the compactability as evidenced by the ease of compaction into the mould was not reduced to the same extent as with chopped randomly aligned fibres. Poor workability of the mix was seen to increase with

fibre additions, and at a fibre reinforcement volume fraction beyond 7%, the mix became very difficult to handle. The effect of this to the overall nature of the composite is the formation of voids, which cause the reduction in strength of the composite. This reduction in flexural strength became apparently the case beyond a fibre reinforcement volume fraction of 8 %. The strength increase trend then shifted from "increase with increase in fibre additions" to "decrease with increase in fibre additions". This was due to the existence of more voids as a result of poor workability of the mix. As more and more fibres were added beyond this value, the formation of voids increased as the mixture became more unworkable; hence a corresponding reduction in flexural strength.

area under the load-deflection curve results as energy is progressively absorbed by the composite to

It is apparent from the results that at the same fibre volume fraction, the results of flexural strength in the case of parallel aligned reinforcement are higher than the corresponding values obtained for chopped randomly aligned reinforcement. This is due to the effect of higher fibre aspect ratio which results in a higher length efficiency factor as predicted by equation 2.11 of the rule of mixtures, and also due to the effect of fibre orientation. This behaviour concurs with section 2.4. The results obtained agree very well with those obtained by Swift and Smith [36] section 2.2, who established that

superior post-cracking ductility and energy absorption is

the flexural strength of cement is greatly improved by addition of parallel aligned sisal fibre, although this improvement consistently improved till deviations appeared at a fibre volume fraction of 7%. Other factors such as fibre length, content and mix preparations accounted greatly to the strength improvement observed. The results of this investigation compare well with those reported by Majumdar [37] and Hannant et al [38], section 2.2.

The flexure behaviour exhibited in flexure test show a great improvement in fracture energy depicted by the increased area under the load-deflection curve, which is also evidence of presence of post-cracking ductility. The increased area under the load-deflection curve results as energy is progressively absorbed by the composite to crack the matrix, and also that which is required to debond the fibres on appearance of the first crack [32]. The cracked specimens showed a diminution of the load as fibres gradually pulled out of the matrix, with the specimens still supporting quite a sizable fraction of the ultimate flexural load. The diminution of the load as fibres pulled out of the matrix on appearance of the first crack agree with the observations of Swift and Smith [30], who have argued that due to the tendency of the fibres to absorb energy as they progressively pull out or crack inside the matrix, the phenomenon of superior post-cracking ductility and energy absorption is

achieved particularly for chopped randomly oriented short fibres whose minimum length exceeds that of the fibre critical length.

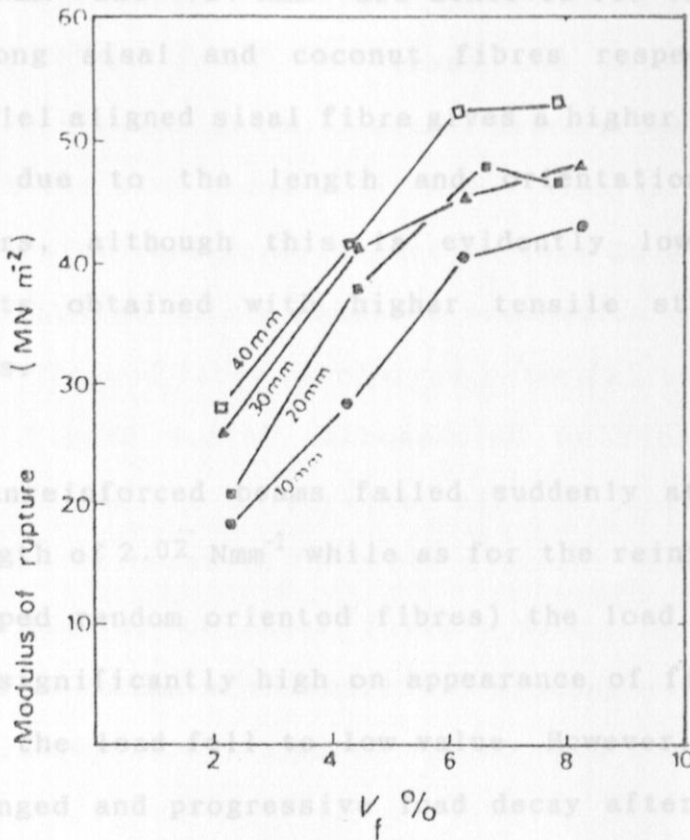


Figure 5.1: Flexural strength of glass reinforced cement composites for different fibre lengths.

Figure 5.1 shows the results of a research work carried by Majumdar [37] in the case of cement composites reinforced by glass fibres. The results show quite a good correlation with the obtained results of cement mortar - sisal/coconut fibre composites. Higher strength results are obtained in the case of glass fibre-cement composites because the fibre used has a higher tensile strength, and therefore in order to satisfy the rule of mixtures,

the glass fibre withstands more load than either sisal or coconut. A maximum strength of  $50 \text{ Nmm}^{-2}$  is shown for 20 mm long glass fibre reinforced cement, while values of  $4.74 \text{ Nmm}^{-2}$  and  $4.24 \text{ Nmm}^{-2}$  are achieved for the case of 20 mm long sisal and coconut fibres respectively. The parallel aligned sisal fibre gives a higher value of  $9.46 \text{ Nmm}^{-2}$  due to the length and orientation efficiency factors, although this is evidently lower than the results obtained with higher tensile strength glass fibres.

Chopped fibre reinforced beams failed by a single crack, Figure 4.4(v), accompanied by fibre pull-out. The unreinforced beams failed suddenly at a flexural strength of  $2.02 \text{ Nmm}^{-2}$  while as for the reinforced beams (chopped random oriented fibres) the load decrease was only significantly high on appearance of first crack at which the load fell to low value. However, there was a prolonged and progressive load decay afterwards, which indicates a gradual failure mode on reaching the ultimate load with the fractured beam still sustaining a certain proportion of the failure load. This was seen to be higher in the case of sisal fibre than for coconut fibre.

introduce points of weakness giving rise to shear failure

For the parallel aligned sisal fibre reinforced beams, a great contrast was observed in the load carried by the beam which increased even after visible fractures occurred. This happened as the load borne before fracture by the fractured matrix was transferred to the fibres, stress exists across the cross-section. A maximum value

which sustained the load, but gradually gave up as individual fibres fractured. A maximum value exists in the middle of the cross-section. Bessel has

Figure 4.4 shows the crack patterns obtained on the chopped fibre reinforced beams and parallel aligned reinforced beams tested. A single crack propagating right through the beam cross-section was observed in the un-reinforced beams tested in four point bending, which resulted into a complete separation of the broken pieces. Chopped fibre reinforced beams failed by a single crack, Figure 4.4(a), accompanied by fibre pull-out, while the failure of parallel aligned fibre reinforced beams was accompanied by crack patterns shown in Figure 4.4(b) similar of shear failure mode. Parallel fibre reinforced beams with small fibre reinforcement volume fraction (up to 4%) however failed with a single crack. otherwise normal flexural failure occurs.

It is quite probable that the alignment of fibres in one direction might contribute to this mode of failure. On the other hand, the existence of voids between fibre layers in a densely reinforced beam is bound to being introduce points of weakness giving rise to shear failure along the fibre direction. strength was seen to attain maximum values at a fibre volume fraction of 7%. Beyond

Two modes of failure are possible in typical bend test as explained by Bessel [34]. When a specimen is loaded in bending, a normal tensile (flexural) stress and a shear stress exists across the cross-section. A maximum value



by the cement mortar matrix. The resulting specimens are of the normal stress exists at the extreme of the cross-section while in the case of shear stress a maximum value exists in the middle of the cross-section. Bessel has further shown that this is quite possible with flexural beams and has evaluated these stresses for the case of three point bending where the maximum normal tensile (flexural) stress is shown to satisfy;

$$\sigma = \frac{[3.P.l]}{[2.b.d^2]}$$

and the maximum shear stress;

$$\tau_s = \frac{[3.p]}{[4.b.d]}$$

which exist at the neutral axis. Further, he explained that for shear failure to occur, the l/d ratio must be less than 6:1 otherwise normal flexural failure occurs.

A critical look into the effect of voids formation that

### 5.2.2 Tensile strength and Modulus of Elasticity

As the fibre volume fraction increases, so does the ultimate tensile strength, with more increase being observed with the parallel aligned reinforcement. The increase in ultimate tensile strength was seen to attain maximum values at a fibre volume fraction of 7%. Beyond this value of reinforcement the strength of the specimens decreased. The observed decrease is likely to be caused by the increase in the number of voids due to improper mixing and leading to improper impregnation of the fibres

by the cement mortar matrix. The resulting specimens are therefore weaker, due to imperfections, hence exhibiting lower strength values.

The results of tensile strength tended to conform to those obtained in earlier work done on cement paste reinforced with sisal fibres [76], in which the maximum tensile strength occurred at a fibre volume fraction of 8%. In the case of cement mortar matrix, maximum strength was attained at a fibre volume fraction lower than in the case of cement paste, because the workability of cement mortar is affected more by fibre incorporation than the cement paste. This results in more number of voids present in cement mortar-fibre composites than the corresponding cement paste-fibre composites. This effect lowers the strength, which explains the little difference observed in the two results.

(i) The Young's Modulus of Elasticity predicted by

A critical look into the effect of voids formation that results in weakening of the composite has been undertaken by Tailor, [77]. Air cured cement products at atmospheric conditions develop portlandite (calcium hydroxide) which can react with carbon dioxide in the air through the process of carbonation, thus causing an increase in volume and mass associated with transformation of calcium carbonate. The resulting increase in volume tends to favour the development of more voids caused by the entrapped unreacted gases, which affects the internal

structure of the composite. This tends to make the composite that is already weak in tension, even weaker when a direct tensile load is exerted on it. This is true at high fibre volume fractions, where more voids are expected to be dominant due to the decreased workability. The tendency of the fibres to ball up during the mixing process at fibre volume fractions in excess of 4 % enhances the possibility of porosity existence, which explains why the rate of strength increase is seen to decrease with fibre reinforcement volume fractions greater than 4%.

Fibre additions have also been seen to lower the Young's Modulus of Elasticity of the composite. The reduction in value of the Young's Modulus of Elasticity could be attributed to the two possible effects;

(i) The Young's Modulus of Elasticity predicted by the rule of mixtures, as  $E_c = E_f V_f + E_m (1 - V_f)$  shows that the composite modulus of elasticity is dependent on the fibre Modulus of Elasticity,  $E_f$ , which is very small compared to the Modulus of Elasticity of the matrix,  $E_m$ . That being the case means that the Modulus of Elasticity of the fibre does not contribute much to the overall composite Modulus of Elasticity. It can be concluded that  $E_c$  is strictly dependent on  $E_m$ . Due to the increase in fibre additions, the term  $E_m(1 - V_f)$  decreases, and consequently  $E_c$  decreases, since the term  $E_f V_f$  has little effect on  $E_c$ .

cement mortar at various fibre volume fraction and the

(ii) The value of the Modulus of Elasticity tends also to be affected by efficiency factors, as does tensile and flexure strength [80]. proper impregnation of the fibres by the cement mortar.

Errors in the results, which are indicated by the observed scatter may possibly have emanated from the difficulties encountered in making the test specimens. It was not easy to obtain a homogeneous mixture in most of the cases because the mixing of the fibres into the matrix was done manually like in the case of parallel aligned reinforced specimens. The fibres also tend to absorb water from the wet matrix, hence reducing the consistency of the latter. fibre cross-sectional area.

Although every effort was made to ensure that the fibres

### 5.2.3 Interfacial bond strength is a large decrease in

The values of the interfacial bond strength obtained seem to vary with fibre reinforcement volume fraction. As the fibre volume fraction is increased, the bond strength seem to go down. The values obtained do not compare well in magnitude to the value of  $0.6 \text{ N/mm}^2$  obtained for cement paste-sisal fibre [76]. The observed difference in magnitude can be attributed to the presence of particles in the cement mortar matrix which tends to hinder proper bonding in the latter, and also the observed decrease in workability and increased percentage of voids [21]. Some values of interfacial bond strength for other fibre cement combinations are shown in Table 2.1. A comparison of the values of the bond strength obtained for sisal-

cement mortar at various fibre volume fraction and the values summarised in the Table show that cement mortar gives a poor bond strength compared to cement Paste, probably due to lack of proper impregnation of the fibres by the cement mortar.

The application of the theory of multiple cracking to cement mortar-sisal composite materials can be used to determine the interfacial bond strength between the fibre and matrix interfaces, although there could be scatter in the results caused by inconsistent cracks at low fibre volume fractions. The scatter in the results is considered to be due in some part to the following:

(i) The large variation in fibre cross-sectional area. Although every effort was made to ensure that the fibres were selected at random, there is a large decrease in cross sectional area between fibres taken from the tip of the sisal leaf and those taken from the butt end [18]. For a specific volume fraction, this affects the total interfacial surface area.

(ii) The high water absorptivity of sisal fibre from the wet matrix which results in voids along the interfacial surface.

(iii) The theory of Aveston et al [53] used in the calculations of interfacial bond strength is based on circular fibre cross section (Appendix 2), properly embedded in the matrix. This is not totally true with a cement mortar matrix.

(iv) There is also considerable variability in cross-sectional geometry. In the calculations, the fibres were assumed to be round and a mean equivalent diameter used. The actual surface area would be greater than that of an equivalent round sisal fibre. It should also be pointed out that the process of producing sisal fibres from the leaves of the sisal plant is likely to produce variability of properties from one sisal estate and factory to another.

(v) The presence air bubbles, as observed in the fracture and misalignment of the fibres, which are common with most composite systems.

In view of these variables, the scatter of the results is acceptable. Since the fibres absorb moisture from the matrix, the value of the interfacial bond strength obtained should be considered to be that between moist sisal fibre and cement mortar matrix. The moisture content of the sisal fibre in the case investigated was not determined, therefore it is unknown.

#### 5.2.4 Density and porosity

Density and porosity (void volume) are inter-related as their magnitude depends on the free space or void volume present in the material.

The graph of density versus fibre reinforcement volume fraction, Figures 5.7 and 5.8, show that the density of

the composite decreases uniformly with fibre additions up to a fibre volume fraction of 6%, above which the rate of decrease increases indicated by the sudden drop in the curve. This sudden drop is due to the increase in the number of voids present in the composite material, which tends to increase with increase in fibre additions. The presence of portlandite affected the observed results, by decreasing the density due to increased volume of the composite while at the same time it increases the degree of porosity and the space left by the expanding matrix [77]. The observed increase in porosity is in agreement with the observations made on air-cured wood pulp fibre reinforced cement mortar [42], where the number of voids increased from 24.4% for the unreinforced mortar, cured for 27 days, to 38.0% at fibre reinforcement volume fraction of 12%. The low percentage voidage in this investigation implies that adequate compaction was achieved during the preparation of the test specimens.

Figure 5.2 and 5.3 show the results of investigations on the variation of density for cement composites with fibre additions carried out by Ali et al [78] and R.S.P Coutts [42]. The results confirm the observed decrease in density of the composite with increase in fibre volume fraction. It was observed that the value of the composite density is affected more by fibre additions at volume fraction above 6% .

Figure 5.3: Graph of density versus percent fibre (by mass) of wood-pulp reinforced cement mortar [42].

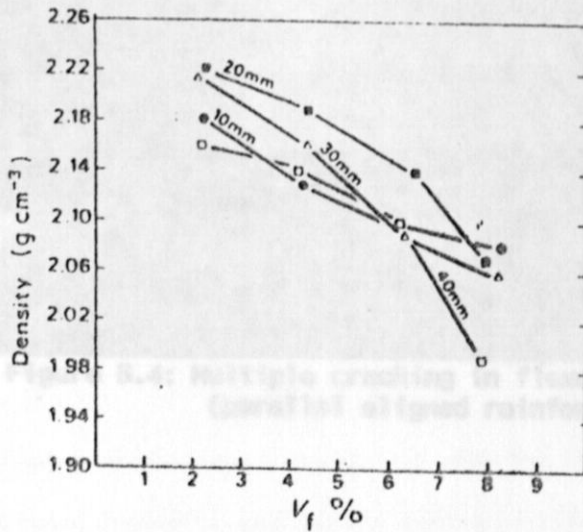


Figure 5.2: Relationship between fibre volume fraction and density of glass reinforced cement composite for different fibre length [78]

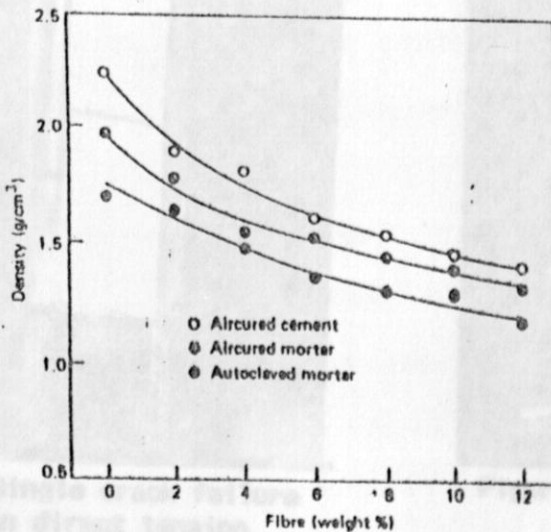
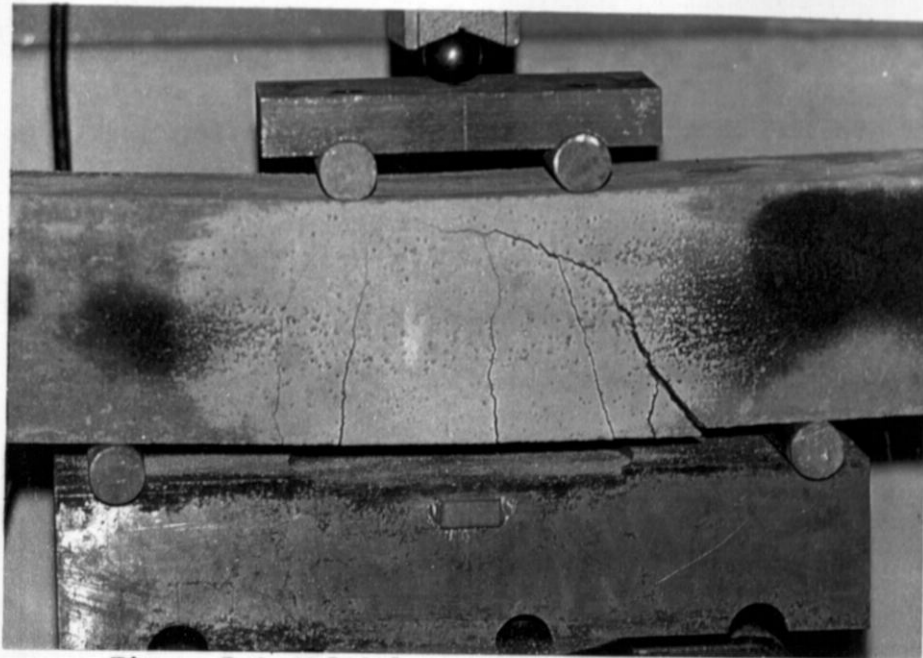
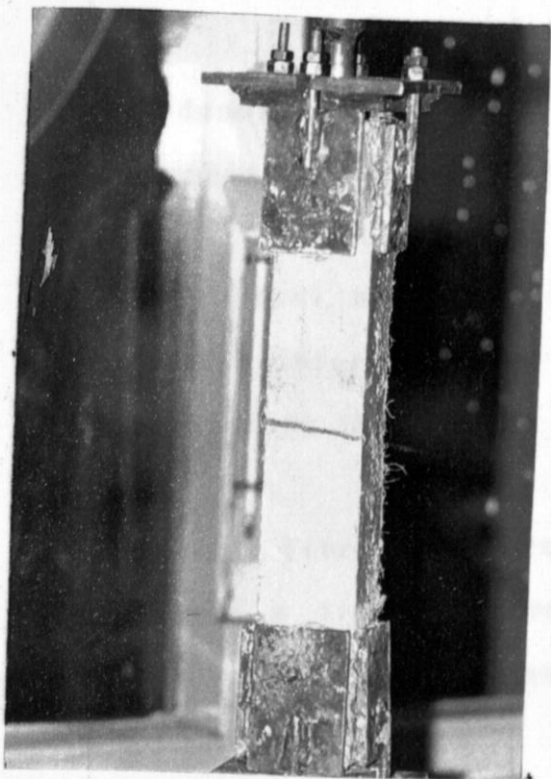


Figure 5.3: Graph of density versus percent fibre (by mass) of wood-pulp reinforced cement mortar [42].





**Figure 5.4: Multiple cracking in flexure test (parallel aligned reinforcement).**



**Figure 5.5: Single crack failure in direct tension (chopped fibre reinforcement).**

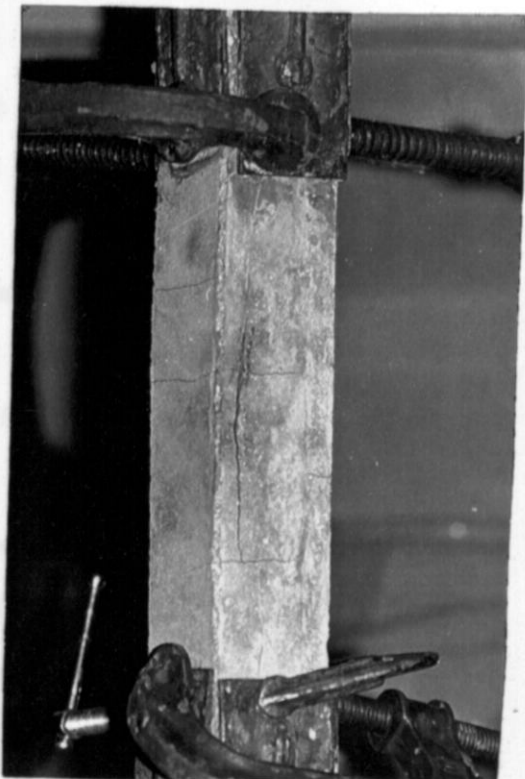


**Figure 5.6: Multiple cracking in direct tension (parallel aligned reinforcement).**

## 6. CONCLUSIONS AND RECOMMENDATIONS FOR FURTHER WORK

### 6.1. Conclusions

The determined properties of coconut fibre are:

(i) Tensile strength:  $159.30 (\pm 70.38) \text{ Nmm}^2$

(ii) Modulus of Elasticity at room atmospheric conditions i.e.  $22^\circ\text{C}$  and 60 % R.H.  $4.02 (\pm 2.26) \text{ GN/m}^2$

(iii) Percentage elongation at break;  $24.20 (\pm 8.15) \%$

The cross sectional area of coconut fibre varies along the fibre length and also between individual fibres.

The density of coconut fibre measured under normal atmospheric conditions is  $0.53 (\pm 0.02) \text{ g/cm}^3$ .

The flexural and tensile strength of cement mortar matrix reinforced with sisal and coconut fibre was greater than that of the un-reinforced matrix.

Parallel fibre reinforced cement mortar composites depicted a linear increase of flexural strength with reinforcement volume fraction.

Chopped, randomly aligned fibre reinforced composites tested both in tension and flexure indicated strength increment of lesser magnitude in comparison to parallel aligned reinforcement.

The matrix with parallel aligned fibre reinforcement failed by multiple cracking, while single crack failure mode with fibre pull-out resulted in chopped fibre reinforcement.

The failure of the un-reinforced matrix was sudden with a brittle fracture. Fibre reinforced composites on the other hand showed a gradual failure mode with the fractured specimens still capable of sustaining a certain amount of load.

Two modes of failure were identified in the flexure test of the cement mortar-sisal composites; flexural failure and shear failure. The un-reinforced beams, chopped fibre reinforced beams and parallel aligned fibre reinforced beams of small reinforcement volume fraction indicated a flexural failure mode, while parallel aligned fibre reinforcement of high reinforcement volume fraction failed in shear. The coconut fibre reinforced cement mortar beams indicated only a flexural failure mode.

The density of fibre reinforced cement mortar composites

The chopped fibre reinforced specimens tested in direct tension failed by single crack, with fibre pull out accompanied by a drastic and sudden decrease of load. The parallel aligned fibre reinforced tensile specimens failed by multiple cracks, with the failed specimens able to carry loads higher than that at first crack. The

The resulting multiple cracks appeared parallel to each other and perpendicular to the direction of the applied load.

post-cracking ductility, and fracture toughness is a

The flexural and tensile strength of fibre reinforced cement mortar composites increase with increase in reinforcement volume fraction, attaining maximum strength at 8 % reinforcement volume fraction. No further strength improvement by fibre additions were achieved above this fibre volume fraction, instead, a decrease in strength resulted. The high density and brittleness of the matrix can be the cause of breakage. The use of sisal or

The Modulus of Elasticity of cement mortar fibre composites is lowered by fibre additions. The results depicted a linear decrease in The Modulus of Elasticity with reinforcement volume fraction.

## 6.2 recommendations for further work

The interfacial bond strength between cement mortar and sisal fibre decreased with fibre addition into the matrix. In plain matrix where crack propagation is unstable and uncontrolled, the presence of these fibres

The density of fibre reinforced cement mortar composites is lowered by fibre additions. They find use in products

meant to last for long time in application. Swift and

Fibre additions to cement mortar matrix introduces porosity in the form of voids. These voids increase with increase in fibre reinforcement volume fraction. and

bacteriological decay. The findings further showed that the sisal fibre removed from the specimens which had been

The increased tensile and flexural strength caused by fibre reinforcement in cement mortar, and the observed post cracking ductility, and fracture toughness is a noted advantage. This would suggest that the resulting products could be valuable in areas of application in which resistance to impact and transverse loading is a noted advantage such as renders in walls and roofs in areas of high usage, eg. schools, shops and factories. An alternative application could be outdoor cement garden products where the high density and brittleness of the matrix can be the cause of breakage. The use of sisal or coconut fibres to reinforce the cement mortar products would lower the density and reduce sudden fracturing hence handleability of such products.

## 6.2 recommendations for further work

sisal and coconut fibre reinforcement in cement mortar matrix have been found to offer the advantage that, unlike the plain matrix where crack propagation is unstable and uncontrolled, the presence of these fibres impart a very slow and controlled crack growth. These fibres therefore would certainly find use in products meant to last for long time in application. Swift and Smith [30], reported that sisal fibre in roofing sheets appeared under normal circumstances to withstand degradation due to alkaline cement environment and bacteriological decay. The findings further showed that the sisal fibre removed from the specimens which had been

kept in contact with soil and exposed to considerable loss of strength due to saprophytic organisms. In order for the fibre in this investigation to find more diverse applications in cement mortar products, a thorough research should be done, to investigate the long term effect and the resulting strength characteristics of cement mortar-fibre composites.

Fibre reinforcement in cement mortar has been

The strength of the bond between the interface has been found to influence the characteristics of composite materials. Proctor [26] have described the interfacial bond between glass fibre and cement as being purely physical in nature. This argument could also be advanced for mortar-sisal fibre composites. The method of assessing the interfacial bond strength in this investigation assumed the existence of a fracture surface between the sisal fibre and cement mortar. In order to develop a more qualitative and quantitative method of measuring the bond strength, further research is therefore recommended to establish the magnitude of the interfacial bond strength.

Parallel aligned sisal fibre reinforced mortar was found to have higher flexural and tensile strength improvement than the chopped random fibre reinforcement, probably due to length and

efficiency factors. In practice, short ran  
fibres find extensive application in ceme  
base products due to the ease of mix  
preparation. Further work is recommended  
and come up with alternative methods  
fabrication that will ensure the fibres a  
aligned in the matrix. metals. pp 1-2

[3] ANTONY KELLY

Fibre reinforcement in cement mortar has  
lower the density of the resulting compos  
noted advantage in cases where there is  
light weight materials, such as in wall  
advertising sign posts. Further work coul  
carried out in this line by introducing o  
into the composite, (eg. wood chips) wi  
making light weight materials, at the same  
with the desired composite strength.

What the Engineer should know about  
Materials pp 16

[7] CARL T. HERAKOVICH

Inelastic behaviour of Composite Ma

[8] HOLISTER, G.S.

Development in Composite Materials

[9] JOURNAL OF MATERIALS SCIENCE LETTER

Vol. 6 No. 11 Nov. 1987.

[10] JACK R. VINSON and TSU-WEI CHOU

Composite Materials and their use

pp 35-102

[11] ROSATO, D.V 7      **REFERENCES**

- History of Composites, Handbook of Fibre glass
- [1] BROUTMAN, J.L. and KROCK, R.H.  
Composite Materials: Mechanics of Composite  
Materials pp 47-48. H. and MILEWSKI, J.
- [2] PATON, W and Properties of Polymers and Composites:  
Fibre reinforced metals. pp 1-2. reinforcements for
- [3] ANTONY KELLY  
[13] The Nature of Composite Materials; a scientific  
American book pp 97-110. brid Technique for
- [4] FIBROUS PLASTER SHEETS isotropic Composites  
Australian Gypsum Ltd. Technical Bulletin (FAO)
- [14] United Nations Hard Fibres Research Series No. 7,  
1970. reinforced metals (Materials group:  
[5] PIATTI, G. gear and stress analysis Division)  
Advances in Composite Materials pp 53-54. Ministry fo
- [6] MOORE, A., and CALOW, C.A.  
[15] What the Engineer should know about Composite  
Materials pp 16. Natural Fibres in Concrete,
- [7] CARL T. HERAKOVICH and Concrete Institute CBI  
Inelastic behaviour of Composite Materials pp 15
- [8] HOLISTER, G.S. HANDBOOK  
Development in Composite Materials pp 5-116. by the
- [9] JOURNAL OF MATERIALS SCIENCE LETTERS of Natural  
Vol. 6 No. 11 Nov. 1987. and Energy,
- [10] JACK R. VINSION and TSU-WEI CHOU  
Composite Materials and their use in Structures  
pp 35-102



- [11] ROSATO, D.V.  
History of Composites, Handbook of Fibre glass  
and Advanced Plastics Composites,  
G. Lubin Edition, New York (1968)
- [12] NIELSEN, L.E., KATZ, H. and MILEWSKI, J.  
Mechanical Properties of Polymers and Composites:  
Handbook of fillers and Reinforcements for  
Plastics.
- [13] CHANDRASHEKHARA, K. and ABRAHAM JACOB, K.  
Experimental-Numerical Hybrid Technique for  
stress analysis of orthotropic Composites  
Indian Institute of Science, Bangalore, India.
- [14] PATON, W.  
Fibre reinforced metals (Materials group:  
fatigue, wear and stress analysis Division)  
National Engineering Laboratory (NEL), Ministry fo  
Technology.
- [15] GRAM, H.E.  
Permeability of Natural Fibres in Concrete,  
Swedish Cement and Concrete Institute CBI  
Stockholm, Sweden.
- [16] SISAL CEMENT HANDBOOK  
A guide to sisal cement roofing application by the  
Kingdom of Swaziland, Ministry of Natural  
Resources, Land Utilization and Energy,  
August, 1985.

- [17] Feasibility Study on the rise of sisal fibre for reinforced plastics in developing countries (F.A.O) United Nations. Hard Fibre Research Series No. 12, 1974.
- [18] MUTULI, S.M.  
The Properties of sisal fibre and sisal fibre reinforced Composite Materials  
MSc. Thesis, 1979, University of Nairobi.
- [19] AVESTON, J., MERCER, R.A. and SILLWOOD, J.M.  
Fibre reinforced cements-Scientific foundations for specifications, Composite Standards, Testing and Design, 1974.
- [20] KRENCHER, H.  
Fibre Reinforced Brittle Matrix Materials.  
SP 44-3 International Symposium.  
Fibre Reinforced Concrete. Ottawa, 1973.
- [21] HANNANT, D. J.  
Fibre Cements and Fibre Concretes  
A Wiley - Interscience publication 1978.
- [22] BIRYUKOVICH, K. L.  
Glass fibre reinforce cement  
Budvel 'nik Publishing House, Kiev, USSR, 1964.
- [23] BLACKMAN, L. C. F.  
Development of glass fibre reinforced cement.  
Pilkington Brothers, Limited.  
St. Helens, England, Paper 10, pp 69-76.

- [24] MAJUMDAR, A. J. and LAWS, V.  
Fibre Cement Composites: Work at the Building  
Research Establishment (BRE), University of Surrey,  
Composites Vol. 10 No. 1 1979. pp 19-27.
- [25] KELLY, A. K. B.  
Pro. Roy. Soc. 282 (1964) 63 Materials Journal of
- [26] OAKLEY, D. R. and PROCTOR, B. A.  
Tensile stress-strain behaviour of glass-fibre  
reinforced cement composites, Fibre reinforced  
cement and concrete, Rilem Symposium, 1975 U.K.
- [27] NAIR, N. G.  
Mechanics of glass fibre reinforced cement.  
Rilem Symposium 1975, UK pp 81-93.
- [28] HALE, D. K.  
Fibre Pull-out in Multiply cracked fibre  
composites. Rilem Symposium 1975, U.K.
- [29] PARAMESWARAN, V. S. and RAJAGOPALAN, K.  
Strength of Concrete Beams with aligned and Random  
Steel Micro-reinforcement,  
Rilem Symposium 1975 pp 95-104.
- [30] SWIFT, D. G. and SMITH, R. B. L.  
The Physical significance of the flexure test for  
fibre cement composites.
- [31] HOLISTER G. S. and THOMAS, C.  
Fibre reinforced composite materials.

- [32] COOPER, G.A. and KELLY A. and HUGHES, D.G.  
Tensile Properties of Fibre Reinforced Materials:  
Fracture Mechanics, Journal of Mech. Physic. Solids,  
[39] Vol. 15, 1967 pp 279-297.
- [33] DHARAN, C.K.H. Materials Science  
The Mechanics of Composite Materials Journal of  
[40] Engineering Materials and Technology,  
1978 pp 233-297 sisal fibres reinforcement in
- [34] BESSELL, T. J. Study sponsored by the United Kingdom  
Morphology related fracture processes in Nylon  
[41] and its fibre reinforced composites.  
PhD Thesis 1973, University of Liverpool.
- [35] LAWS, V. International Conference on Materials  
The tensile or stress/strain curve of brittle  
Matrices reinforced with glass fibre,  
[42] Fibre reinforced materials: Design and  
Engineering Applications.  
Proceedings of the conference held in London  
23-24 March 1977 pp 115-223.
- [36] SWIFT, D.G. and SMITH, R.B.L.  
The flexural strength of cement based composites  
using low modulus (sisal) fibres, Society of  
Composites July 1975 pp 145-148.
- [37] MAJUMDAR, A.J.  
Properties of fibre cement composites  
Rilem Symposium 1975 pp 279-314.

- [38] HANNANT, D.J., ALZONSVELD, J.J. and HUGHES, D.G.  
Polypropylene film in cement base materials  
Composites Vol. 9 April 1978 pp 83-88.
- [39] KELLY, A. and ZWEBEN, C.  
Journal of Materials Science  
Vol. 11 1976 pp 582.
- [40] BUILDING RESEARCH ESTABLISHMENT (BRE)  
Investigation of sisal fibres reinforcement in  
concrete. A study sponsored by the United Hard  
Fibre Study Group, University of Surrey 1969.
- [41] SWIFT D.G. and SMITH R.B.L.  
Sisal fibre reinforcement of cement paste and  
concrete. International Conference on Materials  
of Construction for developing countries  
Bangkok, Thailand, August 1978.
- [42] COUTTS, R.S.P.  
Air-cured woodpulp, fibre/cement mortars.  
composites vol. 18 No. 4 September, 1987.  
Butterworth & Co. Publishers Ltd.
- [43] GRIFFITH, A.A.  
The Phenomenon of rupture and flow in solids.  
Philosophical Transactions, Royal Society of  
London Vol. A221 pp 163-198, 1920.
- [44] ASTM C-496  
Standard Test Method for Splitting tensile  
strength of cylindrical concrete specimens.  
Vol. 6, 1973 pp 523-537.

- [45] LAWS, V. and ALI, M.A. ANLEY and LI VICTOR, C.  
The tensile stress/strain curve of brittle  
matrices reinforced with glass fibre. Journal of  
Fibre reinforced materials: Design and  
Engineering Applications. Paper 13 pp 115-124  
Institution of Civil Engineers, London 1977.
- [46] ALI, M.A., MAJUMDAR, A.J. and RAYMENT, D.L.  
Carbon fibres reinforcement in Cement. Cement and  
Concrete Research Vol. 2, 1972 pp 201-212.
- [47] ALLEN, H.G. Multiple fracture. Conference  
Stiffness and strength of two glass fibre  
reinforced cement laminates, Nov 1971  
Journal of Composite Materials Vol. 5  
April 1971 pp 194-207.
- [48] HANNANT, D.J., WILLIAMS, R.T. and EDINGTON, J.  
Steel Fibre reinforced concrete. Building Research  
Establishment (BRE), University of Surrey, Paper  
CP69/74, July 1974 pp 17.
- [49] HUGHES, B.P. AND FATTUHI, N. I.  
Fibre reinforced concrete in direct tension. Fibre  
reinforced materials: Design and Engineering  
Application paper 16 pp 141-147, ICE,  
London, 1977.
- [50] LAWS, V., LAWRENCE, P. and NURSE, R.W.  
Reinforcement of brittle matrices by glass  
Journal of Physics D. Applied Physics,  
Vol. 6, 1973 pp 523-537.  
Institution of Metallurgists, Nov. 1965.

- [51] YOUJIANG WANG, BACKER STANLEY and LI VICTOR, C.  
An experimental study of synthetic fibre  
reinforced cementitious composites. Journal of  
Materials Science Vol. 22, 1987 pp 4281-4291.
- [52] LAWRENCE J. BROUTMAN and RICHARD H. KROCK  
Composite materials vol. 6: Interfaces in Polymer  
matrix composites Edited by Edwin P. Plueddemann.  
pp 40.
- [53] AVESTON, J., COOPER, G.A., and KELLY, A.  
Single and Multiple fracture. 'Conference  
Proceedings, Properties of fibre composites'  
(National Physical laboratory, Nov. 1971)  
pp 15-26.
- [54] KRENCHER, H.  
Fibre spacing and specific fibre surface.  
RILEM Symposium 1975 on fibre reinforced cement  
and concrete (Construction Press Ltd.)  
Vol. 1 pp 69-80 and Vol. 2 pp 511-513.
- [55] CHAMIS, C. C.  
Mechanical load transfer at the fibre/matrix  
interface. NASA technical note, NASA TN D-6588,  
NASA, Washington D.C, 1972.
- [56] ARGON, A.S. and SHACK, W.J.  
Theories of fibre cement and fibre concrete  
Rilem Symposium, 1975, U.K.
- [57] FORSYTH, P.J.E.  
Composite Materials  
Institution of Metallurgists, Nov. 1965.

- [58] ROBERT VICHOLLS  
Composite construction materials Handbook  
Prentice-Hall Inc. 1978.
- [59] FORSYTH, P.J.E.  
Fibre-strengthened materials; composite materials  
Lectures delivered at the Institution of  
Metallurgists refresher course, Nov. 1965.
- [60] OUTWATER, J.O.  
Modern Plastics Vol. 33, 1956 pp 156.
- [61] McCLINTOCK  
Problems in the fracture of composites with Plastic  
Matrices, 1969.
- [62] KELLY, A. AND DAVIS, G. J.  
Met. Rev. Institution of Metals, 10  
No. 37 (1965).
- [63] ROMAULDI, J.P. and MANDEL, J.A.  
Tensile strength of concrete affected by  
uniformly distributed and closely spread short  
lengths of wire reinforcement A.C.I. Journal, June  
1964 pp 657-677
- [64] PARIMI, S.R. and RAO, J.K.S.  
On the fracture toughness of fibre reinforced  
concrete SP 444. Fibre reinforced Concrete,  
Ottawa 1973.
- [65] TSAI, S.W.  
Fundamental aspects of fibre reinforced  
composites Interscience Ltd., New York, 1968,  
pp 3-11.



- [66] NIELSEN, L.E. - 75.  
 Mechanical Properties of Polymers and Composites.  
 Vol. 2 (1974).  
 pp 72-79.
- [67] COX, H.L.  
 British Journal of Applied Physics  
 Vol. 3 (1952) pp 72-79.
- [68] KRENCHER, H. BESSEL, T.J., AND TALITWALA, B.S.J.  
 Fibre reinforcement  
 Akademisk forlag, Copenhagen 1964.
- [69] ALLEN, H.G.  
 Journal of Physics D: Appl. Phys. 1972  
 Vol. 5 pp 331-343.
- [70] LAWS, V.J.  
 Journal of Physics D: Appl. Phys., 1971  
 Vol. 4 pp 1737-1746.
- [71] BS 1881: Part 109: 1983.  
 British Standards: Method for Making test beams  
 for fibre concrete.  
 British Standards Institution.
- [72] BESSELL, T.J. and MUTULI, S.M.  
 The interfacial bond strength of sisal-cement  
 composites using a tensile test. Journal of material  
 science letters 1 (1982) pp 244-246.
- [73] BS 1881: Part 118: 1983,  
 British Standards: Method for determination of  
 flexural strength British Standards Institution.

[74] ASTM - C 220 - 75.

ASTM method for determination of water absorption and void volume values in concrete.

[75] HUDSON, JOHN

Director: Chiltern Research Laboratories Ltd.

A Review of Coir II, 1952.

[76] MUTULI, S.M, BESSEL, T.J., AND TALITWALA, E.S.J.

The properties of sisal as reinforcing fibre in cement base materials.

African Journal of Science and Technology (AINSTI) Vol. 1 No. 1, April 1982. pp 5-16.

[77] TAILOR, W.H.

Concrete Technology and Practice, 3rd Edition, (Angus and Robertson, Sydney, Australia, 1969).

[79] ALI, M. A., MAJUMDAR, A. J. AND SINGH, B.

Properties of glass fibre cement - the effect of fibre length and content. Building Research Establishment, CP 94/75, October, 1975.

[80] MAJUMDAR, A. J.

Properties of fibre cement composites

RILEM symposium, London, September, 1975

(The Construction Press, Lancaster, 1975)

pp. 279-313.

Table A1.1: Density of coconut fibre.

Specimen Number	1	2	3	4	5
Weight of Plasticine (g)	100.00	100.00	100.00	100.00	100.00
Volume of Plasticine (cm <sup>3</sup> )	52.80	52.80	52.80	52.80	52.80
Density of Plasticine, $\rho$ (g/cm <sup>3</sup> )	1.894	1.894	1.894	1.894	1.894
Weight of fibres (g)	28.87	28.87	28.87	28.87	28.87
<b>APPENDIX 1: DATA</b>					
Volume of Plasticine with embedded fibres (cm <sup>3</sup> )	105.90	97.35	89.75	82.20	74.70
Density of fibres, $\rho_f$ (g/cm <sup>3</sup> )	0.507	0.514	0.523	0.532	0.540
Mean density of fibres			0.52	0.52	
Standard deviation			0.02	0.02	

Table A1.1: Density of coconut fibre.

Table A1.2: Results of tensile test performed on coconut fibre.

Specimen Number	1	2	3	4	5
Weight of Plasticine (g)	100.00	100.00	100.00	100.00	100.00
Volume of Plasticine (cm <sup>3</sup> )	52.80	52.80	52.80	52.80	52.80
Density of Plasticine, $\rho$ (g/cm <sup>3</sup> )	1.894	1.894	1.894	1.894	1.894
Weight of fibres (g)	26.87	22.90	19.50	17.79	14.40
Volume of Plasticine with embedded fibres (cm <sup>3</sup> )	105.80	97.35	88.71	85.20	78.70
Density of fibres, $\rho_f$ (g/cm <sup>3</sup> )	0.507	0.514	0.543	0.549	0.556
Mean density of fibres	0.53		g/cm <sup>3</sup>		
Standard deviation	0.02		g/cm <sup>3</sup>		

Table A1.2 : Results of tensile test performed on coconut fibre.

Specimen Number	X-Section Area (mm <sup>2</sup> )	Modulus of Elasticity E (GN/m <sup>2</sup> )	Yield-stress (N/mm <sup>2</sup> )	Stress at UTS (N/mm <sup>2</sup> )	%age Elongation at failure e <sub>f</sub>
1	0.142	7.042	84.51	197.18	13.60
2	0.086	-	34.88	101.16	-
3	0.035	2.857	40.00	115.14	20.80
4	0.062	6.452	83.87	175.00	22.00
5	0.096	3.255	52.08	76.04	-
6	0.066	6.061	107.58	213.64	25.40
7	0.023	6.522	143.48	391.74	30.12
8	0.038	4.904	118.42	243.68	17.20
9	0.071	3.872	56.34	138.73	26.40
10	0.189	2.910	42.33	72.49	16.80
11	0.132	2.557	56.06	100.00	17.20
12	0.031	5.914	135.48	299.35	28.40
13	0.107	4.439	54.21	154.21	37.12
14	0.132	4.167	56.82	126.52	26.80
15	0.113	1.991	38.94	75.22	17.60
16	0.049	3.081	61.22	118.36	17.00
17	0.108	2.500	71.30	126.67	24.40
18	0.042	4.762	92.62	200.00	-
19	0.066	5.303	61.36	261.91	10.10

20	0.066	2.165	65.71	12
21	0.080	5.357	80.00	26
22	0.086	2.907	37.21	10
23	0.091	5.220	85.71	11
24	0.057	7.018	94.74	21
25	0.166	2.711	28.31	6
26	0.086	3.488	65.12	16
27	0.283	1.555	38.16	6
28	0.145	3.103	57.99	9
29	0.031	7.373	141.93	35
30	0.102	2.131	43.14	5
31	0.102	2.542	50.98	8
32	0.057	-	-	11
33	0.057	2.632	-	7
34	0.053	-	41.51	7
35	0.045	3.333	71.11	20
36	0.057	4.386	77.19	17
37	0.080	1.875	46.25	10
38	0.126	1.488	40.48	11
39	0.071	2.641	66.90	19
40	0.091	3.846	50.55	8
41	0.049	-	75.51	16
42	0.071	2.347	76.06	9
43	0.086	2.50	112.79	28
44	0.035	5.714	171.43	20
45	0.068	4.902	123.53	17
46	0.053	66.04	75.47	18

0.186	3.272	65.31	112.25	9.80
0.189	2.655	49.47	146.03	2-00
0.075	6.333	86.67	215.33	32.00
0.057	4.082	107.90	136.84	32-80
0.075	1.556	42.93	138.93	30.40
0.071	3.521	80.42	178.87	24.80
0.132	-	39.62	128.79	3-80
0.049	4.719	120.41	275.51	36.00
0.071	3.697	91.27	221.83	29.60
0.075	2.154	46.80	109.07	20-80
0.045	5.229	66.67	180.00	22.48
0.031	2.210	20.31	135.48	15.20
0.085	2.647	49.06	150.24	-
0.028	5.357	73.21	150.00	-
0.045	3.889	93.56	166.67	10.80
0.062	5.847	114.36	262.90	25.00
0.075	3.333	42.67	118.67	16.80
0.049	2.551	48.98	200.00	17.88
0.045	2.593	48.89	115.56	20.00
0.028	7.500	116.43	253.57	-
0.125	1.200	33.36	104.96	21.40
0.023	-	95.65	173.91	-
0.053	6.604	62.64	181.13	31.13
0.062	3.102	51.61	117.74	20-80
0.096	2.000	42.23	169.79	32.80
0.049	3.401	73.47	185.71	23.20
0.166	-	30.12	54.52	-

		AVERAGE VALUES		STANDARD DEVIATION	
74	0.071	1.408	25.35	61.69	-
75	0.113	2.655	37.17	103.10	20.00
76	0.076	2.961	42.11	121.05	25.60
77	0.049	4.082	59.18	322.45	32.80
78	0.119	-	43.70	162.19	-
79	0.096	2.431	51.04	193.75	32.80
80	0.075	-	28.00	121.60	34.80
81	0.038	5.921	86.84	251.32	30.40
82	0.119	1.681	40.34	188.66	40.00
83	0.025	6.154	144.00	184.00	20.80
84	0.096	2.734	42.71	162.50	32.40
85	0.159	1.210	20.31	111.32	45.20
86	0.107	3.271	57.01	93.93	-
87	0.042	7.738	114.29	214.26	-
88	0.196	1.470	40.82	142.86	35.20
89	0.113	2.655	54.87	194.96	33.20
90	0.152	1.645	31.58	126.32	38.00
91	0.108	4.398	48.15	153.06	28.80
92	0.145	2.069	36.14	91.52	32.40
93	0.020	7.500	150.00	270.00	-
94	0.123	3.659	52.03	152.85	26.00
95	0.071	-	53.52	138.45	-
96	0.124	2.419	35.48	79.03	29.20
97	0.019	16.667	184.74	278.95	26.80
98	0.041	8.537	108.05	270.49	23.36
99	0.104	3.892	67.31	154.81	27.20



Table A1.3 : Summary of results on tensile test of coconut fibre.

	AVERAGE VALUES	STANDARD DEVIATION
Cross-sectional Area (mm <sup>2</sup> )	0.08	0.04 (N/mm <sup>2</sup> )
Modulus of Elasticity (GN/m <sup>2</sup> )	4.02	2.26
Yield Stress (N/mm <sup>2</sup> )	70.53	35.53
UTS-Stress <sub>2</sub> (N/mm <sup>2</sup> )	159.30	70.38
% <sub>ge</sub> Elongation at failure	24.20	8.15

Table A1.4 : Flexural strength of 100mm x 100mm x 510mm  
sisal fibre reinforced cement mortar beams

SSP. No.	Wt. of added fibres (g)	Fibre Vol. fraction percent ( $v_f$ %)	Mean Fib. vol. fract. percent	Ultimate flexural load (N)	Ultimate flexural stress (N/mm <sup>2</sup> )
1	0	-	-	6789.302	1.88
2	0	-	3.21	7673.202	2.19
3	0	-	-	6221.502	1.77
4	0	-	-	7463.102	2.13
5	0	-	-	7388.002	2.10
6	40.00	-	-	13418.302	3.75
7	40.00	-	3.70	8513.802	2.43
8	40.00	1.06	-	-	-
9	40.00	-	-	7489.602	2.16
10	40.00	-	-	8688.902	2.48
11	60.00	-	-	10373.102	2.86
12	60.00	-	4.37	11984.602	3.32
13	60.00	1.59	-	9594.402	2.60
14	60.00	-	-	11746.902	3.29
15	60.00	-	-	10376.702	2.92
16	80.00	-	-	12718.602	3.54
17	80.00	-	4.83	11291.302	3.19
18	80.00	2.12	-	13239.602	3.51
19	80.00	-	-	12706.102	3.58
20	80.00	-	-	10990.102	3.07

21	100.00		12229.202	3.351	
22	100.00	5.47	11889.702	3.335	4.508
23	100.00	2.63	12315.002	3.349	3.461
24	100.00		13915.002	3.809	
25	100.00		12315.002	3.349	
26	120.00		12693.602	3.661	
27	120.00	6.27	13572.502	3.826	4.546
28	120.00	3.21	13183.002	3.727	3.766
29	120.00		14066.902	3.954	
30	120.00		13469.102	3.662	
31	140.00		18381.202	5.161	
32	140.00	6.66	13413.302	3.755	4.741
33	140.00	3.70	14748.102	3.971	3.930
34	140.00		-	-	
35	140.00		14800.902	4.064	
36	166.00		13094.902	3.606	
37	166.00	7.65	15901.702	4.392	3.820
38	166.00	4.37	14851.802	4.058	4.205
39	166.00		15169.402	4.165	
40	166.00		12749.702	3.676	
41	180.00		15458.002	4.457	
42	180.00	8.08	15975.802	4.722	3.541
43	180.00	4.93	14869.502	4.395	4.485
44	180.00		15087.702	4.411	
45	180.00		15429.602	4.440	
46	200.00		-	-	

Specimen No.	Weight (lb)	Fibre Vol. fraction percent (v <sub>f</sub> %)	Mean fib. vol. fract. percent	Ultimate strength (psi)	Mean Fib. Fraction (v <sub>f</sub> %)
47	200.00			15099.502	4.398
48	200.00		5.47	16488.602	4.708
49	200.00			15005.702	4.413
50	200.00			15594.202	4.505
51	230.00			14905.102	4.298
52	230.00			15523.102	4.611
53	230.00		6.27	15932.502	4.571
54	230.00	1.314		15792.902	4.600
55	230.00	1.327		15972.902	4.652
56	260.00	1.340	1.340	15572.102	4.381
57	260.00	1.360		18361.202	5.161
58	260.00	1.360		17677.402	5.003
59	260.00	2.144		16294.002	4.570
60	260.00	2.139		15763.702	4.590
61	295.00	2.192	2.157	13748.702	3.941
62	295.00	2.133		13094.902	3.806
63	295.00	2.175		14037.002	3.946
64	295.00	2.623		12858.202	3.744
65	295.00	2.706		13751.302	3.861
66	300.00	2.686	2.686	12749.702	3.676
67	300.00	2.727		-	-
68	300.00	2.719		-	-
69	300.00	3.828	8.08	11893.502	3.356
70	300.00	3.769		12553.402	3.591
18	140.00	3.751	3.775		
19	140.00	3.777			
20	140.00	3.751			

Results of flexure test mortar beams reinforced by parallel aligned glass fibre

Sl. No.	Wt. of Fibres (%)	Fibre Vol. Fraction percent (V <sub>f</sub> , %)	Mean fib. vol. frat. percent	Ultimate load	Ultimate stress	Mean Ult. flexural stress (N/mm <sup>2</sup> )
47	200.00			15099.502	4.398	
48	200.00		5.47	16488.602	4.708	4.506
49	200.00			15005.702	4.413	
50	200.00			15594.202	4.505	
51	230.00			14905.102	4.298	
52	230.00			15523.102	4.611	
53	230.00		6.27	15932.502	4.571	4.546
54	230.00			15792.902	4.600	
55	230.00			15972.902	4.652	
56	260.00		1.340	15572.102	4.381	4.217
57	260.00			18361.202	5.161	
58	260.00		6.86	17677.402	5.003	4.741
59	260.00			16294.002	4.570	
60	260.00			15763.702	4.590	
61	295.00		2.157	13748.702	3.941	4.913
62	295.00			13094.902	3.606	
63	295.00		7.85	14037.002	3.946	3.820
64	295.00			12858.202	3.744	
65	295.00			13751.302	3.861	
66	300.00			12749.702	3.676	
67	300.00			-	-	
68	300.00		8.08	-	-	3.541
69	300.00			11893.502	3.356	
70	300.00		3.775	12553.402	3.591	6.337
18	140.00			21531.02	6.057	
19	140.00			20771.02	5.942	
20	140.00			25950.02	7.329	

Table A1.5 : Results of flexure test on 100mm x 100mm x 510mm cement mortar beams reinforced by parallel aligned sisal fibres

SSP No.	Wt. of added fibres (g)	Fibre Vol. fraction percent ( $v_f$ %)	Mean fib. vol. frat. percent	Ultimate flexural load (N)	Ultimate flexural stress ( $N/mm^2$ )	Mean Ult. flexural stress ( $N/mm^2$ )
1	50.00	1.314	5.408	15166.02	4.144	8.201
2	50.00	1.327		16763.02	4.647	
3	50.00	1.340	1.340	16031.02	4.510	4.217
4	50.00	1.360		12222.02	3.506	
5	50.00	1.360		14829.02	4.276	
6	80.00	2.144	6.237	17156.02	4.850	8.051
7	80.00	2.139		16731.02	4.698	
8	80.00	2.192	2.157	17781.02	5.167	4.913
9	80.00	2.133		19542.02	5.471	
10	80.00	2.175		15192.02	4.380	
11	100.00	2.623	6.825	20031.02	5.478	8.377
12	100.00	2.706		19931.02	5.690	
13	100.00	2.666	2.688	19791.02	5.513	5.844
14	100.00	2.727		25009.02	7.232	
15	100.00	2.719		18451.02	5.309	
16	140.00	3.826	7.615	19907.02	5.797	6.480
17	140.00	3.769		21431.02	6.059	
18	140.00	3.751	3.775	21531.02	6.057	6.237
19	140.00	3.777		20771.02	5.942	
20	140.00	3.751		25950.02	7.329	

21	170.00	4.600		27907.02	7.967	
22	170.00	4.622	8.874	30945.02	8.922	8.858
23	170.00	4.577	4.611	24281.02	6.864	7.753
24	170.00	4.618		27857.02	8.000	
25	170.00	4.636		24249.02	7.012	
26	200.00	5.465		26616.02	7.712	
27	200.00	5.438		27796.02	8.014	
28	200.00	5.385	5.408	27281.02	7.712	8.201
29	200.00	5.332		31213.02	8.738	
30	200.00	5.422		30743.02	8.829	
31	230.00	6.285		33443.02	9.690	
32	230.00	6.254		30844.02	8.893	
33	230.00	6.223	6.237	30728.02	8.816	9.051
34	230.00	6.192		32202.02	9.103	
35	230.00	6.229		30599.02	8.753	
36	250.00	6.798		31683.02	9.135	
37	250.00	6.865		32396.02	9.433	
38	250.00	6.764	6.825	33834.02	9.659	9.377
39	250.00	6.865		30658.02	8.927	
40	250.00	6.831		33586.02	9.731	
41	280.00	7.613		31548.02	9.051	
42	280.00	7.613		28156.02	8.118	
43	280.00	7.651	7.615	31351.02	9.084	9.460
44	280.00	7.606		35709.02	10.265	
45	280.00	7.591		37620.02	10.783	
46	330.00	8.973		29901.02	8.665	

21	170.00	4.600		27907.02	7.967	
22	170.00	4.622	8.974	30945.02	8.922	8.858
23	170.00	4.577	4.611	24281.02	6.864	7.753
24	170.00	4.618		27857.02	8.000	
25	170.00	4.636		24249.02	7.012	
26	200.00	5.465		26616.02	7.712	
27	200.00	5.438		27796.02	8.014	
28	200.00	5.385	5.408	27281.02	7.712	8.201
29	200.00	5.332		31213.02	8.738	
30	200.00	5.422		30743.02	8.829	
31	230.00	6.285		33443.02	9.690	
32	230.00	6.254		30844.02	8.893	
33	230.00	6.223	6.237	30728.02	8.816	9.051
34	230.00	6.192		32202.02	9.103	
35	230.00	6.229		30599.02	8.753	
36	250.00	6.798		31683.02	9.135	
37	250.00	6.865		32396.02	9.433	
38	250.00	6.764	6.825	33834.02	9.659	9.377
39	250.00	6.865		30658.02	8.927	
40	250.00	6.831		33586.02	9.731	
41	280.00	7.613		31548.02	9.051	
42	280.00	7.613		28156.02	8.118	
43	280.00	7.651	7.615	31351.02	9.084	9.460
44	280.00	7.606		35709.02	10.265	
45	280.00	7.591		37620.02	10.783	
46	330.00	8.973		29901.02	8.665	



Table A1.6: Results of flexure test of 100mm x 100mm x 200mm cement fibre beams 8.974

47	330.00	8.963		315683.02	9.070	
48	330.00	8.990	8.974	33242.02	9.603	8.659
49	330.00	9.017		28709.02	8.304	
50	330.00	8.929		26801.02	7.651	

SSP. No.	Wt. of added fibres (g)	Fibre vol. fraction parent (v <sub>f</sub> )	Mean fib. vol. fract. percent	Ultimate flexural load (N)	Ultimate flexural stress (N/mm <sup>2</sup> )	Mean Ult. flexural stress (N/mm <sup>2</sup> )
1	30.00	1.084		9558.52	1.901	
2	30.00	1.050		7548.92	2.199	
3	50.00	1.655	1.075	8384.02	2.375	2.235
4	30.00	1.102		8050.02	2.415	
5	30.00	1.073		7889.72	2.289	
6	50.00	1.782		8875.52	2.559	
7	50.00	1.748		7194.12	2.914	
8	50.00	1.765	1.775	8941.52	2.553	2.435
9	50.00	1.783		8779.02	2.499	
10	50.00	1.818		8585.02	2.550	
11	66.00	2.306		9290.92	2.601	
12	66.00	2.282		10853.22	2.951	
13	66.00	2.241	2.285	9707.62	2.589	2.845
14	66.00	2.330		8780.92	2.510	
15	66.00	2.285		9283.72	2.574	
16	100.00	3.461		10253.42	2.815	
17	100.00	3.600		11934.02	3.510	
18	100.00	3.564	3.528	11185.42	3.225	3.200
19	100.00	3.516		10836.02	3.052	
20	100.00	3.448		12102.02	3.398	

Table A1.6 : Results of flexure test of 100mm x 100mm x 510mm cement mortar beams reinforced with 20mm long chopped coconut fibre

SSP. No.	Wt. of added fibres (g)	Fibre vol. fraction percent ( $v_f\%$ )	Mean fib. vol. fract. percent	Ultimate flexural load (N)	Ultimate flexural stress <sub>2</sub> (N/mm <sup>2</sup> )	Mean Ult. flexural stress <sub>2</sub> (N/mm <sup>2</sup> )
1	30.00	1.064	4.648	6558.52	1.901	3.853
2	30.00	1.080		7548.92	2.198	
3	30.00	1.055	1.075	8384.02	2.375	2.235
4	30.00	1.102		8050.02	2.415	
5	30.00	1.073		7889.72	2.286	
6	50.00	1.782	5.247	8875.52	2.559	4.105
7	50.00	1.748		7194.12	2.014	
8	50.00	1.765	1.775	8941.52	2.553	2.435
9	50.00	1.763		8770.02	2.499	
10	50.00	1.818		8585.02	2.550	
11	66.00	2.306	5.910	9290.92	2.601	4.235
12	66.00	2.262		10853.22	2.951	
13	66.00	2.241	2.285	9707.62	2.589	2.645
14	66.00	2.330		8790.92	2.510	
15	66.00	2.285		9283.72	2.574	
16	100.00	3.461	7.134	10253.42	2.815	4.115
17	100.00	3.600		11934.02	3.510	
18	100.00	3.564	3.528	11185.42	3.225	3.200
19	100.00	3.516		10838.02	3.052	
20	100.00	3.449		12102.02	3.398	

21	115.00	4.099		12885.02	3.715	
22	115.00	4.019		13206.22	3.697	
23	115.00	4.059	4.031	12966.42	3.702	3.610
24	115.00	3.980		11783.22	3.235	
25	115.00	4.000		13355.12	3.702	
26	133.00	4.626		12896.02	3.575	
27	133.00	4.626		13621.02	3.813	
28	133.00	4.648	4.649	13699.52	3.835	3.853
29	133.00	4.690		14914.42	4.250	
30	133.00	4.653		13505.52	3.792	
31	150.00	5.325		15318.52	4.395	
32	150.00	5.187		14055.22	3.855	
33	150.00	5.243	5.247	14617.22	4.092	4.105
34	150.00	5.238		14871.02	4.159	
35	150.00	5.243		14375.02	4.024	
36	170.00	5.930		14179.62	3.954	
37	170.00	5.971		16529.42	4.650	
38	170.00	5.884	5.910	15022.32	4.165	4.235
39	170.00	5.827		14913.42	4.055	
40	170.00	5.936		15573.02	4.351	
41	200.00	7.130		14331.22	4.132	
42	200.00	7.200		14433.02	4.245	
43	200.00	7.200	7.134	14297.02	4.205	4.115
44	200.00	7.059		13056.42	3.691	
45	200.00	7.105		15009.32	4.302	
20	15.00	2.387		4197.50	1.888	

Table A1.7 : Ultimate tensile strength of 50.8mm x 50.8mm x 350mm tensile specimens reinforced with 20mm long chopped sisal fibre

SSP. No.	Wt. of added fibres (g)	Fibre vol. fraction percent ( $v_f\%$ )	Mean fib. vol. fract. percent	Ultimate tensile load (N)	Ultimate tensile stress ( $N/mm^2$ )	Mean ult. tensile stress ( $N/mm^2$ )
1	-	-	-	2610.80	0.996	
2	-	-	-	2873.80	1.071	
3	-	-	-	2515.90	1.008	0.997
4	-	-	-	2330.20	0.896	
5	-	-	-	2652.80	1.014	
6	5.00	0.797	-	2555.50	0.998	
7	5.00	0.796	-	2353.10	0.917	
8	5.00	0.803	0.797	3269.80	1.287	1.040
9	5.00	0.799	-	2555.50	1.000	
10	5.00	0.791	-	2575.60	0.998	
11	10.00	1.575	-	3721.20	1.436	
12	10.00	1.623	-	2972.90	1.182	
13	10.00	1.633	1.582	2666.00	1.066	1.211
14	10.00	1.524	-	3171.60	1.184	
15	10.00	1.554	-	3117.60	1.187	
16	15.00	2.474	-	2634.40	1.064	
17	15.00	2.387	-	3120.30	1.216	
18	15.00	2.309	2.384	3196.80	1.205	1.273
19	15.00	2.363	-	3137.50	1.211	
20	15.00	2.387	-	4197.50	1.669	

21	20.00	3.214		3401.10	1.399	
22	20.00	3.151	6.731	5405.20	2.086	2.934
23	20.00	3.201	3.153	4401.60	1.726	1.724
24	20.00	3.090		4081.90	1.545	
25	20.00	3.108		4895.80	1.864	
26	25.00	3.774		6750.00	2.495	
27	25.00	3.774	6.811	5911.00	2.186	2.921
28	25.00	3.900	3.856	4928.60	1.884	2.095
29	25.00	3.939		5273.10	2.035	
30	25.00	3.894		4906.10	1.872	
31	30.00	4.671		6540.10	2.495	
32	30.00	4.581	7.918	6126.80	2.292	2.514
33	30.00	4.563	4.662	7068.80	2.634	2.387
34	30.00	4.710		5512.00	2.120	
35	30.00	4.783		6129.70	2.394	
36	35.00	5.680		7147.60	2.842	
37	35.00	5.569		7306.30	2.848	
38	35.00	5.613	5.582	7431.60	2.920	2.805
39	35.00	5.714		6580.30	2.632	
40	35.00	5.334		7452.90	2.783	
41	40.00	6.217		7434.40	2.831	
42	40.00	6.216		7269.90	2.768	
43	40.00	6.302	6.305	7622.00	2.942	2.871
44	40.00	6.428		7267.00	2.861	
45	40.00	6.364		7574.80	2.953	
46	42.00	6.926		8425.00	3.404	

47	42.00	6.682		7268.00
48	42.00	6.617	6.731	6264.80
49	42.00	6.709		8306.80
50	42.00	6.723		7073.70
51	45.00	6.953		7761.00
52	45.00	6.993		7700.00
53	45.00	6.793	6.911	7933.50
54	45.00	6.793		8677.40
55	45.00	7.021		6780.70
56	50.00	7.877		6199.00
57	50.00	7.893		7118.40
58	50.00	7.877	7.918	6583.00
59	50.00	7.955		5928.70
60	50.00	7.987		6571.60
	2.00	1.884	1.890	3512.80
	2.00	1.928		3827.80
	2.00	1.872		3513.80
	7.00	2.568		4458.00
	7.00	2.737		4428.00
	7.00	2.616	2.852	4825.50
	7.00	2.627		4802.00
	7.00	2.716		5164.00
	2.00	3.487		6780.00
	2.00	3.386		7470.80
	2.00	3.321	3.396	6100.00
	2.00	3.453		7364.00
	2.00	3.353		7276.10

Table A1.8 : Ultimate tensile strength of 50.8mm x 50.8mm x 350mm tensile specimens reinforced with parallel aligned sisal fibre

SSP. No.	Wt. of added fibres (g)	Fibre vol. fraction percent ( $v_f\%$ )	Mean fib. vol. fract. percent	Ultimate tensile load (N)	Ultimate tensile stress ( $N/mm^2$ )	Mean ult. tensile stress ( $N/mm^2$ )
1	5.00	0.773		3307.30	1.252	
2	5.00	0.770		2797.20	1.065	
3	5.00	0.804	0.787	3823.00	1.505	1.265
4	5.00	0.788		3248.90	1.254	
5	5.00	0.800		3185.00	1.249	
6	12.00	1.847		3157.00	1.190	
7	12.00	1.921		3427.20	1.344	
8	12.00	1.884	1.890	3512.60	1.351	1.347
9	12.00	1.928		3827.80	1.507	
10	12.00	1.872		3513.60	1.343	
11	17.00	2.566		4456.00	1.648	
12	17.00	2.737		4423.60	1.745	
13	17.00	2.616	2.652	4625.50	1.744	1.780
14	17.00	2.627		4602.00	1.742	
15	17.00	2.716		5164.00	2.021	
16	22.00	3.467		6780.00	2.618	
17	22.00	3.386		7470.60	2.817	
18	22.00	3.321	3.396	6100.00	2.256	2.648
19	22.00	3.453		7364.00	2.832	
20	22.00	3.353		7276.10	2.717	

21	27.00	4.076		749.50	2.765	
22	27.00	4.280		7838.30	3.044	
23	27.00	4.115	4.201	7610.00	2.842	2.947
24	27.00	4.213		7698.60	2.943	
25	27.00	4.322		8035.00	3.151	
26	33.00	5.231		8119.00	3.153	
27	33.00	5.149		8410.00	3.215	
28	33.00	5.030	5.156	8082.20	3.018	3.170
29	33.00	5.219		8704.50	3.373	
30	33.00	5.149		8086.70	3.091	
31	37.00	5.582		8658.00	3.202	
32	37.00	5.585		9047.60	3.346	
33	37.00	5.898	5.736	9245.00	3.611	3.370
34	37.00	5.784		9021.20	3.455	
35	37.00	5.829		8383.80	3.236	
36	42.00	6.401		9589.90	3.581	
37	42.00	6.553		9852.60	3.766	
38	42.00	6.451	6.542	10036.00	3.777	3.781
39	42.00	6.643		10387.00	4.025	
40	42.00	6.660		9671.70	3.756	
41	47.00	7.095		9642.50	3.566	
42	47.00	7.277		9897.00	3.754	
43	47.00	7.163	7.245	9707.80	3.625	3.762
44	47.00	7.303		10458.70	3.982	
45	47.00	7.378		10095.80	3.883	
46	55.00	8.383		9458.7.	3.532	



Wt. added fibres (g)	Fibre fraction percent (v <sub>f</sub> %)	Mean Fib. vol. fract. percent	Ult. tensile load (N)	Ultimate tensile stress (N/mm <sup>2</sup> )	Mean ult. tensile stress (N/mm <sup>2</sup> )
47 55.00	8.415		8424.60	3.158	
48 55.00	8.383	8.396	9467.00	3.535	3.490
49 55.00	8.334		9944.00	3.692	
50 55.00	8.465		3.533		
5.00	1.009		4841.00	1.750	
5.00	1.049		2274.80	0.882	
5.00	1.000	1.019	1883.30	0.821	1.090
5.00	0.988		3778.00	1.393	
5.00	1.047		2018.50	0.790	
10.00	2.057		4850.50	1.803	
10.00	2.057		3553.00	1.368	
10.00	2.035	2.057	4882.00	1.851	1.643
10.00	2.078		4583.80	1.772	
10.00	2.057		3441.10	1.323	
15.00	3.028		5250.80	1.980	
15.00	3.068		6084.00	2.318	
15.00	3.086	3.073	4852.00	1.873	2.094
15.00	3.088		5891.00	2.308	
15.00	3.075		5185.00	1.990	
20.00	4.114		8838.90	2.887	
20.00	4.155		6832.80	2.653	
20.00	4.051	4.108	6921.00	2.820	2.483

Table A1.9 :Ultimate tensile strength of 50.8mm x 50.8mm x 350mm tensile specimens reinforced by 20mm long chopped coconut fibre

No.	Wt.of added fibres (g)	Fibre vol. fraction percent ( $v_f\%$ )	Mean fib. vol.fract. percent	Ultimate tensile load (N)	Ultimate tensile stress ( $N/mm^2$ )	Mean ult. tensile stress ( $N/mm^2$ )
1	5.00	1.009		4841.00	1.750	
2	5.00	1.049		2274.80	0.892	
3	5.00	1.000	1.019	1863.30	0.621	1.090
4	5.00	0.989		3778.00	1.397	
5	5.00	1.047		2018.50	0.790	
6	10.00	2.057		4950.50	1.903	
7	10.00	2.057		3553.00	1.366	
8	10.00	2.035	2.057	4862.00	1.851	1.643
9	10.00	2.078		4583.80	1.772	
10	10.00	2.057		3441.10	1.323	
11	15.00	3.026		5250.90	1.980	
12	15.00	3.068		6064.00	2.318	
13	15.00	3.098	3.073	4852.00	1.873	2.094
14	15.00	3.098		5981.00	2.309	
15	15.00	3.075		5195.00	1.990	
16	20.00	4.114		6936.90	2.667	
17	20.00	4.155		6832.80	2.653	
18	20.00	4.051	4.108	6921.00	2.620	2.483

No.	Fibre vol. fraction (%)	Average Interfacial bond strength (N/mm <sup>2</sup> )	Standard deviation (N/mm <sup>2</sup> )	Average Interfacial bond strength (N/mm <sup>2</sup> )
19	20.00	4.130		5751.60
20	20.00	4.090		5876.00
21	25.00	5.113		7563.40
22	25.00	5.044		7918.90
23	25.00	5.073	5.079	7409.00
24	25.00	5.083		6729.00
25	25.00	5.084		7422.00
26	30.00	6.053		7600.00
27	30.00	6.053		8667.00
28	30.00	6.135	6.050	6935.50
29	30.00	6.017		7280.40
30	30.00	5.994		8037.00
31	35.00	6.926		5959.60
32	35.00	7.061		6519.00
33	35.00	7.446	7.144	6933.80
34	35.00	7.158		6765.50
35	35.00	7.130		7117.80
9	1.928	57.13		0.0559
10	1.872	51.75		0.0636
11	2.586	54.00		0.0442
12	2.737	54.82		0.0409
13	2.816	57.25		0.0408
14	2.627	54.00		0.0431
15	2.716	59.17		0.0380
16	3.467	58.40		0.0299
17	3.386	55.50		0.0323
18	3.321	57.93		0.0316

Table A1.10: The interfacial bond strength of cement-sisal matrix measured by the method of Aveston et al [53]

SSP. No.	Fibre vol. fraction (v <sub>f</sub> %)	Average crack-spacing (mm)	Interfacial bond strength $\tau$ (N/mm <sup>2</sup> )	Standard deviation (N/mm <sup>2</sup> )	Average interfacial bond-strength $\tau$ (N/mm <sup>2</sup> )
1	0.773	-	-	-	-
2	0.770	75.70	0.1069		
3	0.804	81.00	0.0957	0.0056	0.1013
4	0.788	-	-		
5	0.800	-	-		
6	1.847	61.13	0.0546	0.0012	0.0182
7	1.921	56.25	0.0570		
8	1.884	61.50	0.0532	0.0036	0.0569
9	1.928	57.13	0.0559		
10	1.872	51.75	0.0636	0.0069	0.0185
11	2.566	54.00	0.0442		
12	2.737	54.62	0.0409		
13	2.616	57.25	0.0408	0.0021	0.0414
14	2.627	54.00	0.0431		
15	2.716	59.17	0.0380		
16	3.467	58.40	0.0299	0.0069	0.0142
17	3.386	55.50	0.0323		
18	3.321	57.93	0.0316	0.0016	0.0319

45	7.378	53.13	0.0148		
46	8.383	63.50	0.0108		
47	8.415	66.30	0.0103		
48	8.383	71.00	0.0097	0.0041	0.0103
49	8.334	65.00	0.0106		
50	8.465	68.75	0.0099		

---

APPENDIX 2

Theory for minimum crack spacing 'X' of long fibres with Frictional Bond

The idealized stress-strain curve for a fibre reinforced brittle matrix composite is shown in Figure A2.1.

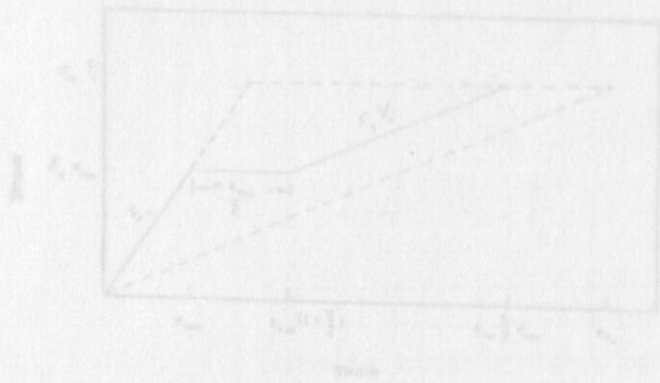


Figure A2.1.

## APPENDIX 2

The initial Young's modulus ( $E_c$ ) has been given by equation 2.11(a) of chapter two. The derivation of the rest of the curve in Figure A2.1 is as follows:

If the fibre diameter is not too small, the matrix will fail at its normal strain ( $\epsilon_m$ ) and the subsequent behaviour will depend on whether the fibres can withstand the additional load without breaking, i.e. whether:

## Theory for minimum crack spacing 'X' of long fibres with Frictional Bond

The idealized stress-strain curve for a fibre reinforced brittle matrix composite is shown in Figure A2.1.

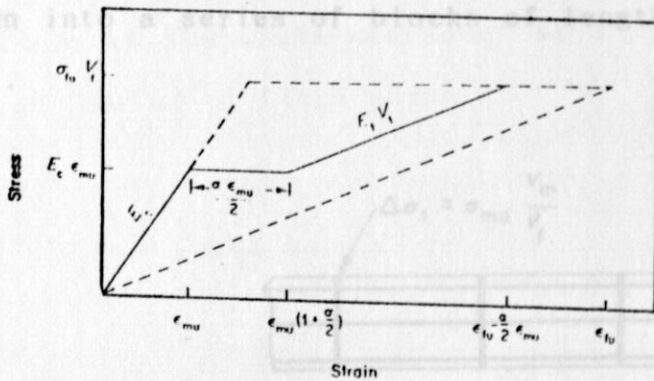


Figure A2.1.

The initial Young's modulus ( $E_c$ ) has been given by equation 2.11(a) of chapter two. The derivation of the rest of the curve in Figure A2.1 is as follows:

If the fibre diameter is not too small, the matrix will fail at its normal strain ( $\epsilon_{\mu}$ ) and the subsequent behaviour will depend on whether the fibres can withstand the additional load without breaking, i.e. whether;

$X'$  can be calculated from a simple balance of the load ( $\sigma_{\mu} V_f$ ) needed to break unit area of matrix and the load carried by  $N$  fibres across the same area cracking. This load is transferred over a distance  $X'$  by the limiting maximum shear stress,  $\tau$ . From Figure A2.3, for aligned fibres,

$$\sigma_{fu} V_f > E_c \epsilon_{mu} \dots [A2.1]$$

If they can take this additional load they will be transferred back into the matrix over a transfer length  $X'$ , Figure A2.2, and the matrix will eventually be broken down into a series of blocks of length between  $X'$  and  $2X'$ .

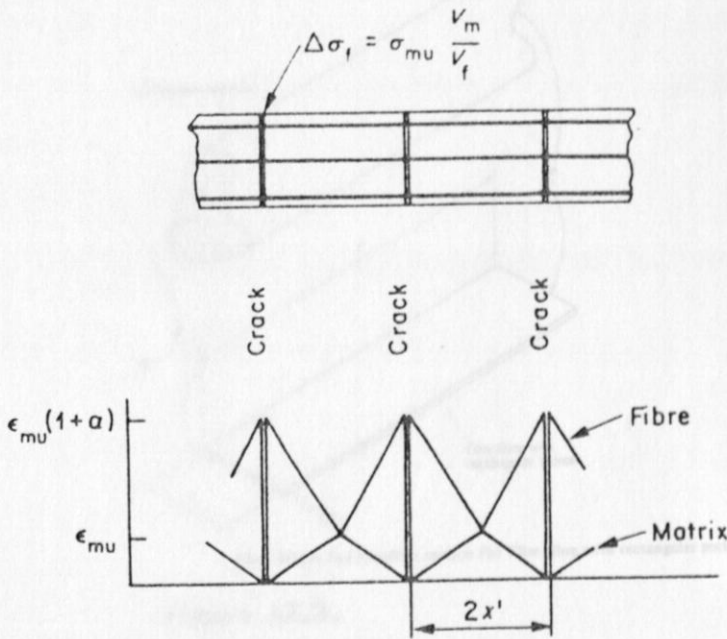


Figure A2.2.

$X'$  can be calculated from a simple balance of the load ( $\sigma_{fu} V_f$ ) needed to break unit area of matrix and the load carried by  $N$  fibres across the same area cracking. This load is transferred over a distance  $X'$  by the limiting maximum shear stress,  $\tau$ . From Figure A2.3, for aligned fibres,



$$N = \frac{V_f}{A_f} \dots [A2.1]$$

$$P_f N \tau X' = \sigma_{mu} V_m \dots [A2.2]$$

where  $A_f$  is the cross-sectional area of fibre and  $p_f$  is the perimeter of fibre shown.

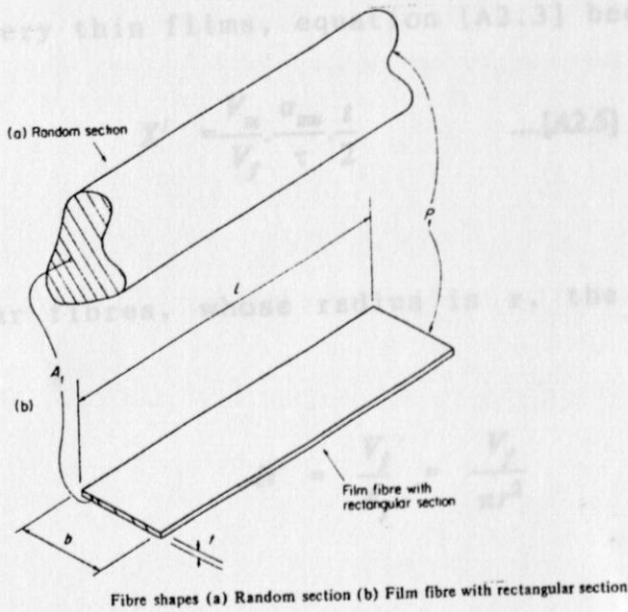


Figure A2.3.

From [A2.1] and [A2.2]

$$X' = \frac{V_m \sigma_{mu} A_f}{V_f \tau P_f} \dots [A2.3]$$

The crack spacing will eventually be between  $X'$  and  $2X'$ .  
For film fibres with a rectangular section,

$$\frac{A_f}{P_f} = \frac{b.t}{2.(b+t)} \quad \dots[A2.4]$$

and for situations where

$$t \ll b, \quad \frac{A_f}{P_f} = \frac{t}{2}$$

Hence for very thin films, equation [A2.3] becomes,

$$X' = \frac{V_m}{V_f} \cdot \frac{\sigma_{mu}}{\tau} \cdot \frac{t}{2} \quad \dots[A2.5]$$

For circular fibres, whose radius is  $r$ , the number of fibres,

$$N = \frac{V_f}{A_f} = \frac{V_f}{\pi r^2}$$

Hence equation [A2.2] becomes

$$2.\pi.r.N.X' = \sigma_{ms} V_m \quad \dots[A2.6]$$

or

$$X' = \frac{V_m}{V_f} \cdot \frac{\sigma_{ms} \cdot r}{2.\tau} \quad \dots[A2.7]$$

The stress distribution in the fibres and matrix (crack spacing  $2X'$ ) will then be as shown in Figure A2.2.